VOLUME 3 (1957) No. 5

NUCLEAR PHYSICS

MONTHLY JOURNAL DEVOTED TO THE EXPERIMENTAL AND THEORETICAL STUDY OF ATOMIC NUCLEI, NUCLEAR FIELDS AND THE FUNDAMENTAL ASPECTS OF COSMIC RADIATION

EDITOR: L. ROSENFELD - MANCHESTER

E. ARBMAN, Excited levels in Bi^{206} from the decay of Po^{206} 625

S. WAHLBORN, Levels in Bi^{206} 644

E. CORINALDESI, Dispersion relations for the decay of the τ-meson . . . 649

C. M. CLASS and U. MEYER-BERKHOUT, The Coulomb excitation of Eu^{151} and Eu^{153} 656

A. BISI, E. GERMAGNOLI and L. ZAPPA, The low-lying energy levels of ^{151}Eu 670

H. A. TOLHOEK and J. R. LUYTEN, A theoretical estimate of the influence of the character of the four-fermion interaction on the muon capture rate . . . 679

A. PETERMANN, Magnetic moment of the electron 689

Book Reviews 691

Erratum 692

Author Index. 693

Book Reviews (Index) 697

Subject Index 697

NORTH-HOLLAND PUBLISHING COMPANY - AMSTERDAM

July 1957

EDITORIAL BOARD

AUSTRIA:	B. Karlik (Vienna), H. Thirring (Vienna)
BELGIUM:	M. de Hemptinne (Louvain), J. Verhaeghe (Ghent)
CANADA:	G. Volkoff (Vancouver)
DENMARK:	C. Møller (Copenhagen), S. Rozental (Copenhagen)
EGYPT & ARAB COUNTRIES:	F. El Bedewi (Alexandria), M. G. Nooh (Cairo)
FINLAND:	L. Simons (Helsinki)
FRANCE	A. Berthelot (Saclay), S. Gorodetzky (Strasbourg), F. Joliot (Paris)
GERMANY (FED. REP.):	W. Gentner (Freiburg i. B.), J. H. D. Jensen (Heidelberg)
GERMANY (DEM. REP.):	G. Hertz (Leipzig)
GREAT BRITAIN:	S. Devons (Manchester)
HUNGARY:	L. Janossy (Budapest)
INDIA:	H. Bhabha (Bombay), B. Peters (Bombay), R. Ramanna (Trombay)
IRISH REPUBLIC:	J. McConnell (Maynooth)
ISRAEL:	G. Racah (Jerusalem)
ITALY:	E. Amaldi (Rome)
JAPAN:	S. Kikuchi (Tokyo), S. Tomonaga (Tokyo)
NETHERLANDS:	H. Brinkman (Groningen), S. R. de Groot (Leiden)
NORWAY:	E. Hylleraas (Oslo), A. Lundby (Oslo), H. Wergeland (Trondheim)
POLAND:	L. Infeld (Warsaw)
PORTUGAL:	J. M. Araújo (Porto), J. R. de Almeida Santos (Coimbra)
SOUTH AMERICA:	G. Beck (Saõ Paulo), J. Leite Lopes (Rio de Janeiro)
SPAIN:	J. M. Otero (Madrid), C. Sanchez del Rio (Madrid)
SWEDEN:	O. Klein (Stockholm), K. Siegbahn (Uppsala), I. Waller (Uppsala)
SWITZERLAND:	P. Huber (Basel), P. Scherrer (Zürich)
U.S.S.R.:	M. A. Markov (Moscow), I. S. Shapiro (Moscow), D. V. Skobeltzyn (Moscow)
YUGOSLAVIA:	I. Supek (Zagreb)
U.S.A. & MEXICO:	V. Weisskopf (Cambridge, Mass.)
AUSTRALIA & NEW ZEALAND:	H. Messel (Sydney), M. L. Oliphant (Canberra)

CONTRIBUTIONS may be sent to the Editor, Professor L. Rosenfeld, Dept. of Theoretical Physics, The University, Manchester, either directly, or preferably through the intermediary of one of the members of the Editorial Board of the country or region in which the author is working. They may be written in English, French or German.

NUCLEAR PHYSICS is published in monthly issues. The subscription price is fl 57.00; 114s; $ 15.00. Postfree.

SUBSCRIPTIONS should be sent to the publishers, NORTH-HOLLAND PUBLISHING COMPANY, P.O.Box 103, Amsterdam or to any subscription-agent. Subscriptions for U.S.A. are to be sent exclusively to INTERSCIENCE PUBLISHERS, INC., 250 Fifth Avenue, New York 1, N.Y.

BOOKS FOR REVIEW should be sent to Professor Rosenfeld.

No part of this issue may be reproduced in any form, by print, photoprint, microfilm or any other means without written permission from the publisher. Reprints, photoprints or microfilms are obtainable at cost from the publisher.

Printed in the Netherlands

NUCLEAR PHYSICS

EDITORIAL BOARD

AUSTRIA: B. Karlik (Vienna), H. Thirring (Vienna)
BELGIUM: M. de Hemptinne (Louvain), J. Verhaeghe (Ghent)
CANADA: G. Volkoff (Vancouver)
DENMARK: C. Møller (Copenhagen), S. Rozental (Copenhagen)
EGYPT & ARAB COUNTRIES: F. El Bedewi (Alexandria), M. G. Nooh (Cairo)
FINLAND: L. Simons (Helsinki)
FRANCE A. Berthelot (Saclay), S. Gorodetzky (Strasbourg), F. Joliot (Paris)
GERMANY (FED. REP.): W. Gentner (Freiburg i. B.), J. H. D. Jensen (Heidelberg)
GERMANY (DEM. REP.): G. Hertz (Leipzig)
GREAT BRITAIN: S. Devons (Manchester)
HUNGARY: L. Janossy (Budapest)
INDIA: H. Bhabha (Bombay), B. Peters (Bombay), R. Ramanna (Trombay)
IRISH REPUBLIC: J. McConnell (Maynooth)
ISRAEL: G. Racah (Jerusalem)
ITALY: E. Amaldi (Rome)
JAPAN: S. Kikuchi (Tokyo), S. Tomonaga (Tokyo)
NETHERLANDS: H. Brinkman (Groningen), S. R. de Groot (Leiden)
NORWAY: E. Hylleraas (Oslo), A. Lundby (Oslo), H. Wergeland (Trondheim)
POLAND: L. Infeld (Warsaw)
PORTUGAL: J. M. Araújo (Porto), J. R. de Almeida Santos (Coimbra)
SOUTH AMERICA: G. Beck (Saõ Paulo), J. Leite Lopes (Rio de Janeiro)
SPAIN: J. M. Otero (Madrid), C. Sanchez del Rio (Madrid)
SWEDEN: O. Klein (Stockholm), K. Siegbahn (Uppsala), I. Waller (Uppsala)
SWITZERLAND: P. Huber (Basel), P. Scherrer (Zürich)
U.S.S.R.: M. A. Markov (Moscow), I. S. Shapiro (Moscow), D. V. Skobeltzyn (Moscow)
YUGOSLAVIA: I. Supek (Zagreb)
U.S.A. & MEXICO: V. Weisskopf (Cambridge, Mass.)
AUSTRALIA & NEW ZEALAND: H. Messel (Sydney), M. L. Oliphant (Canberra)

NUCLEAR PHYSICS

MONTHLY JOURNAL DEVOTED TO THE EXPERIMENTAL AND THEORETICAL STUDY OF ATOMIC NUCLEI, NUCLEAR FIELDS AND THE FUNDAMENTAL ASPECTS OF COSMIC RADIATION

EDITOR: L. ROSENFELD - MANCHESTER

VOLUME III

MARCH 1957—JULY 1957

NORTH-HOLLAND PUBLISHING COMPANY - AMSTERDAM

PRINTED IN THE NETHERLANDS BY
BOEKDRUKKERIJ VOORHEEN GEBROEDERS HOITSEMA N.V., GRONINGEN

Nuclear Physics **3** (1957) 625—643; *North-Holland Publishing Co., Amsterdam*

EXCITED LEVELS IN Bi^{206} FROM THE DECAY OF Po^{206}

E. ARBMAN

The Gustaf Werner Institute for Nuclear Chemistry,
University of Uppsala, Uppsala

Received 5 February 1957

Abstract: The energies and intensities of conversion electrons from the decay of Po^{206} have been studied in a double focusing beta-spectrometer. Relative gamma intensities were measured in a scintillation spectrometer. Coincidences between pairs of conversion lines were studied in a coincidence spectrometer. No positons were observed. A decay scheme is proposed, which contains 9 excited levels and includes 20 of the observed transitions.

1. Introduction

The investigation of the energy levels in Bi^{206} from the decay of Po^{206} to be described in this paper was initiated in connection with studies at this institute of alpha-spectra of polonium isotopes by Rosenblum and Tyrén [1]). Energies and intensities of the conversion electron lines and relative gamma intensities have been obtained from measurements in a double focusing beta-ray spectrometer [2]) and a single-channel scintillation spectrometer. Electron-electron coincidences were measured in a coincidence spectrometer [3]) at the Physics Department of this University.

Po^{206} was first identified by Templeton *et al.* [4]), who reported 9 days half-life and branched decay for this isotope. 90 per cent of the nuclei were found to decay by electron capture to 6.4 day Bi^{206} and 10 per cent by alpha-emission to Pb^{202}. Absorption measurements indicated gamma rays of energies about 300 and 800 keV. Later Momyer *et al.* [5]) determined the alpha-branching of Po^{206} to be 5 ± 1 per cent.

Before the commencement of this work little was known about the excited levels in Bi^{206}. From an investigation of the alpha-decay of At^{210} Asaro [6]) reported three alpha-groups of energies 5.519 (32 %), 5.437 (31 %) and 5.355 (37 %) MeV, thus indicating levels in the Bi^{206} nucleus at about 82 and 164 keV.

Recently, after most of the work reported here had already been carried out, an extensive investigation of the decay of Po^{206} by Stoner [7]) appeared. Energies and intensities of electron lines and gamma rays were studied in different kinds of spectrometers. Stoner reports gamma transitions of energies 60, 286, 311, 338, 463, 472, 511, 522, 807, 980 and 1031 keV. Based on gamma-gamma coincidences a decay scheme was proposed with excited levels at 807, 1031, 1318, 1369, 1378, 1688 and 1840 keV. Further,

July 1957

from coincidences with the K X-rays, half-lives less than 2×10^{-9} sec were assigned to the 286, 311, 338, 511, 807 and 1031 keV transitions.

2. Experimental Procedures

2.1. PREPARATION OF SPECTROMETER SOURCES

Po^{206} was produced by the Bi^{209} (p, 4n) Po^{206} reaction by bombarding bismuth with 50 MeV protons in the Uppsala synchro-cyclotron. In order to get rid of the simultaneously produced 5.7 h Po^{207} and 4 h Po^{204} activities the target was left to decay for four or five days before the separation of the polonium fraction.

Spectrometer sources were prepared by electroplating the polonium from the hot target solution (about 6 N in HCl) on suitable silver backings[8]). Silver strips of 1 mm width and a thickness of a few mg per cm^2 were used for the double focusing spectrometer and small disks of 2 mm diameter (2.7 mg/cm^2) for the coincidence spectrometer. In each case the back side of the foil was masked off by nail-polish. If the solution was stirred and the volume kept small (about 1 cm^3), 15 to 30 min plating gave high yields.

The plating method was found to be very convenient. To get rid of the Bi^{206} daughter, sources could be dissolved and replated several times without appreciable loss of polonium activity. The fact that the strong K line of the 184.1 keV transition in Pb^{206} scarcely was observable from a freshly prepared source proves that practically no bismuth plated out together with the polonium.

To reduce the number of back-scattered electrons, which introduce a background counting rate especially at low electron energies, thin silver foils should be used as source backings. Since extremely thin silver foils are difficult to handle, thin polythene films were coated with a silver layer ($\approx$ 50 $\mu g/cm^2$) by vacuum evaporation. Strips of these films were then used as source backings for investigation of the low energy part of the conversion spectrum. The background in the 50 keV region was found to be reduced by a factor of 10 as compared to the background from a source plated on a silver foil of a thickness of about 10 mg/cm^2.

2.2. ELECTRON SPECTRA

Conversion electrons of energies above about 20 keV were studied in the double focusing spectrometer. Survey runs, repeated several times for four weeks, were performed with the automatic recording arrangement. Analysis of the records gave half-lives and approximate energies of the conversion lines. In several cases lines from the daughter Bi^{206} were found to grow up close to or coinciding with lines from the decay of Po^{206}. No originally present lines with a half-life different from that of the 9 day Po^{206} activity were observed.

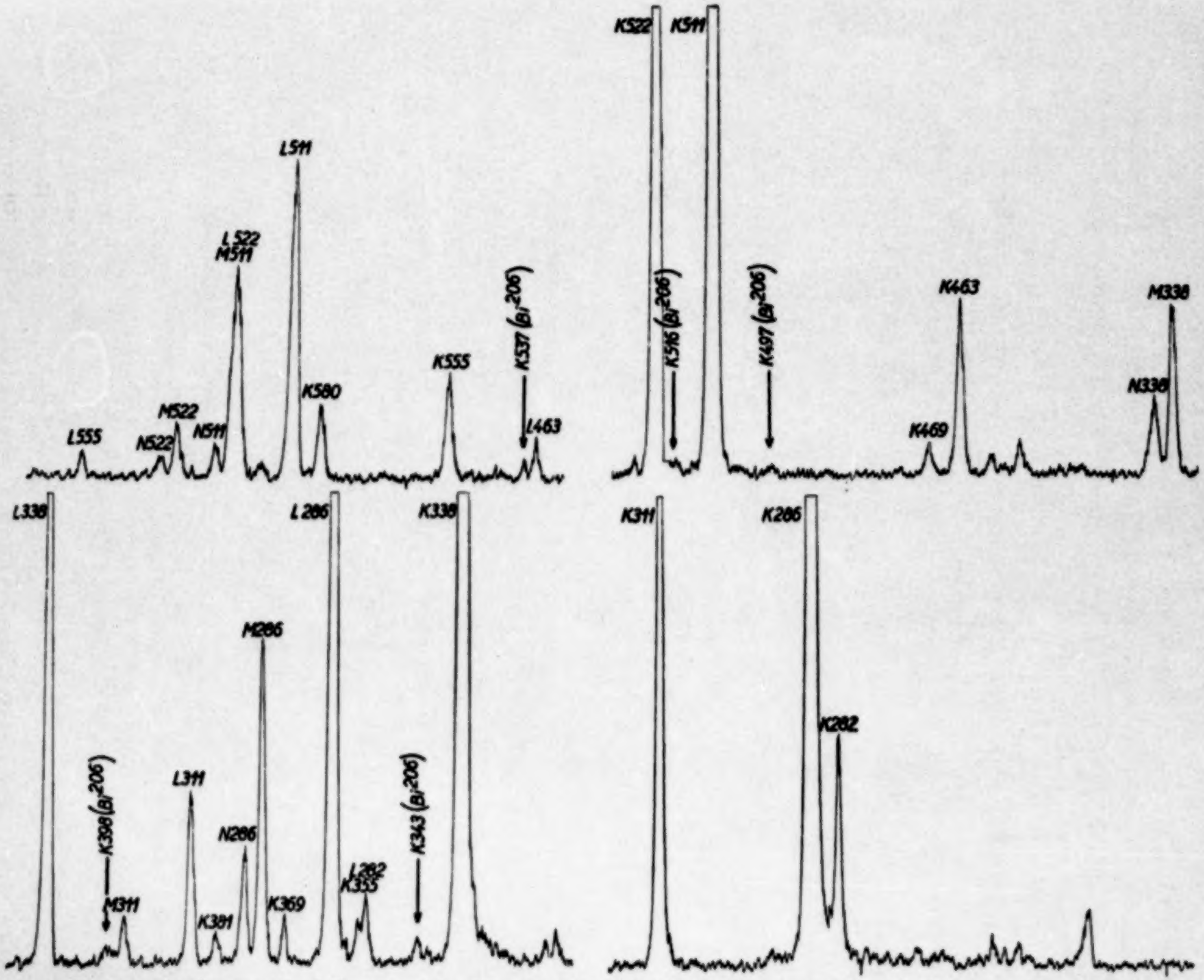

Fig. 1. Photograph of a record of the conversion lines from Po^{206} in the energy range 190 to 525 keV, run about 2 hours after the preparation of the sample. Growing Bi^{206} lines are marked with arrows. Scanning time for the part shown = 36 min. Full scale deflection = 100 c/sec. Peak counting rate of the 286.5 keV K line ≈ 2000 c/sec. Source plated on 1 × 15 mm^2 polythene sheet (2 mg/cm^2) coated with a thin silver layer.

Fig. 1 is a photograph of a part of a record in the energy range 190 to 525 keV, run about two hours after the preparation of the sample. The places where strong Bi^{206} lines are growing are marked with arrows on the record. With the resolution used in the figure (about 0.3 %) the spectrum from 15 keV to 1 MeV can be recorded in three hours. Thus it was possible to obtain the whole conversion spectrum practically undisturbed by the Bi^{206} lines.

In order to improve the energy and intensity values, all lines observed from the decay of Po^{206} were remeasured by point to point plotting. Care was taken to investigate from freshly plated sources the energy regions where the Bi^{206} lines were known to grow up. A small part of the spectrum of the high energy region, measured at 0.24 per cent resolution, is shown in fig. 2.

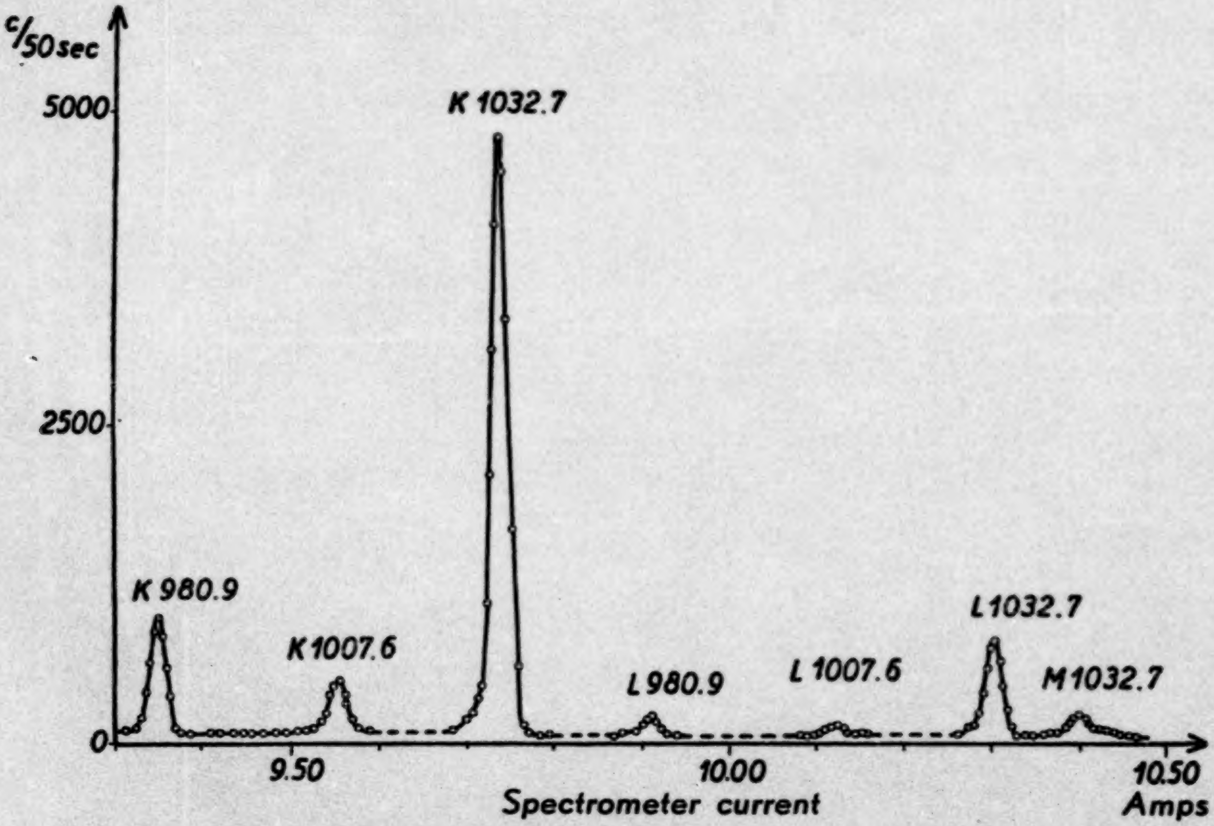

Fig. 2. Conversion lines of the 980.9, 1007.6 and 1032.7 keV transitions, measured with 0.24 % resolution.

The energies of the lines were determined relative to the strong K lines of the 184.1, 497.1, 516.1 and 803.3 keV transitions in Pb^{206}. According to Alburger and Pryce [9]), the energies of these transitions are accurate to 5 parts in 10 000.

The information obtained from the investigation of conversion electron lines is summarized in tables 1 and 2.

Table 1

Gamma transitions in Bi^{206}

γ-ray energy (keV)	Lines observed	K line intensity (%)	K/L	L/M	Remarks
59.9(3)	L_I, L_{II}, L_{III}, M_{II}, M_{III}, N_{III}, O_{III}	31.3[1]	—	4.0	$L_I : L_{II} : L_{III} = 0.030 : 1.1 : 1.0$
82.9	L_I, M_I, N_I	0.31[2]	—	≈3	
117.6	K, L_I, M_I	0.55	4.5±1.0	≈2	
140.6	K, L_I, M_I	0.32	4.7±1.0	≈3	
170.8	K, L_I	0.41	5.3±1.0	—	
171.5	K, L_I	0.10	3.5±1.0	—	
282.1	K, L_I	0.32	5.8±1.0	—	
286.5 †	K, L_I, M_I, N	9.75	5.6±0.6	4.1	$(L_I+L_{II})/L_{III} > 80$
311.5 †	K, L_I, M_I, N	1.54	6.0±0.6	3.7	$(L_I+L_{II})/L_{III} > 10$
338.4 †	K, L_I, M_I, N	5.20	5.6±0.6	4.2	$(L_I+L_{II})/L_{III} > 30$
354.8	K, L_I	0.090	5 ±2		L line composite with 338.4 keV N line
463.5	K, L_I, M	0.21	6.5±0.7	3.0	
469.1	K, L_{II}	0.032	4 ±2		
511.4 †	K, L_I, M_I, N	2.09	5.6±0.6	—	$(L_I+L_{.I})/L_{III} > 20$
522.4 †	K, L_I, M_I, N	1.32	5.5±1.0	—	L line composite with 511.4 keV M line
554.6	K, L_I, M_I	0.11	6.2±1.0	3.3	
579.8	K, L_I	0.076	5.6±1.0	—	
645.6	K, L_{II}	0.017	4.3±1.0	—	
669.0	K, L_I	0.038	5.6±1.0	—	
677.8	K, L_{II}	0.014	3 ±2	—	
807.6 †	K, L_I, M_I, N	0.64	5.6±0.6	3.6	
861.6	K, L_I	0.026	5.4±0.9	—	
980.9 †	K, L_I, M_I	0.10	5.7±0.9	3.3	
1007.6	K, L_I	0.045	4.5±1.0	—	
1032.7 †	K, L_I, M_I, N	0.50	6.0±0.6	3.6	
1320.0	K	0.002	—	—	

[1] Intensity of L_{II} line.

[2] Intensity of L_I line.

† Energy accuracy 5 parts in 10 000.

Table 1 contains those gamma transitions which are considered to be certain. The energies of the transitions listed in column 1 are, when possible, derived from the K line energies by adding the appropriate binding energy[10]. Generally the spread in energies for each gamma ray, when derived from the different lines assigned to that gamma ray (column 2), is less than 5 parts in 10 000. The accuracies of the transition energies marked with a cross are believed to be comparable with the accuracy of the calibration lines, since the lines were measured from the same source in continuous runs. The

TABLE 2

Auger lines and other weak lines from the decay of Po^{206}

Electron energy (keV)	Line intensity (%)	Possible assignment	Remarks
16.1	0.4	K 106.6	
37.2	0.12		
39.2	0.11		
53.8	0.067		
57.5	< 0.50	$K L_I L_I$	Composite with 59.9 keV M_V line
58.3	0.56	$K L_I L_{II}$	
60.6	0.24	$K L_I L_{III}$	
61.2	0.40	$K L_{II} L_{III}$	
63.5	0.17	$K L_{III} L_{III}$	
70.9	0.47	$K L_I M$	
71.6		$K L_{II} M$	
73.3	0.39	$K L_{III} M$	
74.1		$K L_{II} N$	
76.5	0.04	$K L_{III} N$	
89.1	0.07		
90.4	0.11	K 181.0 or L_I 106.8	
129.9	0.05	L_I 146.3	
142.4	0.01	M_I 146.4	
168.2	0.06		
232.4	0.04		
234.3	0.03		
278.4	0.04	K 368.9	
290.3	0.04	K 380.8	
352.9	0.007	L_{II} 368.6	
362.2	0.04	K 452.7	
365.0	0.01	L_{II} 380.7	
367.3	0.01	L_{III} 380.7	
436.1	0.01	L_I 452.5	
447.3	0.03	K 537.8	
727.5	0.01	K 818.0	

energies of the remaining transitions should be accurate to 1 part in 1000. Table 2 includes the Auger lines and other weak lines, for which certain assignment was not possible.

Relative line intensities corrected for absorption in the counter window (0.5 mg/cm^2) according to the curves by Saxon [11]), were determined by comparing the areas of the different lines. The relative intensities were then converted into electrons per 100 disintegrations in accordance with the following considerations. The first excited level of Pb^{206} is assumed to decay to 100 per cent by the 803.3 keV E2 transition [9]). With this assumption every decay of Po^{206} leading to Bi^{206} will be followed by the 803.3 keV transition. The disintegration rate A_2 of Bi^{206}, fed by Po^{206}, is at any time given by the relation

$$A_2 = \frac{\lambda_2 A_1}{\lambda_2 - \lambda_1} \left[1 - \exp\{-(\lambda_2 - \lambda_1)t\}\right] \tag{1}$$

where indices 1 and 2 refer to Po^{206} and Bi^{206} respectively, A_1 and A_2 are disintegrations per unit time, t is the time counted from the preparation of the source and λ_1 and λ_2 are the disintegration constants. With the use of relation (1) and the intensities of the K lines of the 803.3 and 807.6 keV transitions the number of K conversion electrons for the 807.6 keV transition was calculated. As the mean of three different measurements on a sample 10, 22 and 33 days old a value of 0.64 ± 0.04 electrons per 100 disintegrations of Po^{206} feeding Bi^{206} was obtained. In the calculation the experimentally found half-lives 8.83 and 6.30 days for Po^{206} and Bi^{206} respectively and α_K equal to 0.0082[12]) for the 803.3 keV E2 transition were used.

A search for positons was made with the spectrometer set at a transmission of 2 per cent. No positons were observed. From the intensities of the L+M lines of the 1032.7 keV transition, measured at the same transmission, it was estimated that a hypothetical positon distribution with a maximum at about 0.5 MeV and of comparable intensity would have been observed. Thus positon emission seems to occur in less than 0.1 per cent of the disintegrations.

2.3. SCINTILLATION SPECTRUM AND MULTIPOLARITY ASSIGNMENTS

Scintillation spectra — part of one is shown in fig. 3 — were measured

TABLE 3

Multipolarity assignments and intensity of transitions in Bi^{206}

Gamma energy (keV)	Measured gamma intensity, K X-ray peak = 100	Calculated gamma intensities for different multipoles (%)			Assumed multipolarity	Total transition intensity (%)
		M1	E1	E2		
59.9				1.1 †	E2	85
170.8		0.2	4.2		M1 or E1	0.7 or 4.7
282.1	43	0.46	11		M1	0.8
286.5		22	360		M1	34
311.5		4.1	63		M1	5.8
338.4		18	270		M1	24
463.5		1.8	22		M1	2.0
511.4	46	23	260	100	M1	25
522.4		16	176	68	M1	18
554.6		1.4	16		M1	1.5
579.8		1.1	12		M1	1.2
807.6	30	23	195	78	M1	24
980.9	47	6.1	43	17	M1	6.2
1007.6		3.1	20	8.2	M1	3.2
1032.7		34	240	94	M1	35

† Calculated from the intensity of the L_{II} line.

with a single-channel analyser, equiped with a 1″×1″ NaI(Tl) crystal.

The resolution of the 662 keV gamma ray in Cs^{137} was 7.5 per cent. No gamma ray of energy higher than 1320 keV was observed. The relative gamma ray intensities obtained, corrected for the crystal efficiency according to the curve by Kahn and Lyon [13]), are tabulated in column 2 of table 3. The intensity of the K X-ray peak is arbitrarily set equal to 100.

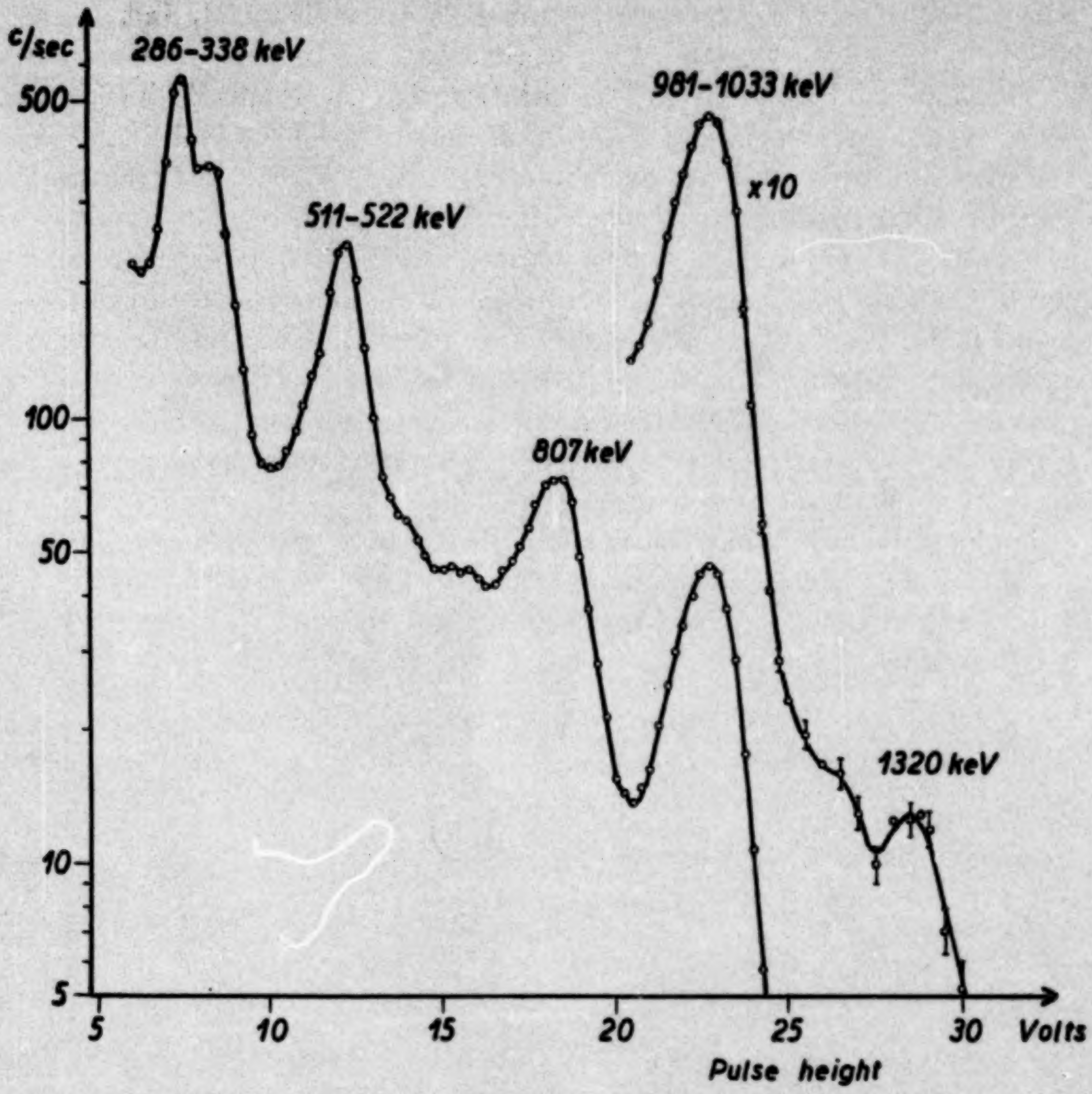

Fig. 3. High energy part of the scintillation spectrum from a freshly prepared Po^{206} sample, measured with a single-channel analyser.

On the basis of K/L ratios, L and M shell conversion coefficients [14]), and gamma intensities derived from experimental K line intensities and theoretical K conversion coefficients [12]), multipolarities have been assigned to the transitions listed in table 3. For comparison some calculated intensities for M1, E1 and E2 transitions are included in columns 3—5. All strong transitions, except that of energy 59.9 keV, seem to be of multi-

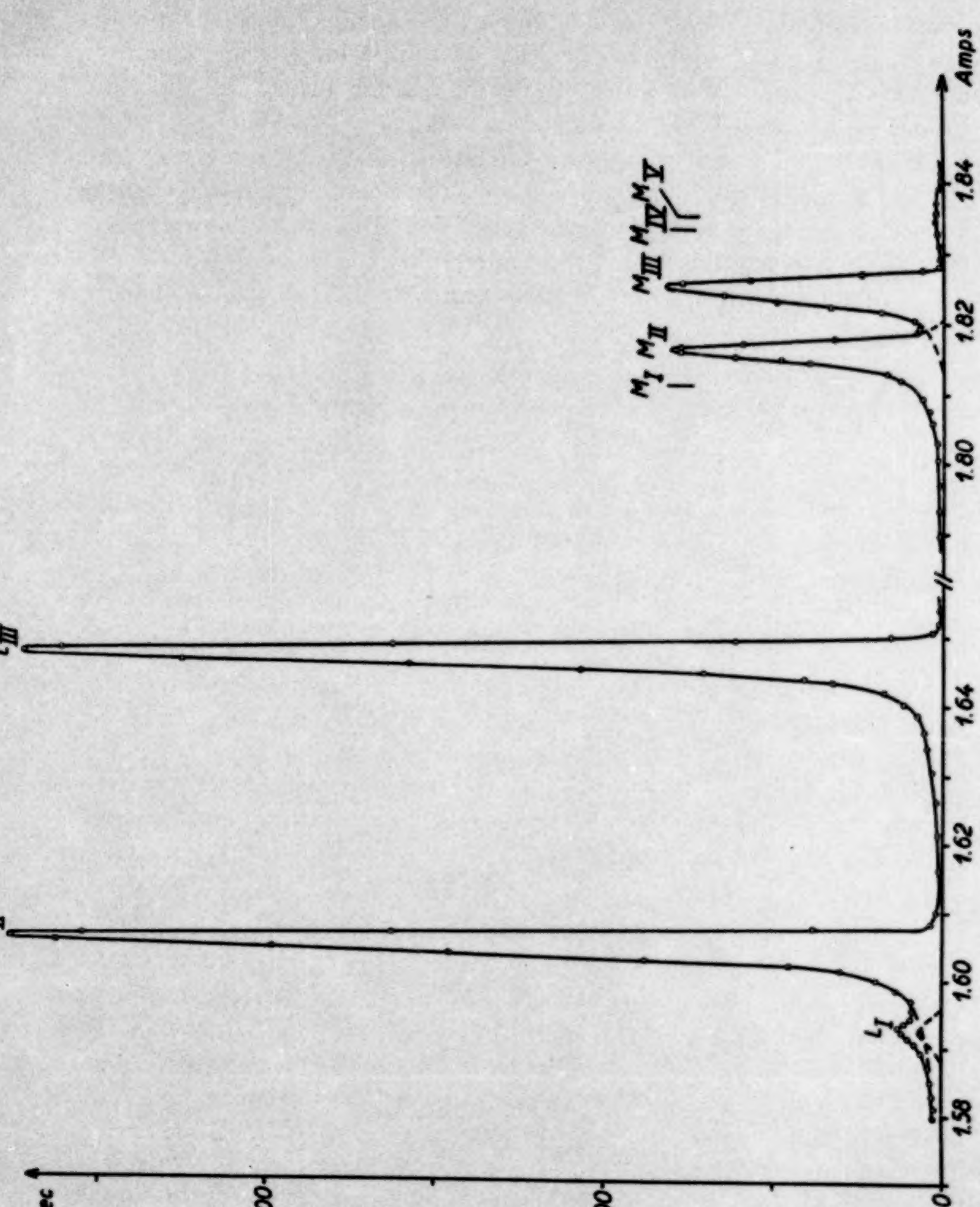

Fig. 4. L and M shell conversion lines of the 59.9 keV transition in the decay of Po^{206}, measured with 0.20 % resolution. Places were the M_I, M_{IV} and M_V lines should appear are indicated.

polarity M1 with a possible E2 admixture. The 463.5, 554.6 and 579.8 keV transitions are according to their large K/L ratios probably M1 or E1 transitions, and as they are not seen in the gamma-ray spectrum, the assignment M1 is most reasonable. The transition intensities (column 7) are derived with the assumption of pure M1, though a small E2 admixture cannot be excluded.

The 59.9 keV transition is predominantly converted in the L_{II}, L_{III}, M_{II} and M_{III} subshells (cf. fig. 4) and should accordingly be classified as an electric multipole transition. The experimental L and M line ratios are tabulated in table 4 together with the corresponding theoretical ratios [14]), derived for different electric multipoles and $Z = 85$. The small difference in Z-value is not assumed to introduce any appreciable errors in the ratios. The agreement between experimental and theoretical E2 ratios is convincing. Though the L line ratios seem to be less conclusive in this case, the M_{III}: $(M_{IV}+M_V)$ ratio strongly supports the assignment of multipolarity E2 to the 59.9 keV transition.

TABLE 4

Experimental and theoretical L and M line ratios for the 59.9 keV transition

	Multipolarity	$L_I : L_{II} : L_{III}$	$M_I : M_{II} : M_{III} : (M_{IV}+M_V)$
Experimental		$(0.030\pm0.006) : (1.08\pm0.10) : 1$	$(<0.05) : (1.02\pm0.10) : 1 : (<0.04)$
Theoretical	E2	0.034 : 1.13 : 1	0.037 : 1.04 : 1 : 0.034
	E3	0.036 : 1.21 : 1	0.041 : 1.22 : 1 : 0.22
	E4	0.035 : 1.28 : 1	0.040 : 1.35 : 1 : 1.38
	E5	0.032 : 1.30 : 1	0.038 : 1.51 : 1 : 4.50

2.4. COINCIDENCE MEASUREMENTS

Electron-electron coincidence measurements were performed with the double lens spectrometer at the Physics Department [3]). The transmission of each spectrometer was adjusted to about 3 per cent, corresponding to a resolution of about 2.5 per cent with a source of 2 mm diameter.

Freshly prepared sources were used in every case where the Bi^{206} lines were expected to interfere. For intensity reasons only about 30 of the 300 possible combinations were investigated. In cases where the conversion lines were well resolved in both spectrometers the coincidence rate was measured only for the peaks of the lines. In several cases of unresolved lines, however, the whole line had to be measured in order to decide which component was really in coincidence, as illustrated by fig. 5.

The coincidence information obtained from 6 sources of different strengths are summarized in table 5. The genuine coincidence rate N_{cg} (column 4) is obtained by subtraction of the random coincidence rate from the measured coincidence rate. The random rate was directly measured by introducing in one spectrometer channel a time delay long compared to the resolving time of the coincidence circuit. The errors in N_{cg} are pure statistical errors.

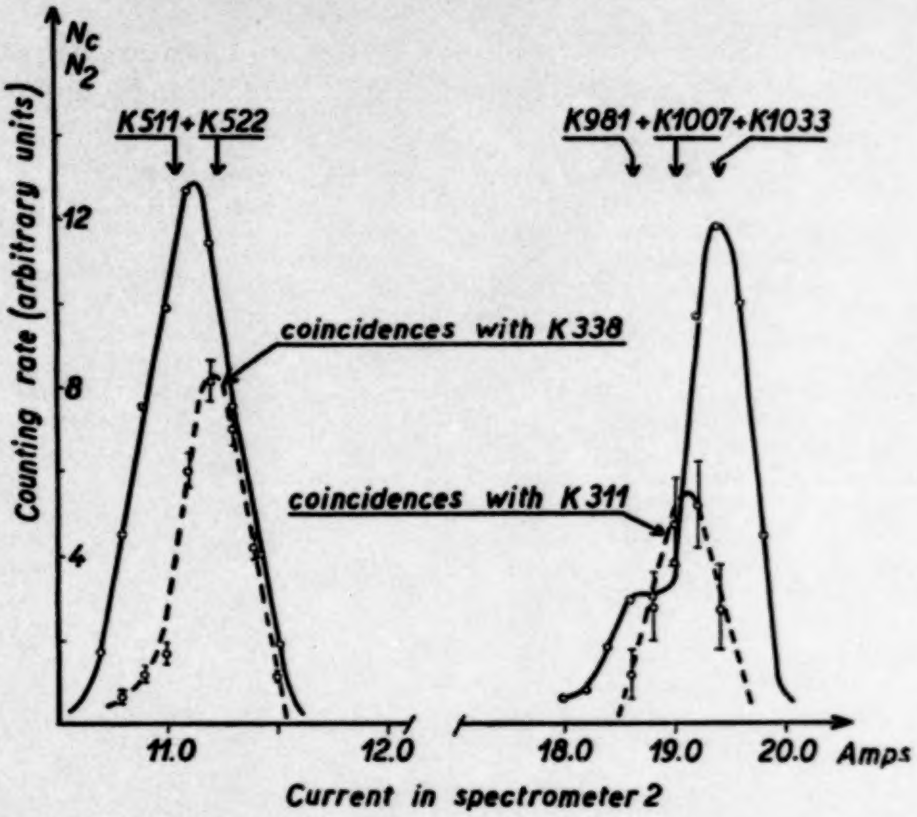

Fig. 5. Coincidence lines in Po^{206} (dotted lines), measured in the coincidence spectrometer with a resolution of about 3 %. The K lines of the 311 and 338 keV transitions are focused in spectrometer 1, while spectrometer 2 is scanning over the K lines of the 511 – 522 and 981 – 1033 keV transitions respectively. The full curves correspond to counting rate in spectrometer 2.

Only weak coincidence effects were obtained with the strong 59.9 keV transition, probably due to the low efficiency of the detectors at this electron energies [15]). The M+N lines could hardly be resolved from the dark current pulses of the photomultiplier. In an attempt to measure the lifetime of the 59.9 keV transition relative to the 286.5 keV transition in the coincidence spectrometer no delayed coincidences were observed. This indicates a half-life for the 59.9 keV transition less than the resolving time of the coincidence circuit ($\approx 10^{-7}$ sec). On account of the poor statistics, however, no definite conclusion can be made.

The coincidence results were analysed using the treatment given by Gerholm [15]). If the efficiencies of the detectors and coincidence circuit are assumed to be 100 per cent (valid for electron energies above about 100 keV) and angular correlation effects are neglected, simplified expressions for the genuine coincidence counting rate N_{cg} can be written

$$N_{cg} \approx N_1 \delta_2 \varkappa_2 \omega_2 \approx N_2 \delta_1 \varkappa_1 \omega_1, \tag{2}$$

where indices 1 and 2 refer to transition 1 (detected in spectrometer 1) and transition 2 (detected in spectrometer 2) respectively, N_1 and $\varkappa_1$ are counting rate and conversion probability [15] respectively for the line of transition 1 focused in spectrometer 1, N_2 and $\varkappa_2$ are counting rate and conversion

TABLE 5

Electron-electron coincidences in the decay of Po^{206}

No.	Transition energy, the conversion line of which is focused in:		N_{cg} c/min [1]	Assumed		Calculated δ_1 or δ_2 (%)	Estimated δ_1 or δ_2 (%)
	spectrometer 1	spectrometer 2		$\varkappa_1$	$\varkappa_2$		
1	59.9	282.1+286.5	2.2±0.7	0.19		1.5±0.6	100
2	59.9	311.5	3.3±0.8	0.19		2.7±0.8	100
3	59.9	338.4	2.5±0.8	0.19		1.6±0.6	100
4	59.9	511.4+522.4	4.8±1.3	0.19		2.2±0.8	100
5	59.9	807.6	0.6±0.3	0.19		1.7±0.9	100
6	59.9	1007.6+1032.7	0.5±0.5	0.19		1.7±1.7	100
7	170.8+171.5	282.1+286.5	5.0±0.9				
8	170.8+171.5	311.5	1.8±0.5		0.25	14 ±2[2]	25
9	170.8+171.5	338.4	3.8±1.2		0.21	3 ±1	
10	170.8+171.5	511.4+522.4	0.9±0.4				
11	282.1	311.5	3.0±0.9		0.25	30 ±9	25
12	282.1+286.5	463.5	5.9±0.9		0.10	1.9±0.5	
13	282.1+286.5	511.4+522.4	3.0±1.4				
14	282.1+286.5	807.6	1.3±0.7		0.027	0.2±0.1[3]	
15	286.5	338.4	3.2±1.4		0.21	0.6±0.3	
16	286.5	1032.7	17.4±2.0		0.014	58 ±8	90
17	311.5	338.4	11.9±1.4		0.21	10 ±3	20
18	311.5	463.5	7.6±0.9		0.10	12 ±2	
19	311.5	522.4	5.9±0.9		0.081	11 ±2	
20	311.5	807.6	0.2±0.3		0.027	3 ±5	
21	311.5	1007.6	2.6±0.6		0.016	31 ±8	55
22	338.4	463.5	3.6±0.7		0.10	1.6±0.4	
23	338.4	522.4	81.5±4.5	0.21		63 ±5	100
24	338.4	807.6	0 ±0.2	0.21		<2	0
25	338.4	980.9	5.1±0.8	0.21		44 ±8	100
26	338.4	1032.7	0 ±0.5	0.21		<5	0
27	511.4+522.4	463.5	1.2±0.5	0.084		9 ±4	
28	511.4	522.4	0 ±0.9	0.084		<2	0
29	511.4	807.6	15.5±1.6		0.027	56 ±11	<100
30	511.4+522.4	1007.6+1032.7	0 ±0.2	0.084		<3	0
31	807.6	1007.6+1032.7	0 ±0.2	0.027		<4	0

[1] The errors in N_{cg} and δ are statistical errors.

[2] 170.8−311.5 assumed to be responsible for the effect.

[3] 286.5−807.6 assumed to be responsible for the effect.

probability for the line of transition 2 focused in spectrometer 2, ω_1 and ω_2 are solid angles of spectrometer 1 and 2 respectively. δ_1 is the fraction of transition 2 in coincidence with transition 1 and δ_2 is the fraction of transition 1 in coincidence with transition 2.

With the use of (2) some δ values have been calculated. In column 5 of table 5 $\varkappa_1$ or $\varkappa_2$ ($\varkappa = \alpha_{\mathrm{line}}/(1+\alpha_{\mathrm{tot}})$) are derived in accordance with the multipolarity assignments of table 3. The corresponding δ values are included in column 6. In the calculations the peak counting rates were used for N_1 (or N_2) and N_{cg} and the ω value was estimated from the spectrometer adjustment [15]. The δ values will be further discussed in section 3.2.

3. Construction of the Decay Scheme

3.1. ENERGIES OF THE EXCITED LEVELS

From the alpha-decay of At^{210} levels in Bi^{206} are indicated at 82 and 164 keV. Gamma transitions of about these energies were found in the conversion spectrum. These transitions being weak, however, attention was paid to the strong transitions and possible energy sum relations as a starting point for the construction of the decay scheme.

TABLE 6

Possible cross over relations in Bi^{206}

Sum no.	E_1 (keV)	E_2 (keV)	E_1+E_2 (keV)	E_3 (keV)	$E_1+E_2-E_3$ (keV)	Agreement with the proposed level scheme
1	140.6	170.8	311.4	311.5	−0.1	No
2	286.5	522.4	808.9	807.6	+1.3	No
3	338.4	469.1	807.5	807.6	−0.1	Yes
4	282.1	579.8	861.9	861.6	+0.3	Yes
5	338.4	522.4	860.8	861.6	−0.8	No
6	311.5	669.0	980.5	980.9	−0.4	Yes
7	511.4	469.1	980.5	980.9	−0.4	Yes
8	338.4	669.0	1007.4	1007.6	−0.2	Yes
9	170.8	861.6	1032.4	1032.7	−0.3	Yes
10	171.5	861.6	1033.1	1032.7	+0.4	No
11	354.8	677.8	1032.6	1032.7	−0.1	No
12	511.4	522.4	1033.8	1032.7	+1.1	No
13	286.5	1032.7	1319.2	1320.0	−0.8	Yes
14	311.5	1007.6	1319.1	1320.0	−0.9	Yes
15	338.4	980.9	1319.3	1320.0	−0.7	Yes
16	511.4	807.6	1319.0	1320.0	−1.0	Yes

In table 6 all pairs of gamma rays are summarized, the sum energies of which differ by less than 2 parts in 1000 from the energy of a third gamma ray. This procedure is justified according to the accuracy of the energy measurements. When compared with the coincidence information in table 5, the sums nos. 2 and 12 seem to be accidental. Sums nos. 13—16 all add up to about 1319 keV and are verified by coincidence results. Further, the unobserved or weak coincidence coupling between transitions of the different pairs and the fact that no gamma ray of energy higher than 1320 keV was observed strongly support the placement of these four cascade pairs in parallel.

The only strong transitions which do not occur in the sums nos. 13—16 are those of energies 59.9 and 522.4 keV. Due to the intensity and observed

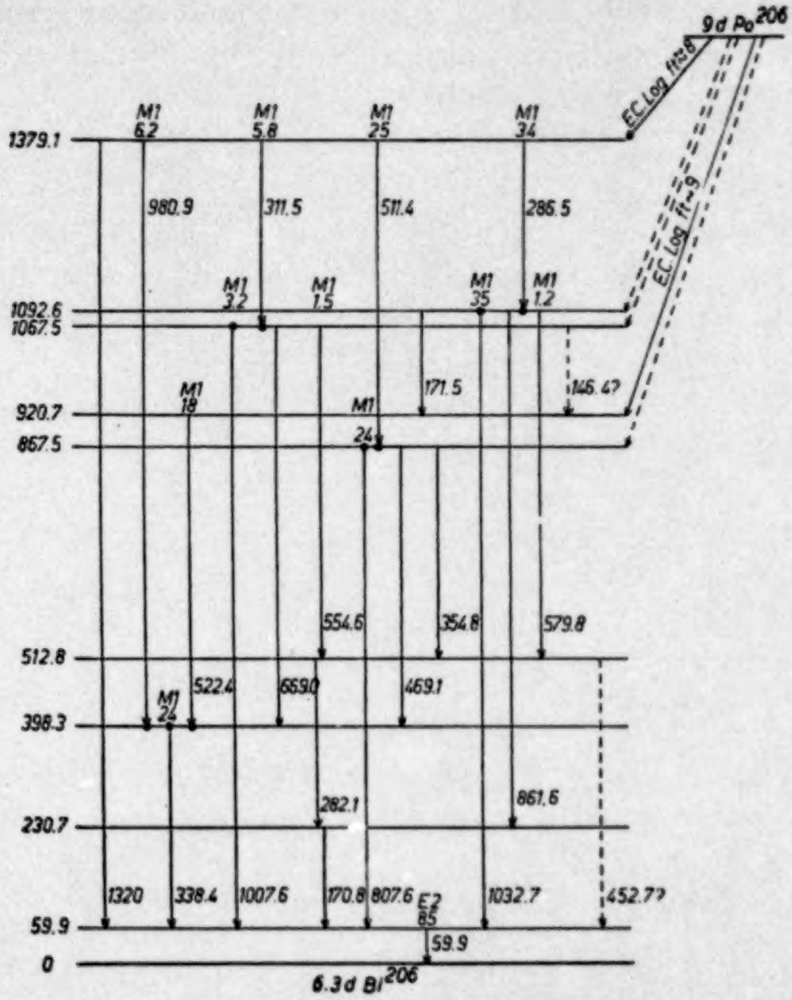
9d Po^{206}
EC Log ft≈8
EC Log ft≈9
1379.1
M1 6.2
M1 5.8
M1 25
M1 34
980.9
311.5
511.4
286.5
1092.6
1067.5
M1 3.2
M1 1.5
M1 35
M1 1.2
920.7
867.5
M1 18
M1 24
171.5
146.4?
554.6
354.8
579.8
512.8
522.4
669.0
469.1
M1 24
398.3
282.1
861.6
230.7
1320
338.4
1007.6
170.8
807.6
E2 85
1032.7
452.7?
59.9
59.9
0
6.3d Bi^{206}

Fig. 6. Proposed decay scheme of Po^{206}. Established coincidences are indicated by large dots. At the head of some transitions the multipolarities and intensities in per cent per disintegration are given. Dotted lines correspond to uncertain transitions.

coincidences, the 59.9 keV transition must either follow or be followed by the 1319 keV cascade transitions. As the 59.9 keV transition is not included in any sum relation and no definite conclusions can be made from the intensity or coincidence information, its position in the decay scheme is difficult to determine from the experimental results obtained so far.

If the 59.9 keV transition is assumed to precede the 1319 keV cascade transitions, then according to the measurements by Stoner 7), the half-life of the 59.9 keV transition should be less than 2×10^{-9} sec. However, from experimental lifetime measurements of E2 transitions in nuclei near the double-closed shell in Pb^{208} 16), as well as from theoretical transition probabilities 17) derived on the basis of the single particle model, a longer half-life may be expected. Recently a half-life of 9×10^{-9} sec has been measured for the 148 keV E2 transition in the odd-odd nucleus Tl^{200} 18). A half-life $> 2 \times 10^{-9}$ sec for the 59.9 keV transition seems therefore probable. Mainly for this reason the 59.9 keV transition is assumed to de-excite a low level at 59.9 keV in the proposed decay scheme of fig. 6. Measurements of its half-life relative to some of the other strong transitions, if possible, would determine its position in the scheme [†].

With the assumption of the low level at 59.9 keV, then, in order to allow for the sum relations nos. 13—16, there must be a strongly excited level at 1379 keV with some intermediate levels. To establish the succession of the transitions in the sum pairs, attention was focused on the sum no. 15 and the strong coincidence effect no. 23. For intensity reasons the 980.9 and 522.4 keV transitions are assumed to precede the 338.4 keV transition, thus giving the levels of energies 398.3 and 920.7 keV. The 1067.5 keV level is then proposed in accordance with the sum relations nos. 6, 8 and 14 together with the coincidence results nos. 17, 19 and 21. Further the 286.5 and 511.4 keV transitions are assumed to precede the 1032.7 and 807.6 keV transitions respectively on account of the weak observed coincidences nos. 7, 8 and 15 and the sum relations nos. 3 and 7. If the energy sum 7 is real, then a weak coincidence effect between the 338.4 and 511.4 keV transitions should be found. Though quite possible (cf. fig. 5) the existence of such an effect is difficult to establish on account of the strong coincidence between the 338.4 and 522.4 keV transitions.

Besides the levels of energies 59.9, 398.3, 867.5, 920.7, 1067.5, 1092.6 and 1379.1 keV already discussed, two additional weakly excited levels at 230.7 and 512.8 keV can be proposed in accordance with the sum relations nos. 4 and 9 and partial coincidence informations.

Of the transitions listed in table 1 there are 6 of energies 82.9, 117.6, 140.6, 463.5, 645.6 and 677.8 keV, most of them being weak, which are not included in the decay scheme. The only one for which some coincidence results are obtained is that of 463.5 keV energy. Since it, however, does not occur in any energy sum relation, its position in the scheme is uncertain. As indicated by the unplaced transitions and the numerous unassigned lines of table 2, other weakly excited levels are probable. Considering the intensities of the placed transitions one may infer that only a few per cent of the disintegrations take place via these undetermined levels. In order to study them, however, stronger sources than those used in this investigation are needed.

[†] *Note added in proof:* A half-life of 7.5 μsec for the 59.9 keV transition has now been measured (E. Arbman and P. A. Tove, in course of publication).

3.2. AGREEMENT WITH THE COINCIDENCE RESULTS

The decay scheme, as constructed in the preceding section, was based on energy sum relations, qualitative coincidence information and intensity considerations. Its agreement with the results of the analysis of the coincidence information (column 6 of table 5) may now be examined. In column 7 the δ values corresponding to those of column 6 have been roughly estimated from the level scheme in cases where the gamma ray intensities are measured or can be estimated.

The calculated δ values for cases where positive coincidence effects were obtained are smaller than the estimated ones. Less importance should be attached to the results concerning the 59.9 keV transition (cf. section 2.4). Somewhat low δ values, calculated according to the expressions (2) are, however, to be expected due to possible unobserved branches. The relations (2) are further derived with the assumption of optimum working conditions of the spectrometer, while the measurements were performed with the primary aim of obtaining qualitative coincidence information and therefore no efficiency check was made with the sources used. Thus the coincidence results seem to be reasonably consistent with the proposed decay scheme.

According to the positive coincidence effect between the 311.5 and 522.4 keV transitions (no. 19 of table 5) a weak branch between the 1067.5 and 920.7 keV levels must be postulated. Conversion lines which may be assigned as the L_I and M_I lines of a possible 146.4 keV gamma ray were found in the conversion spectrum (cf. table 2). The K line which should appear in the vicinity of the M_I line of the 59.9 keV transition was not observed. For intensity reasons, further, there should be a by-pass branch from the 512.8 keV level, which may be identical with the possible 452.7 keV transition (table 2). These transitions are dotted in the decay scheme.

If the δ values are known, the relations (2) can be used to derive the $\varkappa$'s

TABLE 7

Comparison between theoretical K conversion coefficients and the experimental lower limits for the 338.4, 511.4, 807.6 and 1032.7 keV transitions

Transition energy (keV)	Experimental	Theoretical α_K for multipolarity			
		E1	E2	M1	M2
338.4	$\geqq 0.16 \pm 0.01$	0.019	0.052	0.29	0.92
511.4	$\geqq 0.060 \pm 0.007$	0.0079	0.021	0.092	0.25
807.6	$\geqq 0.015 \pm 0.002$	0.0034	0.0085	0.028	0.069
1032.7	$\geqq 0.0081 \pm 0.0011$	0.0021	0.0053	0.015	0.034

and thus the conversion coefficients of the transitions concerned [15]). Table 7 gives the lower limits of the K conversion coefficients for the 338.4, 511.4, 807.6 and 1032.7 keV transitions, calculated from the coincidence results nos. 16, 23 and 29 with the assumption of $\delta \leqq 100$ per cent. The K conversion coefficients [12]) for multipolarities E1, E2, M1 and M2 are included for comparison. It is evident from the table that for the transitions concerned the multipolarities E1 and E2 must be considered improbable. Here again the coincidence results support the assignment of predominantly M1 to these transitions.

4. Discussion

The results obtained in this investigation are mainly in agreement with those reported by Stoner [7]). Of the 11 gamma rays reported by him, all but the one of energy 472 keV were found here. Furthermore, the qualitative gamma-gamma coincidence results obtained by Stoner, except the weak coincidence effect between the (511+522) and 1031 keV gamma rays, are understood when the decay scheme in fig. 6 is considered. In some points, however, the results disagree. The 807 and 1031 keV transitions were assigned multipolarities E2 by Stoner, while according to this investigation they should be mainly M1 transitions (cf. sections 2.3 and 3.2); in addition, the excited levels of energies 1369 and 1840 keV, proposed by Stoner on the basis of the gamma-gamma coincidences, are in contradiction to the more conclusive electron-electron coincidence measurements performed in this work.

The Bi^{206} nucleus has one proton beyond the closed shell of 82 protons and three neutron holes in the 126 shell. Hence coupling between the odd proton and possible neutron configurations may give rise to numerous excited levels. Theoretical calculations of the energy levels in Bi^{206} by the methods introduced by Pryce [19]) and on the basis of the single particle model are now being performed in order to attempt to correlate the experimental levels with the theoretical predictions [20]).

Although the assignment of spin to the different levels is difficult from the experimental data alone, the possible ground state spin of Bi^{206} will be briefly discussed. It is reasonable to assume the 83rd proton in Bi^{206} to be in the $h_{9/2}$ level, and the neutron configuration in the ground state to be the same as that of Pb^{205}. According to the recent investigation by Schmorak *et al.* [21]), the ground state spin of Pb^{205} is most probably 5/2−, due to the configuration $f_{5/2}^{-1}\ p_{1/2}^{-2}$. Then a high ground state spin in Bi^{206} ($\leqq 7$) with even parity is predicted by Nordheim's "weak" rule[22]).

Since no positons were observed in the decay of Po^{206}, the total decay energy is not accurately known. A rough estimate of a decay energy of 3.1±0.6 MeV was, however, made from the masses of Pb^{202} and Bi^{206} given by Huizenga [23]) and the alpha-energy of 5.218 MeV [24]) in the alpha-decay of Po^{206}. According to the proposed level scheme, the electron capture should predominantly feed the level at 1379 keV. By the use of the nomograph of Moszkowski [25]) the log *ft* value for capture to this level is estimated to be 7.9. Though this log *ft* value is high, it seems reasonable to classify the electron capture decay to the 1379 keV level as an allowed transition[26, 27]). Since the ground state of the even-even Po^{206} nucleus in accordance with nuclear shell systematics should have spin 0 with even parity, the spin of the 1379 keV level is probably 0+ or 1+. According to the proposed level scheme and the multipolarities of the transitions concerned, the spin difference between the ground state and the 1379 keV level should be $\leqq 4$. From the experimental results therefore a spin $\leqq 5$ for the ground state of Bi^{206} seems probable.

The author is much indebted to Professor The Svedberg, the head of the institute, for his interest in this work and for the various facilities put at my disposal. I also wish to express my thanks to Professor Kai Siegbahn at the Physics Department, University of Uppsala, for the opportunity of using the coincidence spectrometer, and to Dr. T. R. Gerholm for instructions and valuable suggestions concerning the coincidence investigations. Furthermore stimulating contact with Dr. I. Bergström at the Nobel institute of Physics, Stockholm, is gratefully acknowledged.

This investigation was financially supported by the Swedish Atomic Energy Commission. The support as well as the permission to publish the results is gratefully acknowledged.

References

1) S. Rosenblum and H. Tyrén, Compt. Rend. **239** (1954) 1205
2) E. Arbman and N. Svartholm, Arkiv Fysik **10** (1956) 1
3) T. R. Gerholm, Rev. Sci. Instr. **26** (1955) 1069
4) D. H. Templeton, J. J. Howland, Jr. and I. Perlman, Phys. Rev. **72** (1947) 758
5) F. F. Momyer, Jr. and E. K. Hyde, J. Inorg. Nuclear Chem. **1** (1955) 274
6) F. Asaro, UCRL-2180 (1953)
7) A. W. Stoner, UCRL-3471 (1956)
8) Mme Joliot-Curie, Les Radioéléments Naturels (Paris, 1946) Chapitre XII
9) D. E. Alburger and M. H. L. Pryce, Phys. Rev. **95** (1954) 1482
10) R. D. Hill, E. L. Church and J. W. Mihelich, Rev. Sci. Instr. **23** (1952) 523
11) D. Saxon, Phys. Rev. **81** (1951) 639
12) Sliv and Band, privately circulated tables
13) B. Kahn and W. S. Lyon, Nucleonics **11**, no. 11 (1953) 61
14) M. E. Rose *et al.*, privately circulated tables
15) T. R. Gerholm, Arkiv Fysik **11** (1956) 55
16) A. W. Sunyar, Phys. Rev. **98** (1955) 653
17) S. A. Moszkowski, Beta- and Gamma-Ray Spectroscopy, Ed. Kai Siegbahn (North-Holland Publishing Co., 1955) Ch. XIII
18) I. Bergström, private communication.
19) M. H. L. Pryce, Proc. Phys. Soc. A **65** (1952) 773

20) S. Wahlborn, Nuclear Physics **3** (1957) 644
21) M. Schmorak, R. Stockendal, J. A. McDonell, I. Bergström and T. R. Gerholm, Nuclear Physics **2** (1956/57) 193
22) L. W. Nordheim, Rev. Modern Phys. **23** (1951) 322
23) J. R. Huizenga, Physica **21** (1955) 410
24) J. M. Hollander, I. Perlman and G. T. Seaborg, Rev. Modern Phys. **25** (1953) 469
25) S. A. Moszkowski, Phys. Rev. **82** (1951) 35
26) J. W. Mihelich, A. W. Schardt and E. Segrè, Phys. Rev. **95** (1954) 1508
27) M. H. L. Pryce, Nuclear Physics **2** (1956/57) 226

Nuclear Physics **3** (1957) 644—648; *North-Holland Publishing Co., Amsterdam*

LEVELS in $\mathbf{Bi^{206}}$

S. WAHLBORN

Division of Mathematical Physics, Royal Institute of Technology, Stockholm

Received 4 April 1957

Abstract: A theoretical investigation has been made of energy levels in Bi^{206} following the same principles as used by Pryce. Recent experimental results for the decay scheme of Bi^{206} have been interpreted according to the theoretical results.

From the point of view of the shell model, the neutron deficient Bi-isotopes (with energies lower than the core excitation energy) consist of a rigid, spherical core (collective effects being neglected) plus one proton and a number of neutron holes, all these extra particles occupying nuclear shells [1]) between the magic numbers 82 and 126, namely

$$1h_{9/2},\ 2f_{7/2},\ 1i_{13/2},\ 3p_{3/2},\ 2f_{5/2},\ 3p_{1/2}.$$

The corresponding single-particle energies for neutrons have been accurately measured [2]) in Pb^{207}. For protons the data are as yet uncertain: Two excited levels have been observed [3]) in Bi^{209} (ground state 9/2—) at about 0.90 and 1.56 MeV; we identify them with the first two excited levels, e_1 and e_2, and give them the assignments $f_{7/2}$ and $i_{13/2}$ resp. (in good agreement with shell model calculations [4])).

Pryce [5–7]) has treated nuclei in the Pb^{208}-region with δ-force interaction between the extra particles (assuming the ratio between triplet and singlet potential strengths to be 1.5); see also ref. [8]). In general, the theoretical energy levels are calculated by diagonalizing (in some approximate way) the energy matrix obtained from the shell model and *jj*-coupling. The resulting algebraic expressions for the energies involve known quantities and central force radial integrals. If configuration interaction is neglected, and the δ-force approximation is used, all the radial integrals reduce to the configuration parameters ε_{ik} (denoted $-\varepsilon_S$ in ref. [5])). Pryce [7]) gives some of the ε_{ik}'s as calculated from Pb^{206}-data. If we interpolate between Pryce's values (assuming j-independence and smooth l-dependence), we get for the cases $ik = (n_i l_i,\ n_k l_k) = (3p,\ 1h)$ and (2f, 1h), the values $\varepsilon_{ik} \approx 0.20$ and 0.23 MeV resp. (in qualitative agreement with results for a harmonic oscillator central field [9, 10])).

With the above assumptions, some calculations have been made for the isotope Bi^{206} (constancy of parameters also assumed, cf. ref. [9])). The shell model configurations and their degeneration properties are shown in table 1.

The great complexity, even at rather low zero-order energies, and the large level density, are obvious facts, preventing in practice an explicit, numerical resolution of all but the simplest configurations. In view of all the approximations made, a detailed treatment is also rather meaningless, especially as configuration mixing, which is a very important effect [7, 11]), cannot be rigorously accounted for.

TABLE 1

Configurations of Bi^{206}

Configuration (three neutron holes plus one proton)	No.	Zero-order Energy (MeV)	Parity	Spin-values (exponents = multiplicities)
$(p_{1/2})^2\ f_{5/2}\ h_{9/2}$	Ih	0	+	2, 3, 4, 5, 6, 7
$(p_{1/2})^2\ p_{3/2}\ h_{9/2}$	IIh	0.32	+	3, 4, 5, 6
$p_{1/2}\ (f_{5/2})^2\ h_{9/2}$	IIIh	0.57	+	$0,\ 1^2,\ 2^3,\ 3^4,\ 4^5,\ 5^5,\ 6^4,\ 7^3,\ 8^2,\ 9$
$p_{1/2}\ f_{5/2}\ p_{3/2}\ h_{9/2}$	IVh	0.89	+	$0,\ 1^3,\ 2^5,\ 3^7,\ 4^8,\ 5^8,\ 6^7,\ 7^5,\ 8^3,\ 9$
$(p_{1/2})^2\ i_{13/2}\ h_{9/2}$	Vh	1.06	—	2, 3, 4, 5, 6, 7, 8, 9, 10, 11
$(f_{5/2})^3\ h_{9/2}$	VIh	1.14	+	$0,\ 1,\ 2^2,\ 3^3,\ 4^3,\ 5^3,\ 6^3,\ 7^2,\ 8,\ 9$
$p_{1/2}\ (p_{3/2})^2\ h_{9/2}$	VIIh	1.21	+	$2,\ 3^2,\ 4^3,\ 5^3,\ 6^2,\ 7$
$(f_{5/2})^2\ p_{3/2}\ h_{9/2}$	VIIIh	1.46	+	$0,\ 1^4,\ 2^6,\ 3^8,\ 4^9,\ 5^9,\ 6^8,\ 7^6,\ 8^4,\ 9^2,\ 10$
$p_{1/2}\ f_{5/2}\ i_{13/2}\ h_{9/2}$	IXh	1.63	—	$0^2,\ 1^5,\ 2^7,\ 3^9,\ 4^{11},\ 5^{12},\ 6^{12},\ 7^{12},\ 8^{12},$ $9^{11},\ 10^9,\ 11^7,\ 12^5,\ 13^3,\ 14$
$(p_{1/2})^2\ f_{5/2}\ f_{7/2}$	If	$e_1 \approx$ 0.90	+	1, 2, 3, 4, 5, 6
$(p_{1/2})^2\ p_{3/2}\ f_{7/2}$	IIf	1.22	+	· 2, 3, 4, 5
$p_{1/2}\ (f_{5/2})^2\ f_{7/2}$	IIIf	1.47	+	$0,\ 1^3,\ 2^4,\ 3^5,\ 4^5,\ 5^4,\ 6^3,\ 7^2,\ 8$
$(p_{1/2})^2\ f_{5/2}\ i_{13/2}$	Ii	$e_2 \approx$ 1.56	—	4, 5, 6, 7, 8, 9

The first-order energies (i.e. with configuration interaction neglected) are given in the third column of table 2. In the simplest cases they have been explicitly calculated, but in most cases the energies (or, properly speaking, the diagonal elements of the energy matrix) have been estimated by considering the probable effect of coupling a proton-configuration to the first-order levels [7]) of Pb^{205}, and thereby using some obvious regularities (for example that the interaction energy between the extra proton and the neutron-holes is always positive). In the fourth column a proposed level distribution is given. Attempts have been made to account for configuration interaction in a qualitative way, i.e. essentially by inductive reasoning and comparison with known facts about Pb-isotopes [6, 7, 11, 12]). (In the case of the estimated first-order levels one should also notice the effect of the previously neglected non-diagonal elements). It is assumed, that the lowest levels (belonging to the configuration $(p_{1/2})^2 f_{5/2} h_{9/2}$) get an energy shift due to configuration mixing of about 0.5 MeV. The zero-point for the energy in the fourth column of table 2 has been shifted by the same amount (the lowest first-order energy, i.e. the level 6+, is nearly equal to 0). The result should be regarded as highly tentative.

TABLE 2

Level distribution for Bi^{206}

Conf. No. 1)	Spin and Parity	First-order Energy 2) MeV 4)	Proposed and Experimental Levels 3) MeV 4)
Ih	6+	$\underline{0.01}$	0 A
Ih	4+	$\underline{0.11}$	0.0599 B
Ih	5+	$\underline{0.25}$	0.2307 C
Ih	3+	$\underline{0.23}$	0.3983 D
IIh	5+	$\underline{0.29}$	0.4
IIh	4+	$\underline{0.36}$	0.5128 E
Ih	7+	$\underline{0.49}$	0.5
IIh	6+	$\underline{0.52}$	0.6
IIh	3+	$\underline{0.67}$	0.8675 F
Ih	2+	$\underline{0.61}$	0,9207 G
IIIh	4+	0.7	1.0
IIIh	5+	0.7	1.0
IIIh	3+	0.8	1.0675 H
IVh	3+	1.0	1.0926 I
IIIh	7+	0.7	1.1
IIIh	6+	0.8	1.1
Vh	10—	1.1	1.1
IIIh	1+	$\underline{0.82}$	1.2 x5)
IIIh	4+	0.8	1.2
If	5+	$\underline{1.12}$	1.2
Vh	8—	1.2	1.2
IIIh	2+	1.1	1.3 y5)
IIIh	4+	0.9	1.3
IVh	4+	1.1	1.3
IIIh	5+	0.9	1.3
IVh	5+	1.1	1.3
IIIh	6+	0.9	1.3
IVh	6+	1.1	1.3
IIIh	8+	1.0	1.3
Vh	5—	1.3	1.3
Vh	6—	1.3	1.3
IVh	2+	1.3	1.3791 J
If	3+	$\underline{1.28}$	1.4
IIIh	3+	1.1	1.4
If	4+	$\underline{1.36}$	1.4
VIh	4+	1.1	1.4
VIh	5+	1.2	1.4
IVh	7+	1.0	1.4
IVh	8+	1.1	1.4
Vh	4—	1.4	1.4
Vh	7—	1.4	1.4
IVh	1+	1.3	1.5
If	2+	$\underline{1.45}$	1.5
VIh	3+	1.2	1.5
IVh	3+	1.2	1.5
IVh	4+	1.2	1.5
IIf	4+	1.3	1.5
IIIh	5+	1.0	1.5
IVh	5+	1.2	1.5
VIh	6+	1.1	1.5
Vh	3—	1.5	1.5
Vh	9—	1.5	1.5
(IIIh	0+	$\underline{1.32}$	> 1.5
IIIh	1+	$\underline{1.45}$	> 1.5
If	1+	$\underline{2.16}$	> 1.5
If	6+	$\underline{1.58}$	> 1.5
IIIh	9+	$\underline{1.52}$	> 1.5)

1) According to table 1. The number concerns the essential configuration (the real states are mixed).

2) The underlined values are results of first order perturbation calculation. The other values are roughly-estimated diagonal elements of the energy matrix.

3) The experimental values (for the sake of reference denoted by A, B, . . ., J) are taken from ref. 13), as is also the following information. The levels preferably populated in the electron-capture from Po^{206} seem to be J and G. The following multipolarities have been observed:

J → I, J → H, J → F, J → D, I → E, I → B, H → E, H → B, G → D, F → B, D → B all M1; B → A E2; E → C probably M1; C → B M1 or E1.

4) In the third column the zero-point is the same as in table 1. In the fourth column the zero-point has been shifted by about 0.5 MeV (explained in the text).

5) The letters x and y refer to the text.

Ten levels (denoted A, . . ., J in table 2) have been directly identified with the ten levels given by Arbman [13]) in the decay-scheme of Bi^{206} obtained from the β-decay of Po^{206}. The present experimental results do not permit any definite assignments to be made [13]). Table 2 shows those identifications which, according to the theoretical results, are taken to be the most probable. No serious discrepancies seem to arise from this interpretation. Except for the levels denoted by x and y, all the proposed levels below 1.4 MeV that are not seen in the decay, have spin 4 or higher, and such positions that their absence (i.e. weakness) is explained. The levels x and y are probably energetically disfavoured for γ-transitions. The ground state spin 6 is well compatible with Pb^{206}-data [6]). All multipolarities (see note of table 2) fit into the scheme in a unique way, given the assignments of the lowest levels. The ground-state of Po^{206} is 0+ (configuration $(p_{1/2})^2$ $(f_{5/2})^2$ $(h_{9/2})^2$). Thus the assignment 2+ is implied for the levels J and G, as all transitions from them to A proceed via two M1 and one E2. The $\log ft$-values for the electron-capture of Po^{206} to J and G have been estimated [13]) to be about 8 and 9 resp. This does not exclude second forbiddenness [1]) (one should probably not be too strict with the connection between $\log ft$-values and selection rules for β-decay in this nuclear region [12])). The proposed levels x and y belong (essentially) to the configuration $p_{1/2}(f_{5/2})^2h_{9/2}$, giving $|\Delta l| = 4$ for β-decay. The levels J and G both belong to configurations of the type p^2fh, giving $|\Delta l| = 2$, which perhaps makes them more favoured. That higher low-spin levels are not attained in the decay of Po^{206}, may indicate that the energy available is not sufficiently large.

Finally, it should be mentioned that similar calculations have been made for the isotopes Bi^{207} and Bi^{208}, for which, however, no reliable experimental data have as yet been obtained (Bi^{207} is now in course of investigation [14])). We give some simple results of first-order calculations:

The ground state of Bi^{207} is 9/2−, and the first excited states are 11/2− (0.42 MeV), 7/2− (0.55 MeV), 9/2− (0.60 MeV), 13/2− (0.67 MeV), 5/2− (0.77 MeV).

The ground state of Bi^{208} is 4+, and the first excited states are 5+ (0.06 MeV), 6+ (0.39 MeV), 4+ (0.49 MeV), 3+ (0.62 MeV), 5+ (0.64 MeV).

A more detailed account of calculations and results for Bi-isotopes will appear later.

This work has been supported by the State Council of Technical Research.

References

1) M. G. Mayer and J. H. D. Jensen, Elementary Theory of Nuclear Shell Structure (John Wiley and Sons, New York, 1955)
2) D. E. Alburger and A. W. Sunyar, Phys. Rev. **99** (1955) 695
3) R. Kiehn and C. Goodman, Phys. Rev. **95** (1954) 989
4) K. Bleuler, private communication

5) M. H. L. Pryce, Proc. Phys. Soc. A **65** (1952) 773
6) D. E. Alburger and M. H. L. Pryce, Phys. Rev. **95** (1954) 1482
7) M. H. L. Pryce, Nuclear Physics **2** (1956/57) 226
8) W. W. True, Phys. Rev. **101** (1956) 1342
9) N. Zeldes, Nuclear Physics **2** (1956/57) 1
10) R. Thieberger, Nuclear Physics **2** (1956/57) 533
11) C. J. Herrlander, R. Stockendal, J. A. McDonell and I. Bergström, Nuclear Physics **1** (1956) 643
12) M. Schmorak, R. Stockendal, J. A. McDonell and I. Bergström, Nuclear Physics **2** (1956/57) 193
13) E. Arbman, Nuclear Physics **3** (1957) 625
14) E. Arbman, private communication

Nuclear Physics **3** (1957) 649—655; *North-Holland Publishing Co., Amsterdam*

DISPERSION RELATIONS FOR THE DECAY OF THE τ-MESON

E. CORINALDESI[†]

Dept. of Natural Philosophy, The University of Glasgow

Received 13 January 1957

Abstract: The kinematics of the τ-meson decay is formulated so as to make possible the use of dispersion relations for the transition amplitude.

1. Introduction

We have already pointed out [1]) that the amplitude for τ-meson decay is simply related to a causal amplitude $M_{\alpha\beta\gamma,\,k}$. The indices $_\alpha, {}_\beta, {}_\gamma$ take the values 1, 2, 3. On the other hand, the pairs of values 1, 2 and 3, 4 for $_k$ may be deemed to correspond to the two doublets (K^+, K^0) and (K^-, $\overline{K}^0$) in accordance with the view now generally held.

In the "natural" frame in which the energies of the π-mesons are equal, the causal amplitude satisfies the dispersion relation

$$M(\omega) = \frac{1}{i\pi}\,\mathrm{P}\int_{-\infty}^{\infty} \frac{M(\omega')}{\omega'-\omega}\,\mathrm{d}\omega'. \tag{1}$$

The variable ω is the energy of the τ-meson.

The proof of eq. (1) was outlined in ref. [1]) for an amplitude based on the matrix element $\langle 0|\mathbf{j}_\alpha(x_1)\mathbf{j}_\beta(x_2)\mathbf{j}_\gamma(x_3)\mathbf{J}_k(y)|0\rangle$, where $|0\rangle$ denotes the vacuum state, and $\mathbf{j}_\alpha(x)$ and $\mathbf{J}_k(y)$ the π-meson and τ-meson source densities in the Heisenberg picture [††].

This is the correct form for the amplitude if the interaction Hamiltonian is of the type $j_\alpha\phi_\alpha + J_k\Phi_k$, and the (interaction picture) operators ϕ_α and Φ_k commute with j_α and J_k, as is the case if the $\tau-\pi$ interaction arises from the coupling with a third field. The case when a contact $\tau-\pi$ interaction exists is treated briefly in the appendix. The amplitude is then characterized by the occurrence of products of four, three, two operators, giving energy dependent contributions, and by a contact term λ. The latter, which is proportional to the coupling constant of the contact interaction, remains constant when ω tends to infinity, thus invalidating (1). We shall discard as unlikely the possibility that some of the energy dependent terms may not converge for large ω and tend to the very value $-\lambda$ which is required for the contribution of the contact term to be cancelled. We must therefore conclude that the dispersion relation (1) will be satisfied by the function

---

[†] I.C.I. Research Fellow.

[††] In ref. [1]) Heisenberg picture operators were in ordinary italics.

$M(\omega)-\lambda'$, where λ' is a constant which may be equal to λ. To extract from experiments information concerning the behaviour of $M(\omega)$ for large values of ω will clearly be a very rewarding task.

2. The Natural Frame

We shall first concern ourselves with the question of translating the experimental data into the natural frame. In the rest frame of the τ-meson, a decay event is characterized by the π-meson momenta $\mathbf{k}_1$, $\mathbf{k}_2$, $\mathbf{k}_3$, forming the sides of a triangle, hereafter referred to as T. It is convenient to introduce a system of axes (x, y, z) so that T lies in the xy-plane. We must now perform a Lorentz transformation with relative velocity v ($\cosh\alpha = 1/\sqrt{1-v^2}$) in a direction defined by the polar angles (θ, ϕ), so that the transformed π-meson energies become equal, $k'_{10} = k'_{20} = k'_{30} = \frac{1}{3}\omega$. This requirement leads to the equations

$$\begin{aligned} \xi(k_{1x}-k_{2x})+\eta(k_{1y}-k_{2y}) &= k_{20}-k_{10}, \\ \xi(k_{1x}-k_{3x})+\eta(k_{1y}-k_{3y}) &= k_{30}-k_{10} \end{aligned} \tag{2}$$

for the quantities

$$\xi = \cos\phi \sin\theta \operatorname{tgh}\alpha, \qquad \eta = \sin\phi \sin\theta \operatorname{tgh}\alpha. \tag{3}$$

The solution is

$$\xi = -\frac{a_y}{D}, \qquad \eta = \frac{a_x}{D}, \tag{4}$$

where

$$\mathbf{a} = (\mathbf{k}_2-\mathbf{k}_3)k_{10}+(\mathbf{k}_3-\mathbf{k}_1)k_{20}+(\mathbf{k}_1-\mathbf{k}_2)k_{30} \tag{5}$$

and

$$D = 6\ (\text{area of T}). \tag{6}$$

Since $\operatorname{tg}\phi = -a_x/a_y$, the azimuth ϕ is uniquely determined, whereas θ and α are not, as $\sin\theta \operatorname{tgh}\alpha = |\mathbf{a}|/D$. The transformed τ-meson energy is

$$\omega = M\cosh\alpha = \frac{M}{\sqrt{1-\dfrac{\mathbf{a}^2}{D^2\sin^2\theta}}}, \tag{7}$$

which for any given decay event is to some extent arbitrary. (This arises from the fact that the decay of the τ-meson is a two parameter process.) As was stressed in ref. [1]), the structure of the triangle $\mathrm{T_t}$ obtained by projecting T on to a plane perpendicular to the direction of the Lorentz transformation might be used as an additional element of classification. From a given set of events, those corresponding to an arbitrarily chosen $\mathrm{T_t}$ could then be sorted out by the use of a mechanical device of easy construction. In fact, once ϕ is found from eqs. (3), (4), one should only search for the angle θ (if there is one!) such that the projection of T on to a plane normal to the direction (θ, ϕ) has the structure of T_t. The appropriate value of ω would then be yielded by eq. (7). In this note we shall confine ourselves to Lorentz transformations in the xy-plane $(\theta = \frac{1}{2}\pi)$ for which T_t reduces to a line element.

It is now convenient to use the Dalitz-Fabri representation of decay events [2, 3]). The energies of the π-mesons are expressed in terms of two parameters ϱ and φ,

$$\begin{aligned} k_{10} &= \tfrac{1}{3}M[1+\varepsilon\varrho\cos(\varphi-\tfrac{2}{3}\pi)], \\ k_{20} &= \tfrac{1}{3}M[1+\varepsilon\varrho\cos(\varphi+\tfrac{2}{3}\pi)], \\ k_{30} &= \tfrac{1}{3}M[1+\varepsilon\varrho\cos\varphi], \end{aligned} \tag{8}$$

where $\varepsilon = (M-3\mu)/M \approx 0.154$ and M and μ are the τ and π-meson masses. Each event corresponds to a point of polar coordinates ϱ and φ in a plane. The condition $\varrho^2 \leqq [1+\alpha(1+\varrho\cos 3\varphi)]^{-1}$ with $\alpha = \frac{1}{2}\varepsilon(1-\frac{1}{2}\varepsilon)^{-2}$ results from momentum conservation [3]) and defines an "allowed" region (approximately a circle of radius one) in which points representing decay events must be contained.

By an easy calculation ω defined by eq. (7) with $\theta = \frac{1}{2}\pi$ can be expressed in terms of ϱ and φ, yielding

$$\left(\frac{\omega}{M}\right)^2 = \frac{(1-\frac{1}{2}\varepsilon)^2+\varrho^2(-1+\frac{1}{2}\varepsilon(1-\frac{1}{2}\varepsilon)+\varepsilon\cos\varphi\sin^2\varphi(1-\frac{1}{4}\varepsilon\cos\varphi))-\frac{1}{2}\varepsilon\varrho^3\cos\varphi\cos 2\varphi+\frac{1}{4}\varepsilon^2\varrho^4\sin^2\varphi\cos^2\varphi}{(1-\frac{1}{2}\varepsilon)^2+\varrho^2(-1+\varepsilon\cos\varphi\sin^2\varphi(1-\frac{1}{4}\varepsilon\cos\varphi))+\varepsilon\varrho^3\cos\varphi\sin^2\varphi(\frac{1}{2}\varepsilon\cos\varphi-1)-\frac{1}{4}\varepsilon^2\varrho^4\sin^2\varphi\cos^2\varphi}. \tag{9}$$

From this somewhat formidable expression curves of constant ω can be drawn. It is important to stress that the curve $\omega = \infty$ lies inside the "allowed" region though touching its boundary at some points. There are, therefore, events which cannot be reduced to a "natural" frame by a Lorentz transformation in the plane of the triangle T (i.e. $\theta = \frac{1}{2}\pi$). (Note, incidentally, that every event admits at least one natural frame, the one given by a Lorentz transformation with relative velocity $v = 1$ in a direction perpendicular to the plane of T, yielding $\omega = \infty$.)

Instead of the full relativistic expression (9), in the following we shall use for simplicity

$$\left(\frac{\omega}{M}\right)^2 = \frac{1-\varrho^2}{(1-\varrho^2)-\frac{1}{2}\varepsilon\varrho^2(1-\varrho\cos\varphi+4\varrho\sin^2\varphi\cos\varphi)}, \tag{10}$$

which follows from the original non-relativistic treatment of Dalitz [2]), in which the boundary of the "allowed" region reduces to a circle of unit radius. Fig. 1 shows curves of constant ω plotted by using eq. (10). For ϱ near to one, i.e. for large values of ω, the distortion due to the use of the non-relativistic approximation is quite appreciable. Unfortunately, as was stressed in the introduction, this is precisely the decisive region.

3. Analysis of Experimental data

We have taken the preliminary steps in a dispersion relation analysis of Haddock's date [4]) for the decay $\tau^+ \to \pi^+ + \pi^+ + \pi^-$, more with a view to illustrating the method than with the hope of obtaining anything trustworthy.

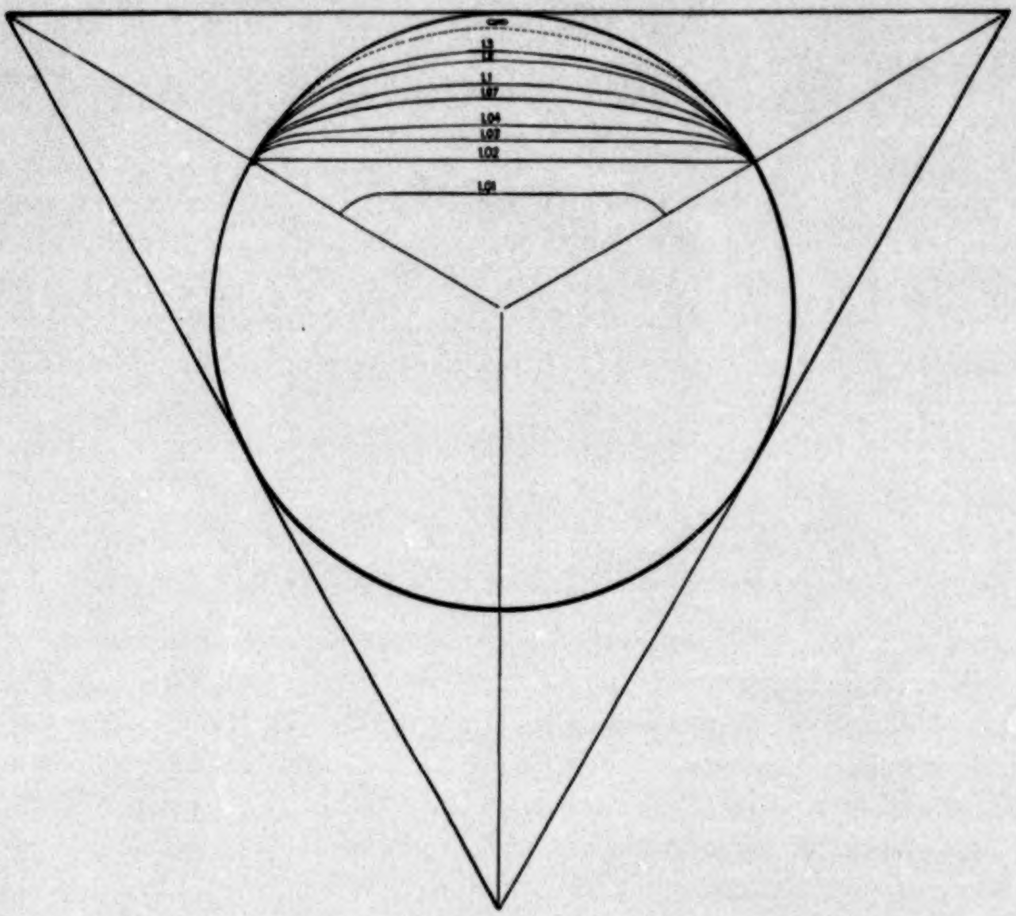

Fig. 1. The Dalitz triangle, and curves of constant ω according to eq. (10). There is a symmetry under rotations of 120°.

Since the amplitude $M_{++-,+}$ is given in terms of $M_{\alpha\beta\gamma,k}$ by the equation

$$M_{++-,+} = \tfrac{1}{4}\{(M_{111,1}+M_{222,2}+M_{211,2}+M_{121,2}-M_{112,2}+M_{122,1}+M_{212,1}-M_{221,1}) \\ +i(M_{222,1}-M_{111,2}+M_{211,1}+M_{121,1}-M_{112,1}+M_{221,2}-M_{212,2}-M_{122,2})\} \quad (11)$$

we may assume that it satisfies dispersion relations like $M_{\alpha\beta\gamma,k}$, but only at the expense of postulating that there is an isotropy in isospin space such that, if ${}_{\alpha}, {}_{\beta}, {}_{\gamma}, {}_{k}$ are each either 1 or 2, $P_{12} M_{\alpha\beta\gamma,k} = M_{\alpha\beta\gamma,k}$, where P_{12} denotes the interchange of 1 and 2. Thus the factor multiplying i in eq. (11)

would vanish and $M_{++-,+}$ satisfy (1). The meaning of this assumption is not at all clear. We are forced into making it by the lack of data for decay of negative τ-mesons, which makes it impossible for the time being to follow the more usual procedure of constructing such linear combinations of the amplitudes $M_{++-,+}$, $M_{+--,-}$ etc. as may satisfy dispersion relations.

In the laboratory frame the lifetime τ is given by 5) †

$$\frac{1}{\tau}=\frac{1}{2\pi}\int\frac{\mathrm{d}\mathbf{k}_1\mathrm{d}\mathbf{k}_2\mathrm{d}\mathbf{k}_3}{k_{10}k_{20}k_{30}M}\delta(\mathbf{k}_1+\mathbf{k}_2+\mathbf{k}_3)\delta(k_{10}+k_{20}+k_{30}-M)\times|M_{++-,+}|^2. \tag{12}$$

In the non-relativistic approximation (12) reduces to

$$\begin{aligned}\frac{1}{\tau}&=\frac{4\pi(3\mu)^3}{M^4}\int|M_{++-,+}|^2\mathrm{d}k_{10}\,\mathrm{d}k_{20}\\&=6\pi\sqrt{3}\left(\frac{\mu\varepsilon}{M}\right)^2\mu\int|M_{++-,+}|^2\,\varrho\mathrm{d}\varrho\mathrm{d}\varphi.\end{aligned} \tag{13}$$

As in fig. 1, the unit circle in the (ϱ, φ) plane is subdivided into portions of area σ_i, each corresponding to an average value ω_i of ω, and containing a number N_i of events. Then

$$|M_{++-,+}(\omega_i)|^2=\frac{16.2}{\tau\mu N}\left(\frac{N_i}{\sigma_i}\right), \tag{14}$$

where $N = 100$ is the total number of events observed. The lifetime would not appear, were the number of parental particles known. We might proceed by taking $\tau \approx 10^{-8}$ sec, and, using the results shown in fig. 2 for N_i/σ_i, determine $|M_{++-,+}(\omega)|^2$. However, a glance at fig. 2 shows that very little can be done for the time being. Not until the behaviour of the amplitude

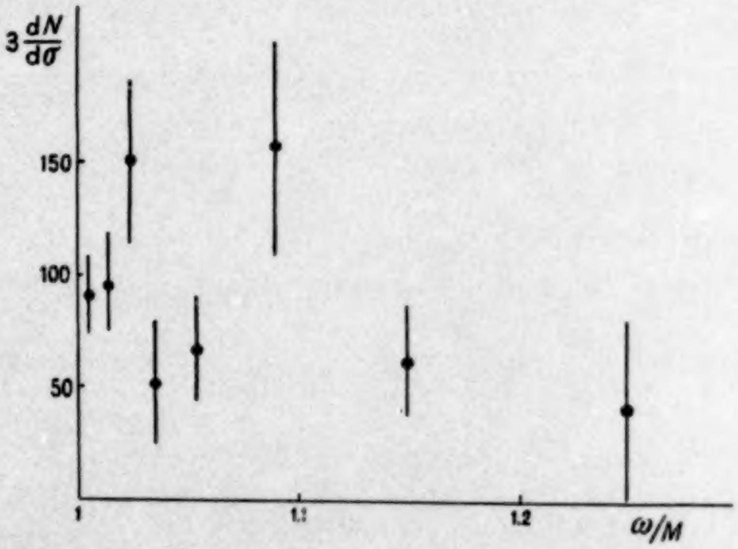

Fig. 2. Number of events per unit area of the Dalitz triangle, $\mathrm{d}N/\mathrm{d}\sigma$, as a function of ω/M.

---

† Our Lorentz invariant amplitude $M_{++-,+}$ is essentially the transition amplitude $(f|M|i)$ as defined in ref. 5) multiplied by the square root of the product of the energies of the particles taking part in the process.

for large values of ω is better ascertained will it be possible to settle the issue as to the existence of a contact interaction. On the other hand, in the non-physical part $-M \leqq \omega' \leqq M$ of the range of integration in (1) an "Ansatz" will have to be made for the amplitude, which can only be done after settling the above-mentioned point.

Thanks are due to Prof. J. G. Gunn, Dr. H. Muirhead and Mr. R. Giles for many helpful comments.

Appendix

For simplicity we ignore the isobaric spin. In the interaction picture the Feynman amplitude for the decay of the τ-meson is

$$F = (0|a(k_1)a(k_2)a(k_3)\sum_{n=0}^{\infty}\frac{(-i)^n}{n!}\int_{-\infty}^{\infty}\mathrm{P}[H(x_1)\dots H(x_n)]\mathrm{d}x_1\dots\mathrm{d}x_n A^{\dagger}(p)|0). \tag{A.1}$$

In this expression $|0)$ is the vacuum state, $A^{\dagger}(p)$ and $a(k_1)$, $a(k_2)$ and $a(k_3)$ are the emission operator for the τ-meson and the absorption operators for the π-mesons, P denotes a chronologically ordered product, and $H(x)$ is the interaction Hamiltonian. If $H(x) = g(\phi(x))^3\Phi(x)$, where $\phi(x)$ and $\Phi(x)$ are the π-meson and τ-meson operators, respectively, by shifting the absorption operators to the right and the emission operator to the left it is easy to show that

$$\sqrt{k_{10}k_{20}k_{30}p_0}\,F = \langle 0|f_1+f_2+\cdots+f_7|0\rangle. \tag{A.2}$$

Here $|0\rangle$ is the Heisenberg vacuum and

$$\begin{aligned}
f_1 &= -6ig(2\pi)^4\delta(p-k_1-k_2-k_3),\\
f_2 &= (-i)^2g^2\int \mathrm{d}x\mathrm{d}y\mathrm{P}[H_{\phi}(x)H_{\Phi\phi\phi}(y)]\\
&\qquad \times (\mathrm{e}^{-ik_1x}\,\mathrm{e}^{i(p-k_2-k_3)y}+\mathrm{e}^{-ik_2x}\,\mathrm{e}^{i(p-k_1-k_3)y}+\mathrm{e}^{-ik_3x}\,\mathrm{e}^{i(p-k_1-k_2)y}), \qquad \text{(A.3)}\\
f_3 &= (-i)^2g^2\int \mathrm{d}x\,\mathrm{d}y\,\mathrm{P}[H_{\phi\phi}(x)H_{\Phi\phi}(y)](\mathrm{e}^{-i(k_1+k_2)x}\,\mathrm{e}^{i(p-k_3)y}\\
&\qquad + \mathrm{e}^{-i(k_1+k_3)x}\,\mathrm{e}^{i(p-k_2)y}+\mathrm{e}^{-i(k_2+k_3)x}\,\mathrm{e}^{i(p-k_1)y}),\\
f_4 &= (-i)^2g^2\int \mathrm{d}x\,\mathrm{d}y\,\mathrm{P}[H_{\phi\phi\phi}(x)H_{\Phi}(y)]\mathrm{e}^{-i(k_1+k_2+k_3)x}\,\mathrm{e}^{ipy},\\
f_5 &= (-i)^3g^3\int \mathrm{d}x\,\mathrm{d}y\,\mathrm{d}z\,\mathrm{P}[H_{\phi}(x)H_{\phi}(y)H_{\Phi\phi}(z)]\\
&\qquad \times (\mathrm{e}^{-ik_1x}\,\mathrm{e}^{-ik_2y}\,\mathrm{e}^{i(p-k_3)z}+\mathrm{e}^{-ik_1x}\,\mathrm{e}^{-ik_3y}\,\mathrm{e}^{i(p-k_2)z}+\mathrm{e}^{-ik_2x}\,\mathrm{e}^{-ik_3y}\,\mathrm{e}^{i(p-k_1)z}),\\
f_6 &= (-i)^3g^3\int \mathrm{d}x\,\mathrm{d}y\,\mathrm{d}z\;\mathrm{P}[H_{\phi}(xH)_{\phi\phi}(y)H_{\Phi}(z)]\mathrm{e}^{ipz}\\
&\qquad \times (\mathrm{e}^{-ik_1x}\,\mathrm{e}^{-i(k_2+k_3)y}+\mathrm{e}^{-ik_2x}\,\mathrm{e}^{-i(k_1+k_3)y}+\mathrm{e}^{-ik_3x}\,\mathrm{e}^{-i(k_1+k_2)y},\\
f_7 &= (-i)^4g^4\int \mathrm{d}x\,\mathrm{d}y\,\mathrm{d}z\,\mathrm{d}u\;\mathrm{P}[H_{\phi}(x)H_{\phi}(y)H_{\phi}(z)H_{\Phi}(u)]\mathrm{e}^{ipu}\,\mathrm{e}^{-i(k_1x+k_2y+k_3z)}
\end{aligned}$$

with $\quad H_{\phi}(x) = 3(\phi(x))^2\Phi(x), \qquad H_{\Phi\phi\phi} = 6\phi(x)$, etc.

References

1) E. Corinaldesi, Nuovo Cimento **4** (1956) 1605

2) R. H. Dalitz, Phil. Mag. **44** (1954) 1068

3) E. Fabri, Nuovo Cimento **9** (1954) 479

4) R. P. Haddock, Nuovo Cimento **4** (1956) 240

5) J. M. Jauch and F. Rohrlich, The Theory of Photons and Electrons (Addison-Wesley Publishing Company, Cambridge, Mass., 1955) p. 163

Nuclear Physics **3** (1957) 656—669; *North-Holland Publishing Co., Amsterdam*

THE COULOMB EXCITATION OF Eu^{151} AND Eu^{153}

C. M. CLASS † and U. MEYER-BERKHOUT ††
Institute for Theoretical Physics
University of Copenhagen

Received 28 January 1957

Abstract: The low lying states of Eu^{151} and Eu^{153} to which transitions occur by means of Coulomb excitation have been studied by observing the spectra of the internal conversion electrons. Thin targets prepared from isotopically enriched europium oxide were bombarded with protons and alpha particles in the energy range between 2 and 4 MeV. The measurements on Eu^{153} confirmed the existence of the previously reported rotational levels at 83 and 190 keV and yield improved values of the reduced transition probabilities. The transitions observed in Eu^{151} were found to fit conveniently into a level spectrum having states at 20, 193, and 304 keV. The first of these levels is known also from the beta decay of Sm^{151}. The 304 keV level decays principally by an M1 transition to the ground state with relatively weaker transitions to the 193 and 20 keV levels. The 193 keV level undergoes transitions to the ground state only, by predominantly E2 radiation. The values of $B(E2)/e^2$ for excitation of the 193 and 304 keV levels were found to be 0.14×10^{-48} cm^4 and 0.40×10^{-48} cm^4, respectively.

1. Introduction

As is well known, nuclei which display rotational spectra when Coulomb excited possess large quadrupole deformations. This correlation is well established for nuclei in the range $153 \leqq A \leqq 190$; but relatively little is known either theoretically or experimentally regarding the spectra of those nuclei immediately adjacent to either end of this range which have somewhat smaller deformations, e.g., isotopes of osmium, iridium, and europium. To begin work on these transition nuclei we chose to investigate Eu^{151}. The deformation of this nucleus having 88 neutrons is about half as large as the deformation of Eu^{153} which has 90 neutrons [1]). One might expect, therefore, that the spectrum of Eu^{151} observed in Coulomb excitation would show marked departures from the rotational order which is conspicuous in the spectrum of the heavier isotope [2]). Indeed, this has been found to be the case, as may be seen in fig. 1, where the levels directly or indirectly populated in Coulomb excitation are shown for both isotopes. Additional consequences of the smaller deformation of Eu^{151} are seen in the location of its levels at higher excitation energies than occur in Eu^{153} and in the reduced magnitude of the transition probabilities to these states, as will be discussed below.

The level scheme given in fig. 1 for Eu^{151} is based on our measurements in which the conversion electrons were observed, and is consistent with the results of Temmer and Heydenburg [3]) [†] who studied the gamma radiation. In addition to our work with Eu^{151}, we found it necessary to reinvestigate Eu^{153}. Although the conversion electrons from the two rotational levels had been studied earlier [2]), the data obtained on the transitions from the second excited state were poor and prevented full use of the Bohr-Mottelson theory [4]) in the analysis of the results. Furthermore, on comparing the positions of the levels of the two isotopes, it is apparent that the second rotational level of Eu^{153} nearly coincides with the formerly unknown level of Eu^{151} at 193 keV. Since all earlier measurements except that of ref. [3]) were made with natural europium, the observed yield corresponding to a transition energy of about 193 keV was completely ascribed to the cross-over transition in Eu^{153}.

---

† On leave from The Rice Institute, Houston, Texas.

†† Now at High Energy Physics Laboratory, Stanford University, Stanford, California.

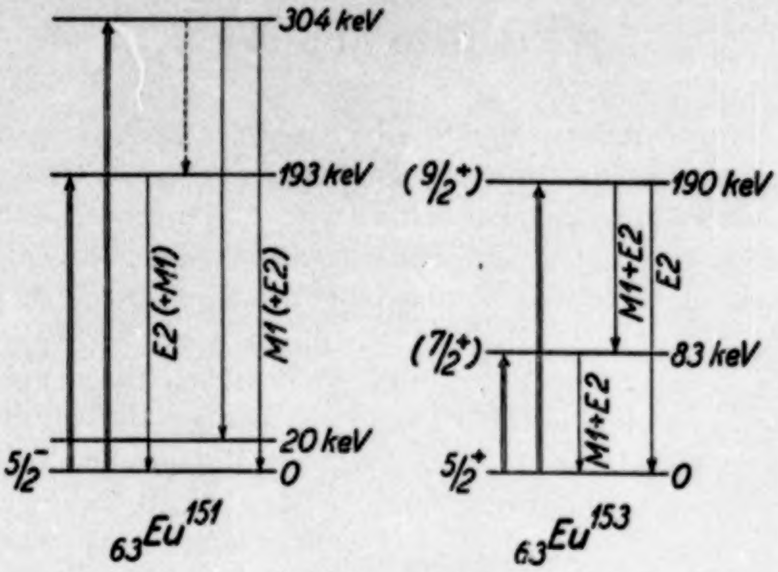

Fig. 1. The energy level diagrams for Eu^{151} and Eu^{153} showing the transitions observed due to Coulomb excitation. The scheme presented for Eu^{151} is based on measurements reported in this paper.

The experimental arrangement and procedure used in the measurements was similar to that described earlier [2]), except that the apparatus was shifted to the new Van de Graaff generator which has recently been put into operation at the Institute. Thin europium oxide targets enriched in either Eu^{151} or Eu^{153} were bombarded with protons or alpha particles accelerated to energies in the range between 2 and 4 MeV. The targets were prepared on thick carbon backings by slowly evaporating a drop containing europium oxide held in an alcohol suspension. The carbon gave only a small background in the range of bombarding energy cited. The thickness of the europium layer in the target at the beam spot was determined by measuring the fractional number of protons which were elastically scattered by the europium nuclei into a known solid angle, using a spectrometer currently available on the Institute's 2MeV Van de Graaff.

[†] We are indebted to Dr. Temmer and Dr. Heydenburg for sending us their results in advance of publication.

2. Results and Discussion

2.1. Eu^{153}

Fig. 2 shows complete spectra of conversion lines corresponding to transitions from the first two rotational states of Eu^{153}. The spectrum in fig. 2a was obtained by bombarding a target which contained 0.7 mg/cm^2 of europium enriched to 95 % in Eu^{153} with 3.7 MeV alpha particles, whereas fig. 2b shows the spectrum obtained by bombardment with protons of 3.4 MeV.

In table 1, all our results on Eu^{153} are summarized. The energies assigned to the levels are accurate to about 1—2 % and confirm the values previously reported. The ratio between the experimentally determined excitation energies for the second and first excited states is 2.29, in agreement with

TABLE 1

Summary of results on Eu^{151} and Eu^{153} derived from measurement of the conversion electron spectra

Nucleus	ΔE (keV)	Line n	$\varepsilon(n)\,\frac{B(E2)}{e^2}$ $(10^{-48}\ cm^4)$	$\frac{1}{\delta^2}$	β	$\frac{1}{\varepsilon(n)}$	$\frac{B(E2)}{e^2}$ $(10^{-48}\ cm^4)$	Q_0 $(10^{-24}\ cm^2)$
Eu^{153}	83	K_1	(0.8)	(0.3)	1	(2.6)	(2.1)	(6.7)
		L_1	(0.8)			(2.6)	(2.1)	(6.7)
		M_1	(0.12)			—	—	—
	107	K_{21}	0.090	0.5	0.41	5.9	0.53	5.7
		L_{21}	0.041			13		
		M_{21}	0.006			—	—	—
	190	K_2	0.045	0	0.59	12	0.53	5.7
		L_2	0.014			37		
		M_2	—			—	—	—
Eu^{151}	193	K_1	0.020 †	$\leqq 0.4$	1	7 ††	0.14 †	
		L_1	0.0065 †			21.5††	0.14 †	
		M_1	—			—	—	
	304	K_2	0.021	$\geqq 1.2$	0.8 †††	18 *	0.38	
		L_2	0.0032			127 *	0.41	
		M_2	—			—	—	
	284	K_2'	0.0031	—	—	—	—	
	111	K_{21}	?	—	0.2 †††	—	—	

† Upper limit; the actual value might be as much as a factor of 2 smaller.

†† Calculated under the assumption of a pure E2 transition.

††† Estimated from the experimental data of Temmer and Heydenburg [3]).

* Calculated under the assumption of a pure M1 transition and the branching fraction given in column 6.

the theoretical value $(2I_0+3)/(I_0+1)$ for a nucleus with ground state spin $I = 5/2$. Apart from the energies all those quantities are given in the table which can be directly derived from the measured conversion electron yields. The values listed are the average of the results of two or more runs in each case. Less certain values are given in parentheses. In general, the results of a single measurement differed by not more than 15 % from the average value. However, systematic errors totaling to about 30 % cannot be excluded.

In interpreting the results presented in the table, one has to keep in mind that, of all those nuclei which are in a given excited state, only a fraction $\varepsilon(n)$ decay by transferring their excitation energy to an electron in the n-th shell. Hence, our measurements do not lead directly to the cross section for exciting a subject state, but to this quantity multiplied by the decay fraction $\varepsilon(n)$. However, upon using the theoretical conversion coefficients † and the mixing and branching ratios derived from these measurements, the cross section can be obtained, and it is then a simple matter to evaluate the total transition probability B(E2) for electric quadrupole excitation. Both this quantity and the partial B-values, $\varepsilon(n)B$(E2), are given in the table.

† For the K-conversion coefficients we used those calculated by L. Sliv *et al.* (taken from privately distributed tables available from O. B. Nielsen of the Institute for Theoretical Physics). The L-conversion coefficients for M1 radiation were derived from Sliv's values by using Rose's theoretical K/L ratios for M1 transitions. For E2 radiation, K/L ratios consistent with experimental data and Rose's and Sliv's tables were used. See ref. 5).

When the information extracted from our measurements is not sufficient or too uncertain to derive the quantities in question reliably this is indicated by a bar.

The nine columns of the table contain:

1. Nuclei investigated.
2. Transition energies.
3. Assignments of the conversion lines observed with respect to atomic shell and nuclear transition. (Subscript $_1$ refers to transition from the first Coulomb-excited state to the ground state; subscripts $_{21}$ and $_2$ refer to transitions from the second Coulomb-excited state to the first, and to the ground state, respectively. A prime (′) indicates that this transition ends on the 20 keV level of Eu^{151}.)
4. Partial B(E2) values for the various conversion lines as computed from the corresponding measured partial cross sections.
5. Reciprocal of the square of the mixing ratios as computed from the experimentally observed K/L ratios and the theoretical conversion coefficients.
6. Branching fractions for the corresponding transitions (i.e., fraction of all excited nuclei in the level considered which decay to the secondary level considered), as computed from the partial B(E2) values of the corresponding cross-over and cascade transition using the mixing ratio from column 5 and the theoretical conversion coefficients.
7. Reciprocal of the decay fractions corresponding to the modes of decay given in column 3, as computed from the data given in column 5 and 6, and the theoretical conversion coefficients.
8. Total B(E2) values as computed from the partial B(E2) values given in column 4 and from the decay fractions as given in column 7.
9. Intrinsic quadrupole moment as computed according to the B−M theory 4) from the total B(E2) value.

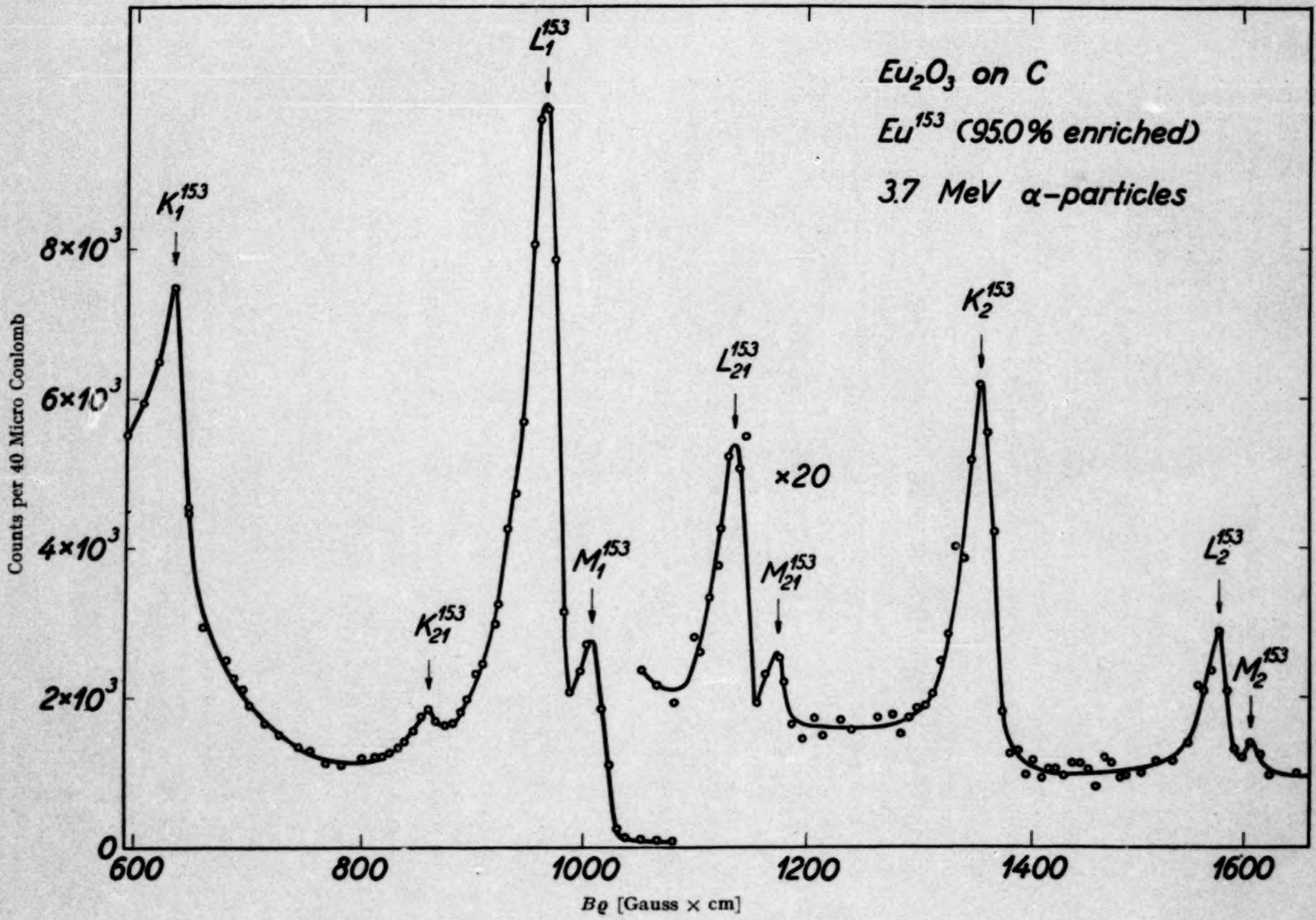

Fig. 2a. The spectrum of conversion electrons from Eu^{153} obtained by bombarding a target of europium oxide, enriched to 95 % in the isotope 153, with alpha particles of 3.7 MeV.

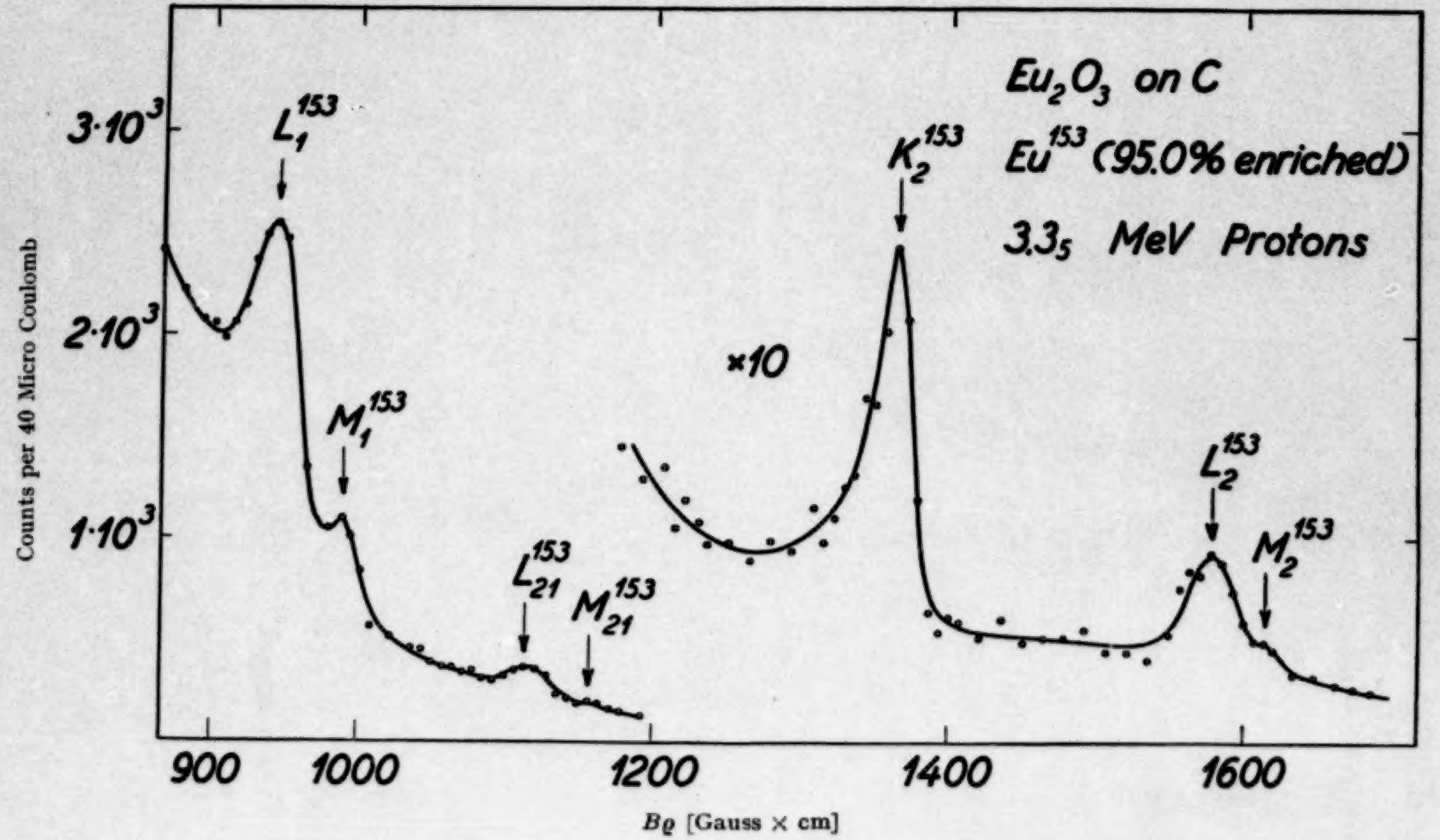

Fig. 2b. The spectrum of conversion electrons from Eu^{153} obtained by bombarding a target of europium oxide, enriched to 95 % in the isotope 153, with protons of 3.4 MeV.

Of the partial B-values quoted for Eu^{153}, those associated with the cross-over transition are derived from measurements in which only protons were used as projectiles. For the cascade transitions, the conversion electrons appear at too low energies to permit reliable measurements to be made with proton bombardment, since the continuous background of electrons present in this case rapidly increases in intensity with decreasing electron energy. This background is much reduced by bombarding with alpha particles, but unless the target is very thin compared to the range of the bombarding particle, the target inhomogeneities can affect the measured yield in such a way that significant errors in the derived B-values may result. In the case of proton bombardment, this effect is of no great importance, since at a typical bombarding energy of 3.7 MeV, the stopping power of europium oxide for protons is about 50 keV/mg·cm². However, for alpha particles of the same energy, the stopping power is about 8 times greater than for the protons, and in this case the derived B-values would be less reliable since the inhomogeneities of the target were comparable with the thickness itself. To circumvent this difficulty for the (2,1) transition, we compared the yields of the K_{21} and L_{21} conversion lines obtained under alpha bombardment with those of the K_2 and L_2 lines measured under identical conditions. From the relative yields and the values of $\varepsilon(K_2)B(E_2)$ and $\varepsilon(L_2)B(E2)$ known from measurements with proton bombardment, one then gets values for $\varepsilon(K_{21})B(E2)$ and $\varepsilon(L_{21})B(E2)$ which are essentially uninfluenced by the target inhomogeneities. Taking into account the different excitation functions of the first and second excited states, the partial B-values of the first excited level were derived by a similar comparison method. For this level, the B-values obtained are of course not independent of target inhomogeneities and are therefore given in our table in parentheses. A direct, although not very precise, measurement of the yield of the L_1 conversion electrons using proton bombardment led to about the same result.

The ratio of the total B-values of the second to first excited states from our data is 0.25, as compared to a value of

$$\frac{B(E2;\, I_0 \rightarrow I_0+2)}{B(E2;\, I_0 \rightarrow I_0+1)} = \frac{2(I_0+1)}{I_0(2I_0+3)} = \frac{7}{20} = 0.35 \text{ for } I_0 = 5/2,$$

which is predicted for strongly deformed nuclei by the B—M theory [4]). Comparison of the Q_0 moments given in the table with the intrinsic quadrupole moment of 7.0×10^{-24} cm² which follows from optical hyperfine structure analysis, shows that the two values are in agreement within the accuracy of the measurements.

In addition to the quantities discussed above, the E2—M1 mixing ratio of the gamma radiation associated with a given transition can be determined from the ratio of the intensities of the corresponding K and L conversion lines.

For the decay of the first excited state, the average of all our measurements gives a K/L ratio of about one. From this, a squared mixing ratio δ_1^2, defined as the ratio of the number of E2 gamma quanta to the number of M1 quanta emitted in decay, of about 3 is obtained. This corresponds to an M1 contribution of about 25 % in the gamma radiation †. For the K/L ratio of the cross-over transition from the second excited state, we get an average value of 3.2, which agrees well with the value expected for the pure E2 transition predicted in this case by the B—M theory [4]). For the transition between the two excited states, the K_{21}/L_{21} ratio is about 2.2, giving a value of δ_{21}^2 of about 2, which corresponds to 33 % M1 and 67 % E2 radiation. Bernstein and Lewis [7]) recently reported that this cascade should be of predominantly M1 character.

In the case of rotational transitions, the two mixing ratios can be expressed in terms of Q_0 and the quantity $|g_K - g_R|$, where g_K is the gyromagnetic ratio of the unpaired proton in its $5/2^+$ orbital in the spheroidal nucleus, and where g_R is the gyromagnetic ratio associated with the collective rotational motion. According to the theory [4, 2]), one has the relation

$$\frac{\delta_1^2}{\delta_{21}^2} = \left(\frac{I_0+1}{I_0+2}\right)^3 \cdot \frac{I_0+3}{I_0} = 1.04 \quad \text{for} \quad I_0 = 5/2,$$

and the measured values are in agreement with this relation to within the experimental uncertainty.

From the mixing ratio given in the table for the cascade transition (2,1), and from the averaged intrinsic quadrupole moment $Q_0 \approx 6.0 \times 10^{-24}$ cm², one gets for $|g_K - g_R|$ the value ≈ 0.1. Using the known magnetic moment of Eu^{153}, the factors g_K and g_R can be computed separately [4]). These turn out to be $g_K \approx +0.6$ and $g_R \approx +0.5$, which is about in order of magnitude what is expected from theory ††.

Finally, from the measured mixing and branching of the transitions from the second excited state one can compare the reduced E2 transition probabilities for the cross-over and cascade decays. Theoretically [4, 2]) one expects the ratio

---

† The uncertainty of this result is rather large, however, since the K_1 and K_{21} conversion lines not only are superimposed on a strong and steeply rising background of electrons but in addition have an energy which is only slightly above the cut-off energy of the mica foil of the Geiger counter. Thus an appreciable correction had to be applied to take into account the absorption of electrons in the foil, whose thickness was 1 mg/cm². The correction factor as function of energy was determined by comparing the intensity ratios of some Th(B+C+C″) lines, as they were measured in our experimental arrangement with the true intensity ratios as determined by O. B. Nielsen (private communication) in the energy range considered. The relative correction factor obtained in this manner was then fitted at high energies to the absolute values obtained by Saxon [8]).

†† Since the theoretical expression for the M1 matrix elements is quadratic in $|g_K - g_R|$, the experimental intensities determined two possible solutions for g_K and g_R, which, however in the present case do not differ appreciably from each other.

$$\frac{B(\mathrm{E2};\ I_0+2 \rightarrow I_0)}{B(\mathrm{E2};\ I_0+2 \rightarrow I_0+1)} = \frac{(2I_0+1)(I_0+3)}{2I_0^2(2I_0+3)} = \frac{33}{100} \quad \text{for} \quad I_0 = 5/2,$$

which is in good accord with the value 0.26 derived from the experimental data in table 1.

Thus, the yield of all six electron lines from K and L conversion of the three transitions can be accounted for in terms of the two nuclear constants Q_0 and $|g_K - g_R|$ with values of the parameters which are in agreement with the theoretical expectations, as well as with other experimental evidence.

2.2. Eu^{151}

The spectra of conversion electrons due to transitions in Eu^{151} are shown in figs. 3a and 3b. They were obtained by bombarding with protons and alpha particles, respectively, a target of europium oxide containing 1.2 mg/cm^2 of europium enriched to 91.9 % in Eu^{151}. The conversion lines of Eu^{153} also appear in these spectra due to an 8 % abundance of this isotope in the target. Our results on Eu^{151} are summarized in table 1. The values listed are based on measurements with protons only and are the average of three or more runs. Corrections have been made where necessary for the effects of the Eu^{153} contamination.

Of the lines obtained under proton bombardment at 3.2 MeV the three of highest energy are attributed to transitions between states of Eu^{151} since their positions occur at energies well above known lines in Eu^{153}. On the other hand, the two lines of lower energy very nearly coincide with the positions of the K_2 and L_2 lines in Eu^{153}. Since, however, no more than 15 % of the yield observed can be due to the Eu^{153} contamination, these lines are also assigned to transitions in Eu^{151}.

When the same target was bombarded with alpha particles at 3.7 MeV under otherwise unchanged experimental conditions, additional conversion lines were distinguished from the continuous electron background in the low energy region as seen in fig. 3b. With one exception all these lines are due to the Eu^{153} contamination. The weak peak at 850 Gauss · cm, however, may be a composite of lines due to transitions in both Eu^{153} and Eu^{151}. A weak line due to Eu^{151} would be expected in this region if the level scheme proposed below is correct. (See fig. 1) Moreover, a careful measurement of the yield of this line indicated that the intensity of the peak is stronger than expected if due solely to K conversion of the (2, 1) transition of Eu^{153}.

The lines marked K_2^{151} and L_2^{151} in fig. 3a are readily identified with conversion in the K and L shells of a transition of 304 keV, since a gamma ray of this energy has also been observed [3]). These lines are presumed to

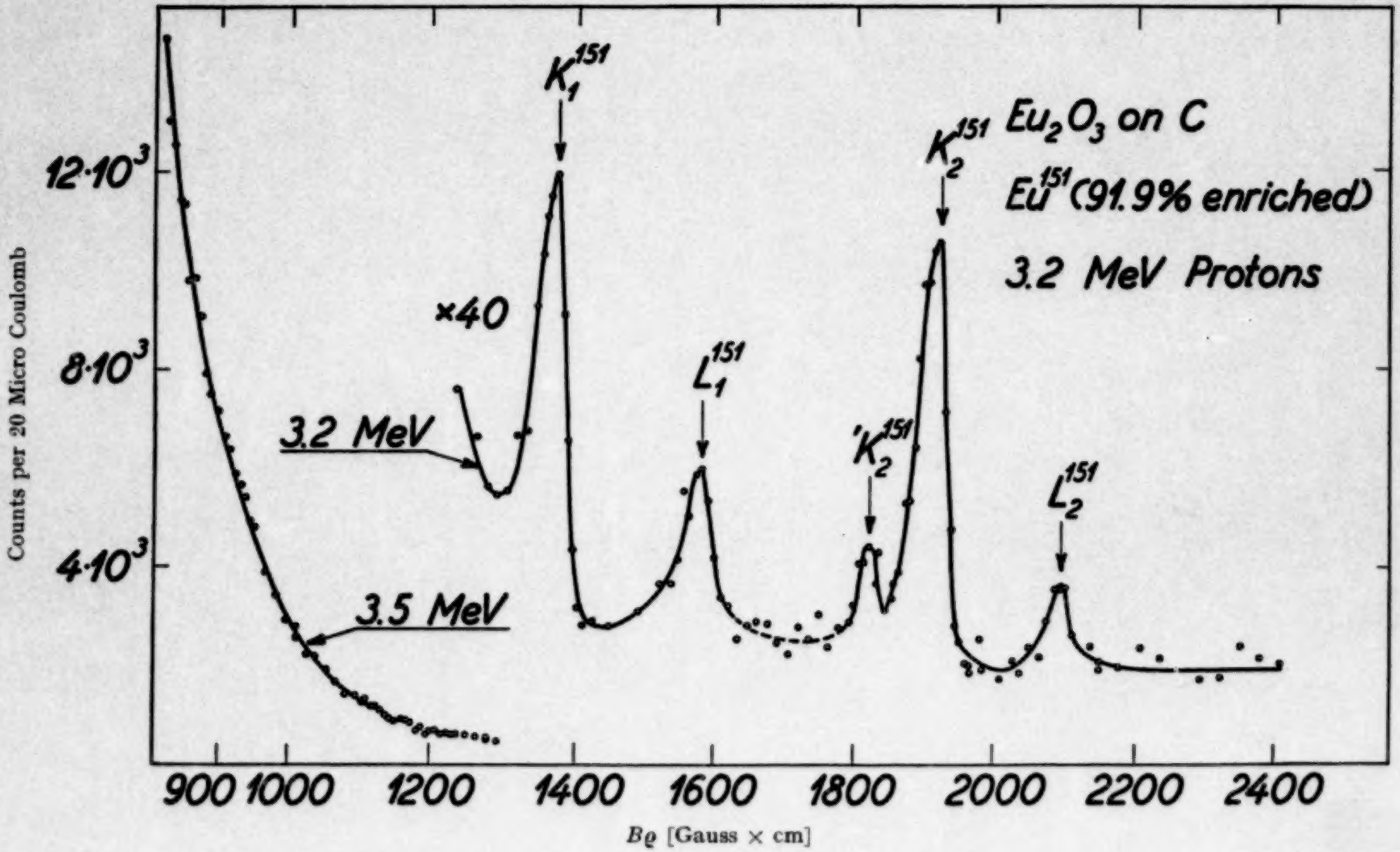

Fig. 3a. The spectrum of conversion electrons from Eu^{151} obtained by bombarding a target of europium oxide, enriched to 91.9 % in the isotope 151, with protons of 3.2 and 3.5 MeV.

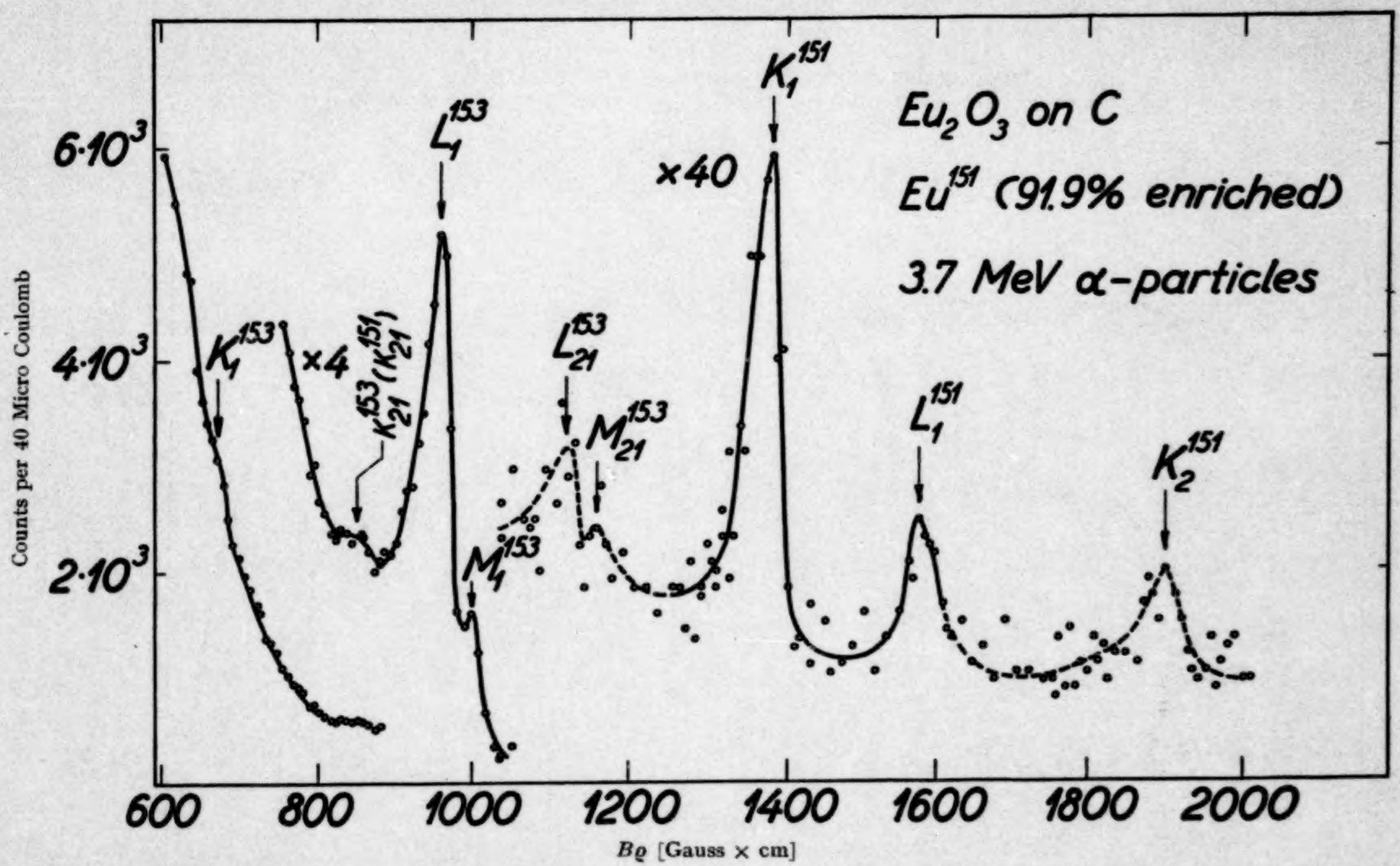

Fig. 3b. The spectrum of conversion electrons from Eu^{151} obtained by bombarding a target of europium oxide, enriched to 91.9 % in the isotope 151, with alpha particles of 3.7 MeV. The lines from Eu^{153} are due to an 8 % abundance of this isotope in the target material.

be due to a state located at 304 keV above the ground state since their intensity varied with bombarding energy as if this were the case. The K/L ratio for this transition given by the average of all our measurements is about 6.5. For pure E2 radiation the theoretical K/L ratio in this case is 4.5, whereas for pure M1 radiation one would expect 7.2. Thus, the 304 keV transition is predominantly M1 in character with possibly some E2 contribution. A spin assignment of $7/2^-$, $5/2^-$, or $3/2^-$ for the 304 keV level is therefore compatible with these data.

A weak satellite line occurs on the low energy side of the K_2^{151} conversion line at about 1815 Gauss · cm (235 keV). A convenient explanation of this line is to assume that it is due to a transition from the state at 304 keV to one at 20 keV which is known from the β^- decay of $_{62}Sm^{151}$ [8]). The energy of the satellite is then in excellent agreement with what one would expect for the K conversion line corresponding to this transition. One would expect that the L conversion peak corresponding to the weak K line should appear at 2000 Gauss · cm (277 keV). Since, however, the K/L ratio to be expected is ≈ 4.5 for an E2 transition and $\geqq 7$ for an M1 or E1 transition, it is not surprising that such a line cannot be distinguished from the continuous background in our experiments. Furthermore, the measurement of the yields of the satellite and K_2^{151} lines showed that their relative intensities of about 1/7 was independent of the beam energy between 2.7 and 3.9 MeV. This result points to a common origin for both lines although experimental uncertainties do not allow one to definitely exclude a level at 284 keV above the ground state. We shall, therefore, assume that the 304 keV level decays partially via a 20 keV level and thus gives rise to the weak satellite.

From the intensity ratio of the K conversion lines of the 284 and 304 keV transition, the intensity ratio of the corresponding gamma rays can be derived by using the theoretical conversion coefficients, provided that the nature of the two transitions is known. As was stated above, the 304 keV transition is of predominantly M1 character. The character of the 284 keV transition is more difficult to determine. Since we do not see the corresponding L conversion line, the K/L ratio for this transition appears to be greater than five, which would be compatible with either an M1 or E1 transition, but not compatible with a predominantly E2 transition. Of the two choices, an E1 transition would require that the 20 keV level be of even parity. This possibility cannot be excluded on the evidence available from the beta decay, but has been avoided in the subsequent discussion since it leads to various inconsistencies. If the M1 assigment is chosen for this transition one gets a ratio of the intensity of the 304 to 284 keV gamma rays of about 10/1 whereas E1 character of the 284 keV line would lead to a value of about 2/1 for the corresponding intensity ratio. A value of

$\varepsilon(\gamma)B(\mathrm{E2})$ can be derived from the tabulated partial B-values $\varepsilon(\mathrm{K}_2)B(\mathrm{E2})$ and $\varepsilon(\mathrm{L}_2)B(\mathrm{E2})$ which can be compared with the value of $\varepsilon(\gamma)B(\mathrm{E}_2) = 0.22\times10^{-48}$ cm^4 given by the gamma ray measurements ^{3}). However, the latter value must be corrected for the branching of the 304 keV level since this complexity in the decay was not detected in the gamma ray measurements. One finds that the comparison of the two values of $\varepsilon(\gamma)B(\mathrm{E2})$ is most favorable if both of the transitions involved are taken to be pure M1 †. In this case, the two values agree to within about 30 % which is compatible with the accuracy of the measurements. If the 284 keV transition is taken to be E1, a much more serious discrepancy between the values results, which is outside the limit of error of the measurements.

Finally, the two strong lines marked K_1^{151} and L_1^{151} in fig. 3b are just of the energy required for conversion in the K and L shells of a transition of 193 keV. A transition of this energy was observed in the gamma ray measurements ^{3}) in which enriched Eu^{151} was also used. As in our case, the intensity of the transition was found to be greater than could be accounted for by the small Eu^{153} contamination.

As a result, it is necessary to assume an additional level in the spectrum of Eu^{151} of 193 keV above the ground state. There is no evidence that this state decays by a cascade transition via the 20 keV level.

Another possible explanation of the 193 keV transition would be to assume that it occurred as the first step of a cascade transition from the 304 keV state via a level at 111 keV above the ground state. This decay scheme, however, was excluded by measuring the yields of the K conversion electrons of the 193 and 304 keV transitions, using successively proton and alpha particle bombardment but under otherwise identical experimental conditions. The ratio of the yields of these conversion electrons should be the same for either projectile provided that the 193 keV transition is the first step in the cascade from the 304 keV level. This result holds even for inhomogeneous and rather thick targets since the electrons emitted have rather high energy. However, as can be seen from the corresponding lines in fig. 3a and fig. 3b, the yield ratio $Y(\mathrm{K}_1)/Y(\mathrm{K}_2)$ increases by a factor of about five when alpha particles are used instead of protons. This change is of the order to be expected at the bombarding energies used if the 193 keV transition originates from a level at 193 keV above the ground state. An estimate of the exact change in the yield ratio however is rather difficult, since it is affected by the target inhomogeneity and furthermore by the fact that the 193 keV level might be populated not only by direct Coulomb excitation, but might be fed by excited nuclei in the 304 keV level. This seems, indeed, to be the case as was indicated by a yield measurement of the K conversion electrons from the 193 keV transition as function of the proton energy.

---

† For the M1 conversion coefficients, the values $\beta_1(\mathrm{K}) \approx 0.08$ and $\beta_1(\mathrm{L}) \approx 0.01$ were used.

The excitation curve which was obtained was between those to be expected for an excited level at 193 keV and at 304 keV.

The partial *B*-values which are given in the table for the 193 keV level were computed under the assumption that the population of the 193 keV level via the state at 304 keV is negligible compared to that occurring by direct excitation. As indicated above, this assumption is not very well justified. From a rough estimate based on the branching in the decay of the 304 keV level ^{3}), one can conclude that the true partial *B*-values may be smaller than those given in the table by as much as a factor of 2. This result is also apparent on comparing the partial *B*-values obtained from the gamma ray measurements with those derived from our work. By taking the 193 keV transition to be pure E2 as is indicated by the K/L ratio of 3.3, one finds a value of $\varepsilon(\gamma)B(\mathrm{E2})$ which is nearly a factor of 1.7 larger than reported by Temmer and Heydenburg ^{3}). In their case where alpha particle bombardment was used, the excitation of the 304 keV level was relatively much weaker than in our case in which protons were used, so that the discrepency in the partial *B*-values may be taken as a measure of the error due to the neglect of cascading. Unfortunately, the yield of the conversion lines due to the 111 keV transition, which would help one to be more quantitative on this point, is weak and this makes it difficult to distinguish the line from the strong and steeply rising background. There seems to be an indication only of the K line, as seen in fig. 3b.

As is not unexpected for a nucleus of small deformation like Eu^{151}, the positions of the Coulomb excited states as well as their transition probabilities and related characteristics are not such that they can be readily interpreted from the point of view of a rotational model.

We should like to express our gratitude to Professor N. Bohr for extending to us the hospitality of his Institute during the time these measurements were made. We also acknowledge with pleasure the advice and help of the members of the Van de Graaff group, especially mag. scient. K. Broström, B. Elbek, S. Holm, and J. Bjerregaard. One of us (U. Meyer-Berkhout) is indebted to the Rask-Oersted Foundation, Copenhagen, and to the Deutsche Forschungsgemeinschaft for financial support during his stay in Copenhagen.

References

1) H. Schüler and T. Schmidt, Z. Physik **94** (1935) 457; **98** (1935) 430; B. R. Mottelson and S. G. Nilsson, Phys. Rev. **99** (1955) 1615
2) Huus, Bjerregaard and Elbek, Mat. Fys. Medd. Dan. Vid. Selsk. **30** (1956) no. 17
3) G. M. Temmer and N. P. Heydenburg, Phys. Rev. **104** (1956) 981, and private communication
4) A. Bohr and B. R. Mottelson, Mat. Fys. Medd. Dan. Vid. Selsk. **27** (1953) no. 16
5) Rose, Goertzel, Spinrad, Harr and Strong, Phys. Rev. **83** (1951) 79
6) Saxon, Phys. Rev. **81** (1951) 637
7) E. M. Bernstein and H. W. Lewis, Bull. Am. Phys. Soc. **1** (1956) 41 and Phys. Rev. (to be published)
8) H. W. Wilson and G. M. Lewis, Proc. Phys. Soc. A **65** (1952) 656; for further references see Hollander, Perlman and Seaborg, Rev. Mod. Phys. **25** (1953) 469

Nuclear Physics **3** (1957) 670—678; *North-Holland Publishing Co., Amsterdam*

THE LOW-LYING ENERGY LEVELS OF ^{151}Eu

A. BISI, E. GERMAGNOLI† AND L. ZAPPA
Istituto di Fisica Sperimentale del Politecnico, Milano

Received 5 February 1957

Abstract: The radioactive decay of ^{151}Gd has been investigated. Measurements of electron conversion spectrum and γ-spectrum show the existence of γ-rays accompanying the electron capture process. The energies of the γ-rays were found to be 21.3, 80, (144), 155, 176, 240, 299 keV. A decay scheme is proposed.

1. Introduction

^{151}Gd is known to decay by orbital electron capture to ^{151}Eu; its half-life is 150 d. No detailed information however is available as far as concerns the transition energy and the γ-rays accompanying the decay and so the energy levels of ^{151}Eu are unknown to date.

Only an intensely converted γ-ray having an energy of 265 keV was found by absorption method by Hein and Voigt [1]).

On the other hand the negaton decay of ^{151}Sm does not represent a valuable source of information about the low-lying levels of ^{151}Eu as its transition energy is only 96 keV[2]): a γ-ray of about 20 keV was found to be emitted in this decay and considered as due to the deexcitation of the first level of ^{151}Eu.

A few data can be drawn from the Coulomb excitation of separated ^{151}Eu, which was recently carried out by Heydenburg and Temmer [3]) with α-particles. γ-rays of 110, 195, 304 keV were found and coincidence measurements made it possible to interpret them as due to the deexcitation of two levels lying at 195 and 304 keV.

The evidence concerning the low energy levels of ^{151}Eu is anyway rather meager; in the following paragraphs experimental techniques used to investigate the radiations emitted from ^{151}Gd will be described, and results discussed.

2. Measuring Techniques

Active Gd was obtained after irradiation of spectroscopically pure Eu_2O_3 with 26 MeV deuterons in the Amsterdam cyclotron. Production of both ^{151}Gd and ^{153}Gd from (d, 2n) reactions in ^{151}Eu and ^{153}Eu was expected to be most important; actually no other intense long lived activities were detected.

Owing to the fact that the spectrum due to the 236 d activity of ^{153}Gd was superimposed on the one to be investigated, during the whole set of measurements accurate comparisons were necessary between the active samples produced by cyclotron irradiation and similar sources of pure ^{153}Gd which had been obtained by irradiating Gd_2O_3 with slow neutrons. These sources had been supplied by AERE (Harwell) and had been allowed to decay long enough that no more activities from short lived isotopes of Gd and Tb were present.

---

† Laboratori C.I.S.E., Milano.

The orbital electron capture of ^{153}Gd has been investigated extensively and, though some features of the decay scheme are not yet fully understood, both the X- and γ-ray spectrum $^{4, 5, 6, 7}$) and the conversion electron spectrum ^{8}) are well known, so that no ambiguities in the interpretation of mixed ^{151}Gd and ^{153}Gd spectra can arise from difficulties in correctly attributing a line to either isotope.

K X- and γ-radiations were investigated by means of a single crystal spectrometer; the low energy region of the X- and γ-spectrum was more satisfactorily studied with the help of an $A-CH_4$ filled proportional counter. Both crystal-crystal and crystal-proportional counter coincidences were also used in several measurements. The conversion electron spectrum was finally investigated by means of an intermediate image beta spectrometer.

3. γ- and X-Radiations from ^{151}Gd

The results which have been obtained with a single NaI(Tl) crystal spectrometer are shown in fig. 1 and fig. 2. In order to avoid contributions to the counting rates from summation peaks due to the known integrating features of the crystal spectrometers, all the spectra were taken with the sources located at a distance of about 20 cm from the crystal (cylindrical in shape, 3.75 cm diameter, 2.5 cm thick). In fig. 1 an account is given of the energy region between 25 keV and 140 keV both with ^{151}Gd$+^{153}$Gd and with the pure ^{153}Gd sources.

A quantitative comparison between the two spectra shows that no intense γ-lines are emitted by ^{151}Gd in this energy interval. The 103 keV γ-line belongs to ^{153}Gd and it can be easily noticed that an intense emission of K X-rays has to be attributed to ^{151}Gd. A weak peak at about 75 keV is present in both spectra and is most probably a composite one: the I K X-rays escape peak due to the 103 keV γ-line (about 75 keV) was interpreted as superimposed on the 72 ± 8 keV line which was observed in the decay of ^{153}Gd by Bhattacherje and Shee Raman ^{5}). Of course contributions of weak lines from ^{151}Gd cannot be excluded in the region between 70 and 90 keV or thereabout. Evidence of a 80 keV line was indeed found from the measurements of the conversion electron spectrum.

Fig. 2 shows the spectrum from ^{151}Gd for energies above 110 keV. In this case the attributions are rather sure because no peaks were noticed in the spectrum of pure ^{153}Gd. The quoted energies result from a calibration of the spectrometer by means of the well known lines from ^{141}Ce (145 keV), ^{203}Hg (279 keV), ^{22}Na (annihilation peak) and ^{153}Gd itself (103 keV).

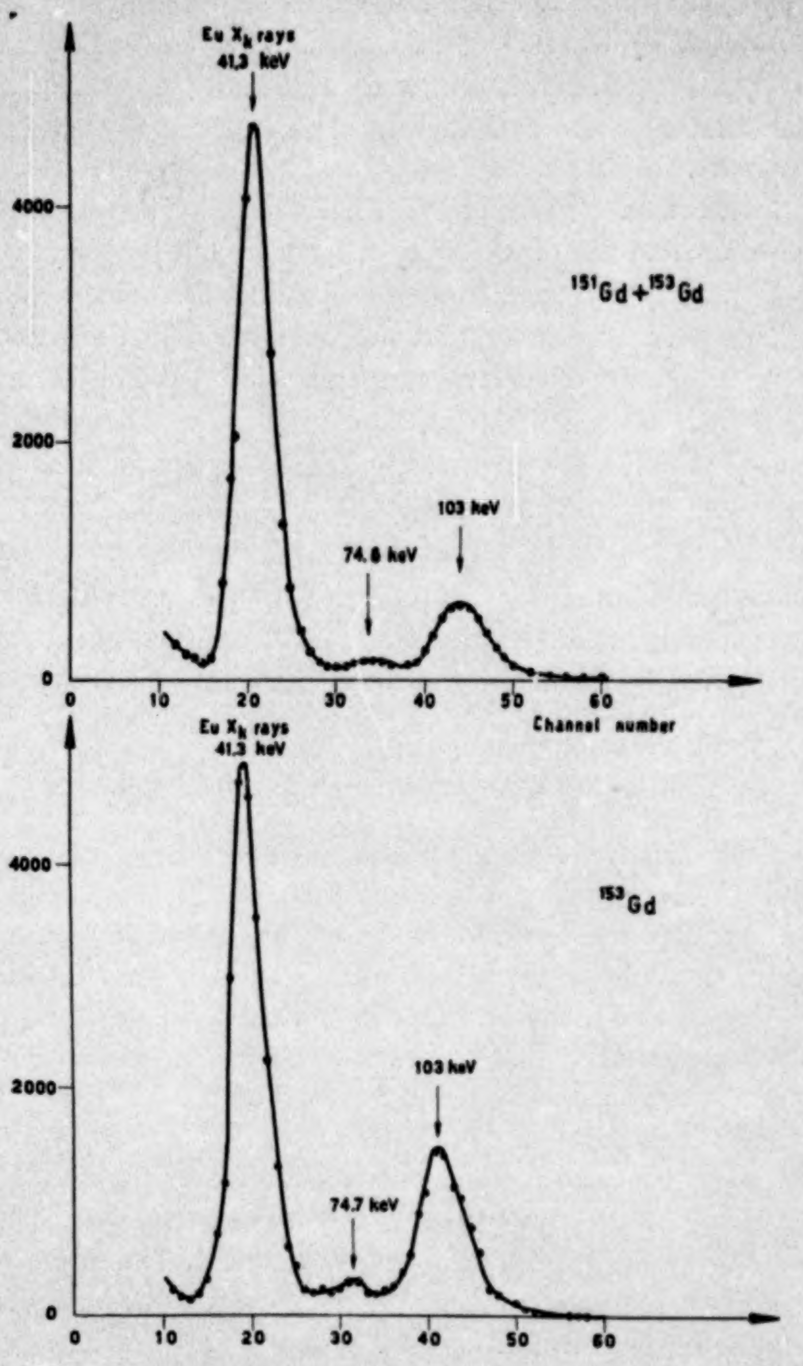

Fig. 1. Gamma ray spectra in the energy interval between 25 keV and 140 keV: sources of ^{151}Gd+^{153}Gd and of pure ^{153}Gd.

No lines of energy higher than 300 keV were found to be emitted from ^{151}Gd: very weak peaks were noticed and their energies roughly calibrated as 700 keV, 950 keV and 1.2 MeV. It was concluded that they do not belong to the spectrum of ^{151}Gd and the following considerations support such a conclusion:

a) in the irradiation of Eu with 26 MeV deuterons the long lived negaton emitter ^{154} Eu is also expected to be produced in a (d, p) reaction and some of the above quoted energies are consistent with what was observed in the decay of ^{154}Eu [4]).

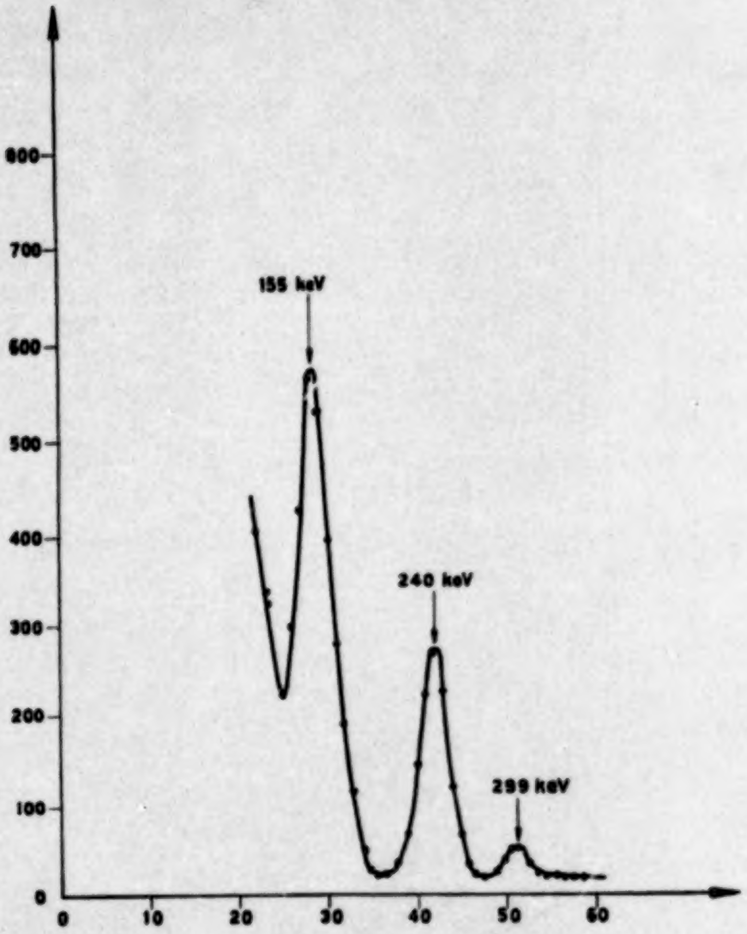

Fig. 2. Gamma ray spectrum from ^{151}Gd for energies above 110 keV.

b) in coincidence measurements, when the K X-rays peak from Eu was used to trigger the coincidence circuit, high energy γ-rays were still found but their total intensity turned out to be lowered by a factor 50 or thereabout, in comparison with the low energy lines. This fact shows that high energy gammas are time coincident with only a few X-rays, as expected for a negaton decay and for very weakly internally converted hard γ-rays.

c) a weak emission of negatons whose end point is more than 500 keV, was observed. This circumstance is consistent with the hypothesis that the spurious activity is due to ^{154}Eu.

d) high energy γ-rays seem to decay with a half-life which is definitely longer than 200 d.

A spectrum of low energy X- and γ-rays from the ^{151}Gd+^{153}Gd source is given in fig. 3. Besides the L X- and K X-peaks a γ-line at 21.3±0.2 keV (belonging to ^{151}Gd) is readily detectable by means of the proportional counter. This line is most probably the one which has been found in the decay of ^{151}Sm.

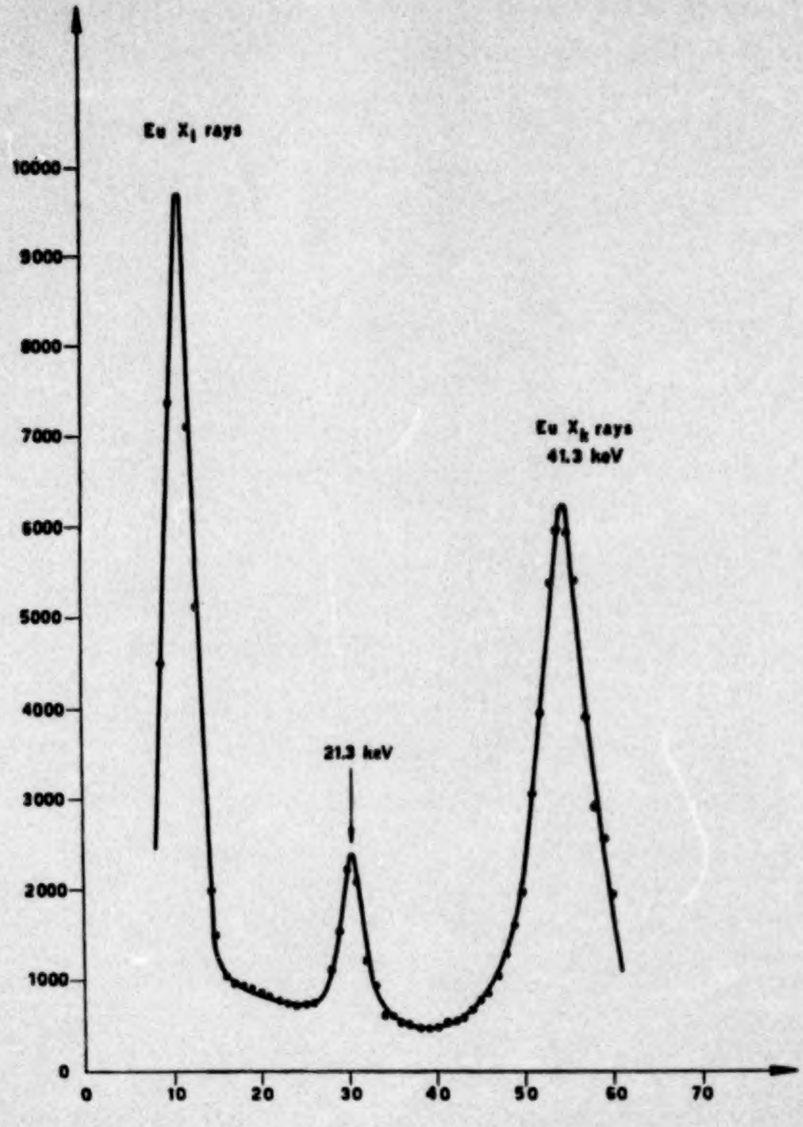

Fig. 3. Low energy radiations from a source of ^{151}Gd+^{153}Gd.

Table 1 summarizes the above results: after a normalization of the intensity of the 103 keV line from ^{153}Gd, the contribution of ^{153}Gd was subtracted. Energies are quoted and relative intensities, corrected if necessary for counter efficiencies and escape peaks, are given.

TABLE I

Energy (keV)	Intensity
21.3±0.2	0.046
K X-rays	1
152 ±5	0.06
240 ±5	0.04
299 ±10	≈ 0.003

4. Coincidence Measurements

Besides the 299 keV line, which was too weak, all the peaks which are listed in table 1 were used in coincidence measurements. In any case, only pulses belonging to one definite photopeak were allowed to trigger the coincidence circuit (2μs resolving time).

A peculiarity of the decay of ^{151}Gd seems to be the absence of reasonably intense $\gamma-\gamma$ coincidence rates, so that the measurements described here were not very helpful in building up a decay scheme of ^{151}Gd.

Satisfactorily high counting rates were obtained when K X-rays acted as triggering peak: the above mentioned lines were all found to be time coincident with K X-rays. Comparison between the intensity ratios resulting from coincidence measurements and from the spectra given in fig. 1 and fig. 2 would in principle give some data about the features of the decay of ^{151}Gd, but the equations involved are too complicated to give reliable results.

The counting rates were extremely low and statistically significant results could not consequently be obtained when 21.3 keV and the 240 keV lines were used to trigger the coincidence circuit. On the other hand a good evidence was obtained that the 152 keV line is in cascade with one weak peak whose energy resulted to be about 140 keV.

5. Internal Conversion Spectrum

The active sample used for the measurements with the β-ray spectrometer was obtained by electroplating thin Cu foils ($\approx$ 0.5 mg/cm^2) in a solution of Gd_2Cl_3 in pyridine, making use of stainless steel rotating anode. The sample was 0.05 mg/cm^2 thick. The window of the Geiger counter, a nylon film, did not introduce any distortions in the spectrum above 45 keV. The resolution of the spectrometer was set at 3.5 %.

The spectrum of internal conversion electrons is shown in fig. 4. By taking into account the energies of the peaks, their relative intensities and a comparison with the conversion spectrum of pure ^{153}Gd, the following conclusions can be easily deduced:

a) the most intense peak, quoted as γ_{0K} peak, is due to the K-conversion of the 103 keV γ-ray from ^{153}Gd. The lower energy peaks can be primarily identified as groups of Auger lines.

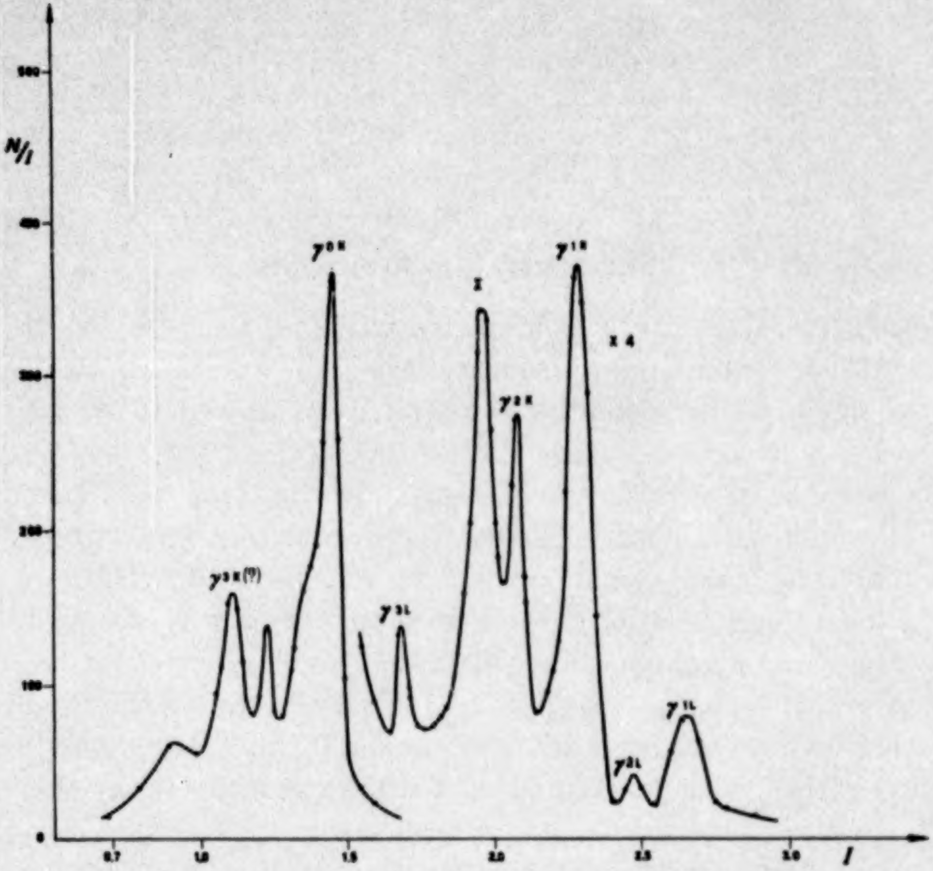

Fig. 4. Spectrum of internal conversion electrons from a source of ^{151}Gd+^{153}Gd.

b) the γ_{1K}- and γ_{1L}-peaks arise respectively from K- and L+M-shell conversion of a γ-ray at 176 keV energy. This γ-ray must be strongly converted as its presence was not noticed in the γ-ray spectrum. The γ_{2K} and γ_{2L} peaks are due to K- and L+M-shell conversion of a γ-ray at 155 keV (the same reported in the previous sections). The weak γ_{3L} peak arises from the L+M shell conversion of a γ-ray at 80 keV whose K-conversion line occurs in the spectral region that was distorted by the presence of the Auger lines and by the absorption of the Geiger window. The Σ peak occurs at the expected value of the energy as required by the L+M-conversion line of the 103 keV γ-ray, but its intensity with respect to that of the γ_{0K} peak differs strongly from the intensity observed in the conversion spectrum of pure ^{153}Gd. It is likely to be a composite peak containing the K-conversion line of a γ-ray of 144 keV energy whose presence was noticed in the coincidence measurements.

As regards the higher energy γ-rays, the conversion was investigated by using a thicker sample. Only the presence of very weak conversion lines of the 250 keV γ-ray was clearly revealed.

The interpretation of the conversion spectrum is summed up in table 2 which includes also a few K/L conversion ratios. No accurate values for the K- and L-conversion coefficients could be obtained, owing to the total absence of the 176 keV peak in the γ-spectrum and to the fact that the 155 keV γ-peak was a composite one.

TABLE 2

Energy of electron line (keV)	Conversion Shell	Corresponding γ-transition (keV)	K/L conversion ratio
54.5	K	103 (^{153}Gd)	
72.5	L+M	80	
95.5	L+M K	103 144	
106.8	K	155.3	> 10
127.5	K	176	4.8
147.4	L+M	155	
167.8	L+M	176	
191.5	K	240	≈ 1
232	L+M	240	

6. Decay Scheme

The level scheme of ^{151}Eu can be tentatively deduced from the reported observations.

The γ-ray of 21.3 keV energy was assumed to arise from the deexcitation of the first level owing to the fact that in the decay of ^{151}Sm (96 keV transition energy) only one γ-ray having this same energy was observed. The values of the energy of the other γ-rays suggest the following conclusions:

a) the 176 keV γ-ray can be interpreted as a crossover transition from a 176 keV level to the ground level. The deexcitation of this level to the 21.3 keV level occurs through the 155 keV γ-ray.

b) the 320 keV level, whose deexcitation leads to all other levels except the fundamental one, accounts in a simple way for the other γ-rays and for the coincidence measurements.

The decay scheme given in fig. 5 is consequently proposed. It will be noticed that in this scheme the 240 keV and the 80 keV γ-rays can be interchanged, provided a level at 240 keV is substituted for the one at 80 keV. No definite reasons could be found to prefer either alternative.

A comparison between the present results and those obtained by Heydenburg and Temmer ^{3}) seems to point out that the Coulomb excitation and the decay from ^{151}Gd lead to a different level succession.

As regards spins and parities of the levels, some reasonable assignements can be made on the basis of the above mentioned K/L values, but as the experimental results do not support them strictly, we prefer to omit the orbitals from the scheme.

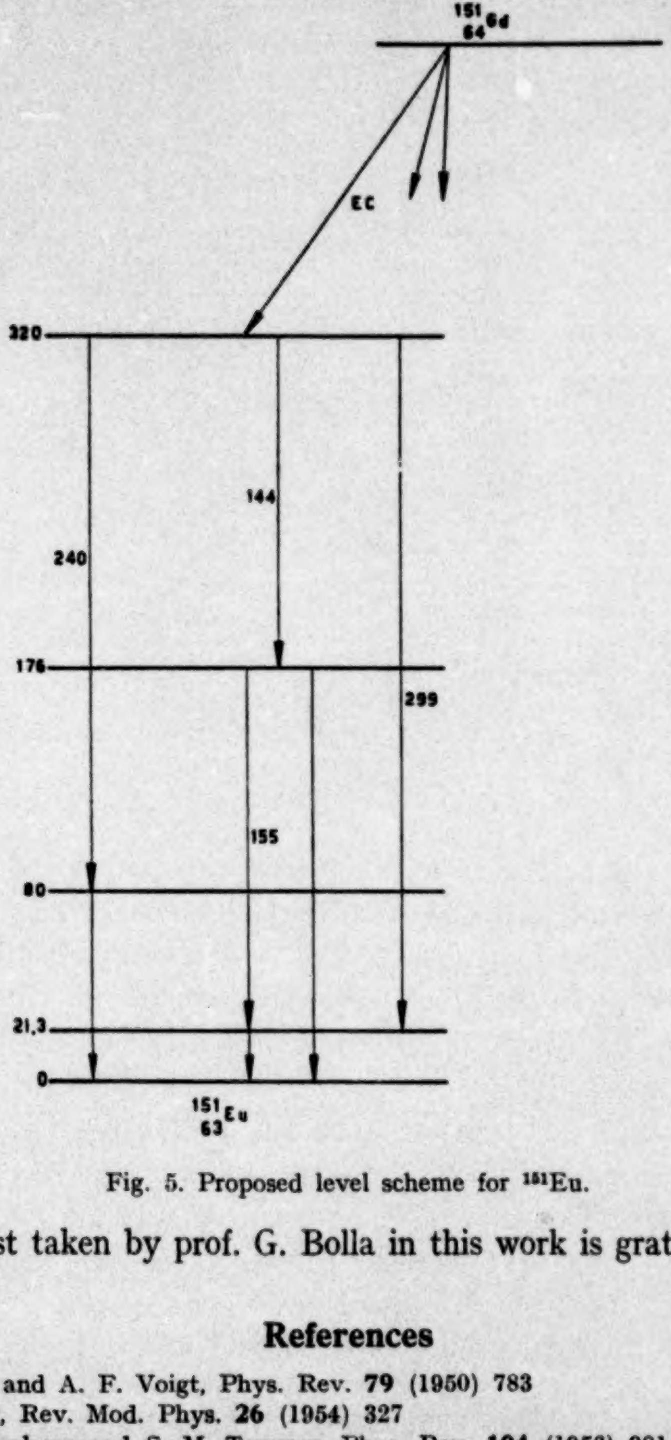

Fig. 5. Proposed level scheme for ^{151}Eu.

The interest taken by prof. G. Bolla in this work is gratefully acknowledged.

References

1) R. E. Hein and A. F. Voigt, Phys. Rev. **79** (1950) 783
2) R. W. King, Rev. Mod. Phys. **26** (1954) 327
3) N. P. Heydenburg and G. M. Temmer, Phys. Rev. **104** (1956) 981
4) J. M. Hollander, I. Perlmann and G. T. Seaborg, Rev. Mod. Phys. **25** (1953) 469
5) S. K. Bhattacherjee and Shree Raman, Nuclear Physics **1** (1956) 486
6) A. Bisi, E. Germagnoli and L. Zappa, Nuclear Physics **1** (1956) 593
7) R. K. Gupta and S. Jha, Nuovo Cimento **4** (1956) 88
8) N. Marty et M. M. Vergnes, Comptes Rendus Acad. Sci. **242** (1956) 1438

Nuclear Physics **3** (1957) 679—688; *North-Holland Publishing Co., Amsterdam*

A THEORETICAL ESTIMATE OF THE INFLUENCE OF THE CHARACTER OF THE FOUR-FERMION INTERACTION ON THE MUON CAPTURE RATE

H. A. TOLHOEK AND J. R. LUYTEN
Lorentz-Institute, University of Leyden

Received 15 March 1957

Abstract: The four fermion interaction for muon capture may contain the Fermi interaction as well as the Gamow-Teller interaction, similar to the situation for the beta radioactivity. Theoretical calculations of the muon capture rate were made for both types of interaction for the nuclei from Ca to Ni, assuming nuclear shell structure. It follows that an experimental determination of the ratio of Fermi to Gamow-Teller interaction should be feasible by measuring the ratio of muon capture rates in suitably chosen nuclei (preferably the separated isotopes, although the use of the natural isotope mixtures is not quite excluded). The ratio of the capture rates for two nuclei differs often up to 50 % for Fermi and Gamow-Teller interaction. As several simplifying assumptions were made, the results of the calculations may have more qualitative than quantitative significance; however, the results obtained seem to justify further theoretical and experimental work on the subject.

The published experimental data do not allow to draw any conclusions with certainty, but may contain an indication for preponderant Gamow-Teller interaction.

1. Introduction

In 1949 several authors [1]) noticed that the coupling constant for the four-fermion processes: beta decay, muon decay and muon capture were equal within the limits of the experimental uncertainties, which at that time were rather large. Since then, a considerable amount of experimental work has made our knowledge of the beta interaction more precise [18, 19]), and has given some information on the muon decay interaction.

In particular data were obtained making possible the determination out of which of the five "pure" interactions: the scalar (S), vector (V), tensor (T), axial vector (A) and pseudoscalar (P) the actual beta interaction is composed; now it can be said that this interaction consists mainly of S and T [19]).

Although quite a number of experimental data on muon capture are available [2–12, 14–16]) they are not so accurate that a conclusion as to the character of the interaction can be drawn. The theory for muon capture was developed by Tiomno and Wheeler [1]), Kennedy [23]), Primakoff [13]) and Rudik [21]). These authors generally do not consider the influence of the character of the interaction on the muon capture rates (except for a calculation by Rudik [21]), and a short remark by Primakoff [13])).

It would be most interesting if experiments could be designed from which the character of the interaction could be deduced, and then to compare the muon capture interaction with beta decay also in this respect (cf. ref. [17])). In this paper we investigate whether shell model effects might influence the ratio of the capture rates of pairs of nuclei in such a way that information on the character of the interaction for muon capture could be obtained from such experimental data.

2. Principle of Calculations

The muon capture process is highly analogous to K-electron capture. The transition probability for a transition between definite initial and final states of one nucleon may be calculated by first-order perturbation theory as

$$\lambda = \frac{2\pi}{\hbar} |M|^2 \varrho_{\mathrm{F}}, \tag{1}$$

where ϱ_{F} is the density of final states and M the matrix element for this transition. M is of the form

$$M = g_{\mu c} \sum_k \int (\psi_{\mathrm{n}}{}^* \Omega_k \psi_{\mathrm{p}})(\psi_\nu{}^* \Omega_k \psi_\mu) \mathrm{d}V, \tag{2}$$

where $g_{\mu c}$ is the coupling constant for muon capture and n, p, ν, μ refer to neutron, proton, neutrino and muon respectively. Ω_k is a Dirac operator, depending on the character of the interaction assumed; the summation Σ_k is a summation over the various components of a particular Dirac operator. The integration is to be extended over a suitably chosen large volume in which the wave-functions are normalized. After accepting some model for the atomic nucleus, the one particle wave-functions ψ_{n}, ψ_{p} can be calculated and (2) can be determined; in this paper the nuclear shell model will be used for this purpose (cf. § 3.)

The total capture probability is then found from the sum of all $|M|^2$ for transitions from all proton states present in the nucleus to all states available as final states for the neutrons; states already occupied by neutrons are not available as final states in consequence of the Pauli principle. The difference between muon-capture and K-capture is, that in muon capture transitions between several nucleon states contribute appreciably to the total capture probability. This is caused by the much higher energy release in muon capture. Consequently in muon capture no definite selection rules, stating when a transition is allowed, can be formulated. Hence it might be expected that because of this averaging over several initial and final proton and neutron states the type of interaction will affect the capture rate less than is usual in beta-processes. However, the calculations show that the number of transitions contributing is not very large, and that measurable effects are to be expected in many nuclei.

3. Details of Calculations and Assumptions

For the present purpose we introduce a number of simplifying assumptions, essentially following the method of calculation of Kennedy [23]).

(1) The muon capture rate may be calculated for a pure interaction. However, the most general interaction is a mixture of the five pure interactions

$$H_{\mu c} = g_{\mu c}[C_S H_S + C_V H_V + C_T H_T + C_A H_A + C_P H_P]. \tag{3}$$

(we shall assume expressions for H_S, $H_V \ldots$ exactly analogous to those, used in beta radio activity, cf. Rose [20])). The constants $C_S, \ldots, C_P$ are real for interactions invariant for time reversal, but may be complex, if this invariance does not hold. Parity non-conserving interactions have a form which differs from (3) [25]), but are equivalent to an interaction (3) as far as one is concerned with lifetimes for muon capture. The kinetic energies of proton, neutron and muon are rather small compared to their rest energy and we may neglect the small components of their Dirac wavefunctions. This has the consequence, that the Dirac operators for S and V reduce to 1, for T and A to $\boldsymbol{\sigma}$, and vanish for P, so that it is no longer possible to distinguish between S and V, or to distinguish between T and A interaction. (In beta processes a different situation exists, since both the neutrino and the electron may be relativistic.)

The interaction energy densities for pure interactions are written in the form

$$H_{\mu c} = g_{\mu c}(\psi_n{}^* \psi_p)(\psi_\nu{}^* \psi_\mu) \qquad \text{for S and V,} \tag{4}$$

$$H_{\mu c} = g_{\mu c}(\psi_n{}^* \boldsymbol{\sigma} \psi_p) \cdot (\psi_\nu{}^* \boldsymbol{\sigma} \psi_\mu) \qquad \text{for T and A.} \tag{5}$$

For a mixed interaction (3) the capture rate, λ, is

$$\lambda = |C_S + C_V|^2 \lambda_S + |C_T + C_A|^2 \lambda_T, \tag{6}$$

in which λ_S, λ_T are the capture rates for pure S and pure T interactions; the result for a mixed interaction thus follows immediately from the results found for pure S and pure T interaction.

(2) When we calculate "average" capture rates for (4) and (5) for the same value of $g_{\mu c}$ the result is 3 times larger for T, A-interaction than for S, V-interaction; so in comparing the results obtained for these interactions it is sometimes convenient to divide the result obtained with T, A interaction by 3. By "average" capture rate we mean the capture rate as one would calculate by averaging over different nuclear structures, or if one calculated the capture rate for a Fermi gas of independent particles.

(3) In finding ψ_n, ψ_p we used the nuclear shell model in its simplest form:

the ψ_n, ψ_p were found as single particle states in a spherical potential well of infinite depth (cf. [23])). The effect of the spin-orbit coupling was incorporated in the angular dependence of the wave-functions, but its effect on the radial dependence and energy were neglected. The order of the levels was assumed to be

$$\begin{array}{l} 1s_{\frac{1}{2}}\,(2);\quad 1p_{3/2}\,(4);\quad 1p_{\frac{1}{2}}\,(2);\quad 1d_{5/2}\,(6);\quad 2s_{\frac{1}{2}}\,(2); \\ 1d_{3/2}\,(4);\quad 1f_{7/2}\,(8);\quad 2p_{3/2}\,(4);\quad 1f_{5/2}\,(6);\quad 2p_{\frac{1}{2}}\,(2); \end{array} \tag{7}$$

(The numbers in parenthesis denote the number of particles possible in each state.)

The calculations were made for nuclei having from 20 to 28 protons and 20 to 32 neutrons, the particles from 21 to 28 thus going into the $1f_{7/2}$-shell and from 29 to 32 into the $2p_{3/2}$-shell (although in the actual nuclei pairs of $1f_{7/2}$ neutrons are not quite excluded for $N = 30$ and $N = 32$). The radius R of the potential well is assumed to be: $R = r_0 A^{1/3}$. Two different values were taken for r_0 ($r_0 = 1.15 \times 10^{-13}$ cm and $r_0 = 1.40 \times 10^{-13}$ cm) in order to see whether the results are sensitive to a change in the radius. (One should not confuse the radius of the (infinite) potential well with the radius of matter distribution; this latter radius found from the wave-functions in an infinite potential well is appreciably smaller than the radius of this well, so that the value of $r_0 = 1.40 \times 10^{-15}$ cm will give a radius for the matter distribution which is closest to reality.)

(4) As we use a potential well of infinite depth the final neutron states are always discrete states; in the actual nucleus free states should be taken as final states. However, one may hope that the behaviour of the wave-function inside the nucleus will not differ too much in both cases. (This same approximation was also made by Kennedy [23]); cf. ref. [16]).)

(5) The meson wave-function was assumed to be a constant throughout the nucleus. Its value was taken from a calculation by Wheeler, who solved the wave equation for the meson in the field of a charge Ze, uniformly distributed over the nuclear volume, cf. ref. [24]).

For the neutrino wave-function the free space solutions with definite angular momentum were taken.

(6) The neutrino is always relativistic and its wave-function has four components of similar magnitude of which only two enter in the calculations, the other two being multiplied into the small components of the muon wave-function. One can show that consequently one should normalize these two components to give $\frac{1}{2}$ when integrated over coordinate space[†].

(7) As in all cases the neutrino wavelength was large, compared to the nuclear radius, the value of the matrix element decreases rapidly for in-

---

[†] In consequence of this our value for the capture rate in Ca comes out $\frac{1}{2}$ of the value found by Kennedy who normalized these two components of the neutrino function to 1.

creasing l_ν because the neutrino wave function behaves as r^{l_ν} for small r. Therefore we calculated the matrix element only for the smallest value of l_ν which gives a non-zero result.

(8) The matrix elements for transitions from specific proton to neutron states are all averaged over the nuclear orientations (magnetic quantum numbers); the total contribution is then obtained by multiplying by the number of initial protons and by the number of final empty neutron states. Such a procedure is justified if either the initial or final states belong to a completely filled (or completely empty) shell; in other cases it means that the influence of the relative orientation or protons and neutrons, such as occurs in the nucleus, is neglected.

TABLE 1

Values of the matrix elements for partial transitions

Transition	$\Sigma\|M\|^2$ (S, V)	$\frac{1}{3}\Sigma\ \|M\|^2$(T, A)
$1f_{7/2} \rightarrow 1f_{5/2}$ (0)	0 (0)	280 (303)
$1f_{7/2} \rightarrow 1f_{7/2}$ (0)	490 (530)	210 (227)
$1d_{5/2} \rightarrow 1f_{7/2}$ (1)	210 (151)	100 (71)
$1d_{3/2} \rightarrow 1f_{7/2}$ (1)	0 (0)	110 (80)
$1d_{5/2} \rightarrow 1f_{5/2}$ (1)	10 (7)	121 (88)
$1d_{3/2} \rightarrow 1f_{5/2}$ (1)	145 (106)	34 (25)
$1f_{7/2} \rightarrow 1g_{9/2}$ (1)	245 (188)	105 (88)
$1f_{7/2} \rightarrow 1g_{7/2}$ (1)	7 (5)	148 (113)
$2s_{\frac{1}{2}} \rightarrow 2p_{3/2}$ (1)	33 (26)	33 (26)
$2s_{\frac{1}{2}} \rightarrow 2p_{\frac{1}{2}}$ (1)	16 (13)	16 (13)

In the column "transition" the spectroscopic notation refers to the states of proton and neutron respectively; the number in parentheses is the angular momentum of the neutrino. The second column has the sum of $|M|^2$ in arbitrary units, where the M are calculated for S or V interaction and the summation is extended over the magnetic quantum numbers of proton and neutron. The numbers in parentheses result from using a radius of the potential well with $r_0 = 1.15\times 10^{-13}$ cm and the others with $r_0 = 1.40\times 10^{-13}$ cm. The third column shows the same thing for the sum of $|M|^2$ calculated for V or A interaction, but now divided by a factor of 3 for the reason mentioned in § 3 (2).

The effect of this division by 3 is, that as soon as the transitions $n, l, j \rightarrow n', l', j' = l'+\frac{1}{2}$ and $n, l, j \rightarrow n', l', j' = l'-\frac{1}{2}$ contribute equally we get the same result for S, V interaction as for T, A interaction (for example: $0+490 = 280+210$, etc.); this result is quite general and forms the basis for the remark § 3 (2).

(9) The expression for the matrix element (2) can be split in a radial and an angular part; we first calculated the radial integrals for all transitions and calculated the angular parts only in those cases where a large radial integral had been found. (We neglected all integrals smaller than 0.1 times the largest one; the capture rate, depending on the square of the matrix element will thus only be slightly affected.)

(10) The integral over the radial part of the wave-function can be written as a product of an expression, containing R, and a dimensionless integral. However, this integral depends on the relative wavelength of the neutrino (i.e. its wavelength compared to the nuclear radius) and this changes somewhat in going from element to element. As this change was rather a slow one, we neglected it.

4. Results of Calculations and Conclusions

The results of these calculations are shown in table 1; the numbers are, in arbitrary units, the squares of the matrix elements summed over the magnetic quantum numbers of proton and neutron; so they give the contribution to the capture rate for all transitions from an entirely filled proton shell to a totally empty neutron shell. From this table it appears that a large difference in calculated capture rate will occur in those cases where the transitions $1\mathrm{f}_{7/2} \rightarrow 1\mathrm{f}_{5/2}$ $(l_\nu = 0)$ and $\mathrm{if}_{7/2} \rightarrow 1\mathrm{f}_{7/2}$ $(l_\nu = 0)$ contribute differently. In a ^{52}Cr nucleus, for example, the latter transition is impossible, as all final $1\mathrm{f}_{7/2}$-states are already occupied by neutrons. The capture rate in ^{52}Cr thus comes out much larger for T, A interaction than for S, V.

From this table we calculated the capture rates for the stable nuclei with 20 to 28 protons and 20 to 32 neutrons; the result is shown in table 2. It is easily seen from this table that the ratio of the capture rates for two nuclei may depend on the character of the interaction and that differences of 20—40 % are quite common; hence it seems feasible to determine the mixing ratio of the two types of interaction by measuring the ratio of capture rates in two suitably chosen nuclei.

According to the average Z^4_{eff}-law for muon capture derived by Wheeler and Tiomno [1, 24]) the capture rates should increase by a factor 2.5 from $Z = 20$ to 28, cf. ref. [22]). One sees from table 2 that our results show an increase, but also very substantial fluctuations from any possible average law.

On the basis of the nuclear shell model, one would not expect the $Z^4{}_{\mathrm{eff}}$-law to hold for the heavier elements; the largest matrix elements come from transitions $nl \rightarrow n'l'$ with $n = n'$, $l = l'$, and in the heaviest elements these transitions are generally impossible as for all proton states the corresponding neutron states are entirely occupied; the heavy

TABLE 2

Muon capture rates λ_S for Fermi interaction (S or V) and λ_T for Gamow-Teller interaction (T or A).

N \ Z	20 Ca	21 Sc	22 Ti	23 V	24 Cr	25 Mn	26 Fe	27 Co	28 Ni
32							146(181) 231(333)	165(206) 268(391)	185(232) 308(452)
31							151(188) 237(342)		
30					119(146) 172(240)	137(170) 207(294)	157(195) 245(351)		198(249) 325(475)
29					124(153) 178(248)				
28			94(114) 118(157)	111(136) 150(204)	129(159) 184(256)		169(210) 259(370)		
27			110(136) 131(175)						
26			127(159) 146(193)		180(233) 222(308)				
25			144(183) 160(211)						
24	101(120) 101(120)	130(162) 136(173)	162(208) 175(231)						
23									
22									
21									
20	146(173) 146(173)								

In each square the upper numbers give λ_S divided by $10^{101}\, g^2_{\mu c}$; the lower numbers give λ_T divided by $3\times10^{101}\, g^2_{\mu c}$. The capture rates were calculated for two values for the radii of the potential wells: the values in parentheses correspond to a value $r_0 = 1.15\times10^{-13}$ cm, the others to $r_0 = 1.40\times10^{-13}$ cm. The values for λ are given in c.g.s. units. The squares surrounded by heavy lines are for nuclei which have a closed shell structure for either neutrons or protons; for these nuclei the results are probably more reliable than for the others.

elements containing much more neutrons than protons, cf. ref. [13]).

In table 3 we have collected, as examples, some ratios of capture rates for pairs of nuclei with a closed shell structure for either protons or neutrons (for which nuclei the results are most reliable, cf. § 3 (8)). The numbers in parentheses denote the results for the smaller of the two radii of the potential well which were chosen. It is seen that the results are affected by the value assumed for this radius, but that qualitative conslusions remain possible in spite of some uncertainty in the wave functions such as resulting from different radii. The ratio of capture rates in ^{40}Ca and ^{44}Ca is included in the table because it might provide a test of the theory: the ratio is independent of the character of the interaction and nearly independent of the potential well radius.

TABLE 3

Ratios of capture rates in some pairs of nuclei

Nuclei being compared	Ratio for S, V	Ratio for T, A
^{52}Cr/^{40}Ca	0.88 (0.92)	1.26 (1.48)
^{58}Fe/^{40}Ca	1.00 (1.05)	1.58 (1.92)
^{54}Fe/^{40}Ca	1.15 (1.22)	1.77 (2.14)
^{54}Fe/^{50}Ti	1.80 (1.85)	2.19 (2.36)
^{60}Ni/^{40}Ca	1.27 (1.34)	2.11 (2.60)
^{51}V/^{40}Ca	0.76 (0.79)	1.03 (1.18)
^{44}Ca/^{40}Ca	0.69 (0.695)	0.69 (0.695)

The second column gives the ratio for S, V, the third column for T, A interaction. These nuclei have all a closed shell structure either for the protons or for the neutrons.

As it will be much simpler to do the experiments for the natural isotopic mixtures than for the pure isotopes we also calculated the capture rates in the natural elements; they are given in table 4. However, the results

TABLE 4

Capture rates for the natural isotopic mixtures of the elements

145(172)	130(162)	128(161)	111(136)	130(161)	137(170)	157(196)	165(206)	194(244)
145(172)	136(173)	147(194)	150(204)	185(257)	207(294)	246(352)	268(391)	320(476)
Ca	Sc	Ti	V	Cr	Mn	Fe	Co	Ni

The numbers are presented in the same way as in table 2.

may be less reliable than those mentioned in table **3** for the reasons given in § **3** (8).

From our results we conclude that further experimental and theoretical work on muon capture in order to find the character of the interaction is justified. A theoretical improvement concerning the wave functions is straightforward: one should use the more realistic wave-functions belonging to a potential well of finite depth and with rounded-off edges. However, also other less straightforward improvements may be desirable; for this purpose critical considerations on the limitations of the nuclear shell model are required, in particular with respect to problems concerning correlations between nucleons and excitations of more than one nucleon. It is therefore not excluded that the experimental study of muon capture will provide a number of data on nuclear structure.

The problem of determining the character of the interaction for muon-capture is to a high extent analogous to the problem of determining the character of the beta interaction. The character of both interactions could in principle be determined from the transition probabilities for two nuclei only. It was suggested by Rudik[21]) and Primakoff[13]) to determine the (very small) muon capture rates for H and D for this purpose. Determinations of muon capture rates for many nuclei, as proposed here, give the possibility of different checks and may teach something on nuclear structure in addition. Also the capture rates for heavier nuclei are larger and are easier to measure; on the other hand the disadvantage is that the theoretical analysis (analogous to some extent to analysis for beta-interaction as given by Kofoed-Hansen and Winther [19])) is much more complicated.

From calculations as those given by Kennedy or ourselves a value can be obtained for the coupling constant $g_{\mu c}$, which depend on the character of the interaction. In beta processes the parameter x, defined by

$$x = |C_{\mathrm{T}}|^2/(|C_{\mathrm{S}}'|^2+|C_{\mathrm{T}}|^2), \tag{8}$$

was determined from the experimental data to be $x = 0.56$ (cf. ref. [19])).

Should one assume the muon-capture interaction to be composed of S and T interaction in this same ratio, the coupling $g_{\mu c}$ for muon capture constant comes out from the measured capture rate in Fe (cf. ref. [6])) as

$$g_{\mu c} = 3.6\times 10^{-49} \text{ erg} \cdot \text{cm}^3. \tag{9}$$

One may compare this with the value of the coupling constant

$$g_{\beta} = 2.11\times 10^{-49} \text{ erg} \cdot \text{cm}^3 \tag{10}$$

for the beta interaction. (This value follows from the value $B = 2787\pm 70$ sec given in ref. [19]).)

The most extensive experimental data which are available seem to be those of Weinrich and Ledermann [14]). The capture rates for the natural isotope mixtures for Ca, Ti and Fe are given as 2.40 ± 0.40; 2.65 ± 0.50; $4.25 \pm 0.50 (\times 10^6 \text{ sec}^{-1})$ respectively. Comparing with table 4 we see that this would agree (within experimental error) with pure T, A interaction, not with pure S, V interaction. However, it should be emphasized that our calculations are of a preliminary nature and are meant to decide whether an observable influence of the character of the interaction on the muon capture rate exists. Therefore our results will only be qualitative or at best semi-quantitative. (For this reason we do not dare to give an estimate of the error in the value (9).)

The authors are indebted to professors J. A. Wheeler, S. R. de Groot, V. L. Fitch and J. Steinberger for valuable discussions. This work is part of the research program of the Foundation for Fundamental Research of Matter (Stichting F.O.M.), which is financially supported by the Netherlands Organization for Pure Scientific Research (Z.W.O.).

References

1) J. Tiomno and J. A. Wheeler, Rev. Mod. Phys. **21** (1949) 153
2) H. K. Ticho, Phys. Rev. **74** (1948) 492
3) H. K. Ticho, Phys. Rev. **74** (1948) 1337
4) C. W. Kissinger and D. Cooper, Phys. Rev. **74** (1948) 349
5) F. B. Harrison, J. W. Keuffel and G. T. Reynolds, Phys. Rev. **83** (1951) 680
6) J. W. Keuffel, F. B. Harrison, T. N. K. Godfrey and G. T. Reynolds, Phys. Rev. **87** (1952) 942
7) T. N. K. Godfrey, Phys. Rev. **92** (1953) 512
8) A. G. Tenner, Physica **20** (1954) 24
9) N. N. Biswas and M. S. Sinha, Phys. Rev. **94** (1954) 1400
10) A. Alberigi Quaranta and E. Pancini, Nuovo Cimento **9** (1952) 959
11) A. H. Benade, Phys. Rev. **91** (1953) 971
12) G. T. Reynolds, Proc. 3rd Rochester Conf. (1952) 94
13) H. Primakoff, Proc. 5th Rochester Conf. (1955) 174
14) M. Weinrich and L. M. Ledermann, Bull. Am. Phys. Soc. (II) **1** (1956) 174; CERN Symposium Vol. 2 (Genève, 1956) p. 427
15) A. Alberigi Quaranta and E. Pancini, Nuovo Cimento **11** (1954) 607
16) A. M. Conforto and R. D. Sard, Phys. Rev. **86** (1952) 465
17) L. Michel and A. Wightman, Phys. Rev. **93** (1954) 354
18) C. S. Wu, Beta and gamma ray spectroscopy (ed. K. Siegbahn) (Amsterdam, 1955) Chapter XI, pp. 314–356
19) O. Kofoed-Hansen and A. Winther, Mat. Fys. Medd. Dan. Vid. Selsk. **27** (1953) no. 14; and a reexamination of the data (1956) in course of publication
20) M. E. Rose, Beta and gamma ray spectroscopy (ed. K. Siegbahn) (Amsterdam, 1955) Chapter IX, p. 277
21) A. Rudik, Dokl. Akad. Nauk. S.S.S.R. **92** (1953) 739
22) F. Ferrari and C. Villi, Phys. Rev. **96** (1954) 1159
23) J. M. Kennedy, Phys. Rev. **87** (1952) 953
24) J. A. Wheeler, Rev. Mod. Phys. **21** (1949) 133
25) C. N. Yang and T. D. Lee, Phys. Rev. **104** (1956) 254

Nuclear Physics 3 (1957) 689—690; *North-Holland Publishing Co., Amsterdam*

MAGNETIC MOMENT OF THE ELECTRON

A. PETERMANN
CERN *Theoretical study division,*
Institute for theoretical physics, Copenhagen

Received 28 May 1957

Recent measurements of the magnetic moment of the electron have cast some doubt either on the validity of quantum electrodynamics in its actual form or on the exactness of the theoretical calculations. In fourth order, the latter are made so lengthy and intricate by the great number of the integrals over auxiliary variables that this possibility cannot a priori be excluded.

The present note explains how the last possibility has been investigated. Owing to the experimental uncertainties, which are at least of the same order of magnitude as the fourth order corrections, many figures in the result are not so interesting. Accordingly, the numerical results for the terms I, IIa—IIe in the work by Karplus and Kroll [1]) have been checked by rigorous upper and lower bounds. Whereas every other term fell well between these bounds, agreement could not be obtained for diagram IIc. Here, therefore, some of the big contributions have been evaluated analytically, the others estimated by analytic upper and lower bounds. The numerical value for this term has been found to satisfy

$$\mu_{\text{IIc}} = (-1.02 \pm 0.53)\alpha^2/\pi^2 \text{ Bohr magnetons.}^{\dagger} \qquad (1)$$

Moreover, to provide some check of the numerous integrations and the tedious algebra, the much less elegant, but safe and fast numerical integrations have been performed for this term. They confirmed every time the bounds derived before. However, here again, analytic integrations have been used to compute the contribution of the logarithmic tails.

It is not claimed here that the numerical results for the terms I, IIa, d, e quoted in Karplus and Kroll are exact, but only that they lie between the bounds found and are not in contradiction with them. If one accepts for these the values given by Karplus and Kroll, the total magnetic moment in fourth order would turn out to be

$$\mu^{(4)} = (-0.81 \pm 0.53)\alpha^2/\pi^2 \text{ Bohr magnetons.} \qquad (2)$$

This result agrees fairly well with the Stanford measurements [2]). As said

---

† After a term $-(\frac{1}{2}\alpha^2/\pi^2) \log \lambda^2/m^2$ (infra-red term) has been separated out. The value quoted by Karplus and Kroll for this term is $-3.18\alpha^2/\pi^2$.

before, it does not need to be refined as long as the experimental error remains so large (about four times the theoretical uncertainty).

It is of course very desirable that other checks of the fourth order magnetic moment should be performed. Mistakes are easily introduced in such long calculations.

The new value would also change slightly the value of the fine structure constant and increase the Lamb shift by an amount of (0.62 ± 0.16)Mc/s. But to assert a definite value to this effect other fourth order corrections computed by Weneser, Bersohn and Kroll [3]) have to be recalculated. Indeed, these authors used some integrals occurring in the magnetic moment calculation and the result is uncertain.

The author is grateful to Dr S. Deser and Dr G. Källen for many interesting discussions. He thanks Prof. N. Bohr for the hospitality extended to him at the Institute.

References

1) R. Karplus and N. M. Kroll, Phys. Rev. **77** (1950) 536
2) P. Franken and S. Liebes Jr, Phys. Rev. **104** (1956) 1197
3) J. Weneser, R. Bersohn and N. M. Kroll, Phys. Rev. **91** (1953) 1257

Nuclear Physics **3** (1957) 691; *North-Holland Publishing Co., Amsterdam*

BOOK REVIEWS

C. J. Gorter (editor), *Progress in low temperature physics*, Volume 2 (North Holland Publishing Co., Amsterdam. 1957. xi-480 pages. *f* 42, 84 s.)

The subject of this important volume falls almost entirely outside the scope of this journal: other reviewers will give it the praise it deserves. The purpose of this notice is to call attention to the 45-page chapter 'Orientation of atomic nuclei at low temperatures' by M. J. Steenland and H. A. Tolhoek, which provides an excellent up-to-date survey of a method of investigation of considerable interest and of the results it has hitherto achieved. The latest Wu experiments on the decay of oriented ^{60}Co nuclei, already world-famous before their publication, are not yet described in this article (even the publishers of *Nuclear Physics* cannot work miracles); but the idea and background of these experiments *is* duly reported by the authors, who also give an interesting outline of possible further applications of the method.

L. R.

J. Bass, *Cours de mathématiques* (Masson et Cie, Paris. 1956. xi-916 pages. Broché 7800 fr. fr., relié 8500 fr.fr.)

This volume contains the substance of the mathematical teaching given to the students of two great institutions of higher technological education in France: the Écoles Nationales Supérieures de l'Aéronautique and des Mines. It sweeps over the vast subject from higher algebra to analytical functions and partial differential equations, somewhat cursorily perhaps, but with typical French lucidity and precision. One should not look in this book for the elucidation of the deeper aspects, which are deliberately left out (but not without being at least mentioned); what it offers is a survey of mathematics as a tool, and from that point of view it may be of great service to physicists as well as to engineers.

L. R.

T. L. Hill, *Statistical mechanics*, Principles and selected applications (McGraw-Hill Book Co., New York, Toronto, London. 1956. xiii-432 pages. $9)

This book does not claim to treat all the aspects of statistical physics; its aim is to give an up-to-date exposition of a few important topics on which research has been and still is most active: imperfect gases and condensation, the liquid state, lattice theory. The brief discussion of the principles which forms the four first chapters of the book is quite neat so far as it goes, but (as usual) rather weak from the epistemological point of view; this matters little, however, since the emphasis of the book is on the systematic treatment of the special problems just mentioned. In this, the author is eminently successful and his work will be hailed not only by the specialists (from whom it will receive more adequate appraisal than this journal can give it), but also by the outsiders. To the latter, who might well feel a bit lost in the maze of difficult and sometimes conflicting papers devoted to these fascinating problems, it offers a clear, complete and well-ordered account of the present state of the questions.

L. R.

ERRATUM

R. E. White and F. J. M. Farley, *Polarisation in the inelastic scattering of neutrons by helium* (Nuclear Physics **3** (1957) 476). On page 477, it is stated that a maximum polarisation P_2 is obtained in theory when $\theta_2 = 76°$. A more detailed study of the theory has shown this statement to be incorrect.

AUTHOR INDEX

Alphonce, R., A. Johansson and G. Tibell, The polarization of 155 MeV protons elastically and inelastically scattered from carbon 185

Andersson, G. and I. Bergström, Note on the decay of Tl^{198m} 506

Andersson, G. and I. Bergström, Anomalous internal conversion ratios of E 3 transitions in the region $Z = 77-82$ 541

Andersson, G., P. A. Tove, B. Jung and I. B. Svensson, The isomeric transitions in Tl^{197} and Tl^{195}. 493

Arbman, E., Excited levels in Bi^{206} from the decay of Po^{206}. . . 625

Austern, N., *see* Levinger

Bartholomew, G. A., *see* Gove

Baumann, K., *see* Wildermuth

Bellicard, J. B., A. Moussa et S. K. Haynes, Étude des électrons Auger-K émis par le zinc 65. 307

Berestetsky, V. B., On interference phenomena in the decay of strange particles 157

Berestetsky, V. B. and Yu. A. Bychkov, K-meson scattering with change of intrinsic parity 153

Bergström, I., *see* Andersson

Bergström, I., *see* McDonell

Biedenharn, L. C., *see* Thaler

Bisi, A., E. Germagnoli and L. Zappa, The low-lying energy levels of ^{151}Eu 670

Bloch, C., La fonction densité (strength function) dans la théorie statistique des réactions nucléaires 137

Bowey, Eleanor M., Isotopic assignment of slow neutron resonances in germanium, rubidium, neodymium and tungsten 553

Burcham, W. E., W. M. Gibson, D. J. Prowse and J. Rotblat, Alpha-alpha scattering at 38.5 MeV 217

Bychkov, Yu. A., *see* Berestetsky

Class, C. M. and U. Meyer-Berkhout, The Coulomb excitation of Eu^{151} and Eu^{153} 656

Corinaldesi, E., Dispersion relations for the decay of the τ-meson 649

Deutsch, M., Electric monopole transition rate in Zr^{90} 83

Dolinsky, E. I., *see* Shapiro

El Bedewi, F. A. and M. A. El Wahab, An investigation of the reaction $^{23}Na(d, n)\ ^{24}Mg$. 385

El Wahab, M. A., *see* El Bedewi

D'Espagnat, B., R. Omnes and J. Prentki, Some remarks on decay rates of heavy mesons 471

D'Espagnat, B., J. Prentki and Abdus Salam, On symmetries in elementary particle interactions 446
Farley, F. J. M. and R. E. White, Neutron alpha particle angular correlation in the reaction ^{7}Li(d, α) and the ground state of ^{5}He 561
Farley, F. J. M., *see* White
Fowler, G. N. and A. W. Wolfendale, On the interactions of fast μ-mesons 299
Fowler, G. N., A possible explanation of the anomalous scattering of μ-mesons 121
Gerholm, T. R., *see* Herrlander
Germagnoli, E., *see* Bisi
Gibson, W. M., *see* Burcham
Gove, H. E., G. A. Bartholomew, E. B. Paul and A. E. Litherland, Erratum 344
Haynes, S. K., *see* Bellicard
Herrlander, C. J. and T. R. Gerholm, Excited levels in Hg^{200} studied from the decay of Tl^{200} 161
Herrlander, C. J., *see* McDonell
Herzenberg, A., Studies in the α-particle model of nuclei III. Calculation of the interaction between α-particles 1
Herzenberg, A. and A. S. Roberts, Studies in the α-particle model of nuclei IV. The polarisation forces between α-clusters in nuclei 314
Hillman, P. *see* Tyrén
Johansson, A., *see* Alphonce
Johansson, A., *see* Tyrén
Jung, B., *see* Andersson
Khalatnikov, I. M., Concerning the elastic scattering of high energy particles 433
Klema, E. D. and R. K. Osborn, Empirical determination of nuclear shape factors and moments of inertia 571
Koppe, H., Zur Theorie der β-Wechselwirkung 585
Lal, D., N. Narasappaya and P. K. Zutshi, Phosphorus isotopes P^{32} and P^{33} in rain water 69
Landau, L., On the conservation laws for weak interactions 127
Landé, A., Foundations of quantum mechanics, an anti-review 132
Lanius, K., Über die Zertrümmerung schwerer Kerne der Kernemulsion durch Teilchen der kosmischen Strahlung 391
Levinger, J. S., N. Austern and P. Morrison, The dipole sum rule with an approximate Hamiltonian 456
Levintov, I. I., A. V. Miller and V. N. Shamshev, A new method of measurement of neutron polarization and n-He^4 phase analysis 221
Levintov, I. I., A. V. Miller, E. Z. Tarumov and V. N. Shamshev,

Dependence of (D+D) neutron polarization on deuteron energy 237
Lindquist, T. and I. Marklund, The influence of *l*-forbiddenness on magnetic dipole transitions in Tl^{203} 367
Litherland, A. E., *see* Gove
Liubimov, A. L., *see* Zastavenko
Luyten, J. R., *see* Tolhoek
Maris, Th. A. J. and H. Tyrén, Inelastic high energy nucleon scattering on light nuclei (see also Erratum p. 344) 35
Maris, Th. A. J., Polarization of high energy nucleons exciting a collective level 213
Maris, Th. A. J., *see* Tyrén
Marklund, I., *see* Lindquist
Marty, C., Niveaux de rotation de noyaux sans axe de symétrie. 193
McCutchen, C. W., X-ray escape gating as applied to a proportional counter 76
McDonell, J. A., R. Stockendal, C. J. Herrlander and I. Bergström Levels in Pb^{202} and Tl^{202} populated from 3.62-h Pb^{202m} 513
Meyer-Berkhout, U., *see* Class
Miller, A. V., *see* Levintov
Mishakova, A. P., *see* Shapiro
Mitra, A. N., The fluctuation problem in μ-meson bursts 262
Morinaga, H. and D. C. Peaslee, Sum rule for optical nuclear reactions. 115
Morrison, P., *see* Levinger
Moussa, A., *see* Bellicard
Narasappaya, N., *see* Lal
Newton, J. O., The Coulomb excitation of U^{235}, Pu^{239} and U^{238} . 345
Nilsson, S., A decay of a negative τ' 364
Ofer, S., The energy levels of Hf^{177} and the unified model . . . 479
Ogievitsky, V. I., *see* Zastavenko
Omnes, R., *see* d' Espagnat
Oneda, S., On the universal interactions II: K-meson decays into pions 97
Oneda, S., Two-component theory of the neutrino and K-meson decays comprising two neutrinos 598
Osborn, R. K. *see* Klema
Paul, E. B., *see* Gove
Peaslee, D. C. Nuclear surfaces and zero-energy scattering . . . 255
Peaslee, D. C., *see* Morinaga
Petermann, A., Invariance properties and identities between renormalization constants 592
Petermann, A., Magnetic moment of the electron 689
Podgoretsky, M. I., *see* Zastavenko

Polkinghorne, J. C., Many-body forces and the many-body problem 94

Prentki, J., *see* d' Espagnat

Prowse, D. J., *see* Burcham

Puzikov, L., R. Ryndin and J. Smorodinsky, Construction of the scattering matrix of a two-nucleon system 436

Rasmussen, John O., *see* Strominger

Reignier, J., Sur la diffusion d'électrons de haute énergie par les noyaux 340

Roberts, A. S., *see* Herzenberg

Rotblat, J., *see* Burcham

Ryndin, R., *see* Puzikov

Salam, Abdus., *see* d' Espagnat

Scobie, J., Electron capture in arsenic 74 and arsenic 76 465

Shamshev, V. N., *see* Levintov

Shapiro, I. S., E. I. Dolinsky and A. P. Mishakova, On the spin and parity of the τ-meson. 60

Sikkema, C. P., Scattering of fast neutrons by neon in the energy region 1.9 to 3.5 MeV. 375

Smorodinsky, J., *see* Puzikov

Stockendal, R., *see* McDonell

Strominger Donald and John O. Rasmussen, Concerning lifetimes of low energy El gamma transitions in odd mass spheroidal nuclei 197

Svantesson, N. L., A scintillation spectrometer study of the photodisintegration of O^{16} 273

Svensson, I. B., *see* Andersson

Tarumov, E. Z., *see* Levintov

Taylor, J. C., Space-time reflections and isobaric spin. 606

Thaler, R. M. and L. C. Biedenharn, A note on the calculation of coulomb penetration and coulomb wave functions 207

Tibell, G., *see* Alphonce

Tolhoek, H. A. and J. R. Luyten, A theoretical estimate of the influence of the character of the four-fermion interaction on the muon capture rate 679

Tove, P. A., *see* Andersson

Tyrén, H. and Th. A. J. Maris, Studies of inelastic scattering of 185 MeV protons on carbon (see also Erratum p. 344). 52

Tyrén, H., Peter Hillman and A. Johansson, The polarization of 173 MeV protons inelastically scattered by carbon 336

Tyrén, H., *see* Maris

Villars, F., A note on rotational energy levels in nuclei 240

Vries, de Hl., Further analysis of the neutron component of the background of counters used for ^{14}C age measurements 65

Wahlborn, S., Levels in Bi^{206} 644
Weisskopf, V. F., The problem of an effective mass in nuclear matter 423
White, R. E. and F. J. M. Farley, Polarisation in the elastic scattering of neutrons by helium (see also Erratum p. 692) 476
White, R. E., *see* Farley
Wildermuth, K. and K. Baumann, Some remarks on self-acceleration and similar effects in quantum field theory 612
Wolfendale, A. W., *see* Fowler
Zappa, L., *see* Bisi
Zastavenko, L. G., A. L. Liubimov, V. I. Ogievitsky and M. I. Podgoretsky. On a possibility of K-meson investigation. . . . 549
Zutshi, P. K., *see* Lal

BOOK REVIEWS

Bass, J., Cours de mathématiques (L. R.) 691
Broda, E. and T. Schonfeld, Die technischen Anwendungen der Radioaktivität (H. J. Axon). 344
Cowling, T. G., Magnetohydrodynamics (L. R.). 624
Gorter, C. J., editor, Progress in low temperature physics (L. R.) vol. II. 691
Hill, T. L. Statistical mechanics (L. R.) 691
Kopfermann, H., Kernmomente (L. R.) 624
Landé, A., Foundations of quantum mechanics, an anti-review. . 132
Rockwell, T., Reactor Shielding Design Manual (J. Diamond). . 491
The Physics of Nuclear Reactors (L. R.) 491
Shamos, M. H. and G. M. Murphy, editors, Recent advances in science-physics and applied mathematics (L. R.) 135

SUBJECT INDEX

Beta and gamma spectroscopy
  Electric monopole transition rate in Zr^{90}, Martin Deutsch 83
  Excited levels in Hg^{200} studied from the decay of Tl^{200}, C. J. Herrlander and T. R. Gerholm 161
  Concerning lifetimes of low energy E1 gamma transitions in odd mass spheroidal nuclei, D. Strominger and J. O. Rasmussen 197
  Étude des électrons Auger-K émis par le zinc65, J. B. Bellicard, A. Moussa et S. K. Haynes 307
  The influence of *l*-forbiddenness on magnetic dipole transitions in Tl^{208}:, Torsten Lindquist and Ingvar Marklund 367
  Electron capture in arsenic 74 and arsenic 76, J. Scobie. 465
  The energy levels of Hf^{177} and the unified model, S. Ofer 479

The isomeric transitions in Tl^{197} and Tl^{195}, G. Andersson, P. A. Tove, B. Jung and I.B. Svensson. 493
Note on the decay of Tl^{198m}, G. Andersson and I. Bergström 506
Levels in Pb^{202} and Tl^{202} populated from 3.62-h Pb^{202m}, J. A. McDonell, R. Stockendal, C. J. Herrlander and I. Bergström 513
Anomalous internal conversion ratios of E3 transitions in the region $Z = 77$-82, G. Andersson and I. Bergström 541
Excited levels in Bi^{206} from the decay of Po^{206}, E. Arbman 625
The low lying energy levels of ^{151}Eu, A. Bisi, E. Germagnoli and L. Zappa . . 670

Cosmic radiation

Phosphorus isotopes P^{32} and P^{33} in rain water, D. Lal, N. Narasappaya and P. K. Zutshi. 69

Elementary Particles

On the spin and parity of the τ-meson, I. S. Shapiro, E. I. Dolinsky and A. P. Mishakova. 60
On the universal interactions II: K-meson decays into pions, S. Oneda 97
A possible explanation of the anomalous scattering of μ-mesons, G. N. Fowler . . 121
On the conservation laws for weak interactions, L. Landau 127
K-meson scattering with change of intrinsic parity, V. B. Berestetsky and Yu. A. Bychkov. 153
On interference phenomena in the decay of strange particles, V. B. Berestetsky . 157
A decay of a negative τ', S. Nilsson. 364
On symmetries in elementary particle interactions, B. d'Espagnat, J. Prentki and Abdus Salam. 446
Some remarks on decay rates of heavy mesons, B. d' Espagnat, R. Omnes and J. Prentki 471
On a possibility of K-meson investigation, L. G. Zastavenko, A. L. Liubimov, V. I. Ogievitsky and M. I. Podgoretsky 549
Zur Theorie der β-Wechselwirkung, H. Koppe 585
Two-component theory of the neutrino and K-meson decays comprising two neutrinos, S. Oneda 598
Space-time reflections and isobaric spin, J. C. Taylor 606
A theoretical estimate of the influence of the character of the four-fermion interaction on the muon capture rate, H. A. Tolhoek and J. R. Luyten. 679

Field Theory

Invariance properties and identities between renormalization constants, A. Petermann 592
Some remarks on self-acceleration and similar effects in quantum field theory, K. Wildermuth and K. Baumann. 612

Methods and instruments

Further analysis of the neutron component of the background of counters used for ^{14}C age measurements, Hl. de Vries 65
X-ray escape gating as applied to a proportional counter, C. W. McCutchen . . 76
A new method of measurement of neutron polarization and n-He^4 phase analysis, I. I. Levintov, A. V. Miller and V. N. Shamshev. 221

News items

Sixth session of the council of CERN (Geneva, 14 December 1956). 136
Conference on liquid scintillation counting (Evanston, August 20-22, 1957) . . . 492

Nuclear states

Properties of low lying levels in Mg^{25}, H. E. Gove, G. A. Bartholomew, E. B. Paul and A. E. Litherland (Nuclear Physics **2** (1956/57) 132—146), Erratum. 344
Levels in Bi^{206}, S. Wahlborn 644
Mgnetic moment of the electron, A. Peterman 689

Passage of particles through matter (*see also* Cosmic radiation)

The fluctuation problem in μ-meson bursts, A. N. Mitra. 262
On the interactions of fast μ-mesons, G. N. Fowler and A. W. Wolfendale . . . 299
Über die Zertrümmerung schwerer Kerne der Kernemulsion durch Teilchen der kosmischen Strahlung, K. Lanius 391

Photonuclear reactions

A scintillation spectrometer study of the photodisintegration of O^{16}, N. L. Svantesson 273

Reactions induced by particles (*see also* Nuclear states)

La fonction densité (strength function) dans la théorie statistique des réactions nucléaires, C. Bloch. 137
A note on the calculation of coulomb penetration and coulomb wave functions, R. M. Thaler and L. C. Biedenharn 207
The Coulomb excitation of U^{235}, Pu^{239}, and U^{238}, J. O. Newton 345
An investigation of the reaction ^{23}Na (d, n) ^{24}Mg, F. A. El Bedewi and M. A. El Wahab 385
Isotopic assignment of slow neutron resonances in germanium, rubidium, neodymium and tungsten, Eleanor M. Bowey 553
Neutron alpha particle angular correlation in the reaction ^{7}Li (d, α) and the ground state of ^{5}He, F. J. M. Farley and R. E. White. 561
The Coulomb excitation of Eu^{151} and Eu^{153}, C. M. Class and U. Meyer-Berkhout 656

Scattering

Inelastic high energy nucleon scattering on light nuclei, Th. A. J. Maris and H. Tyrén (see also Erratum p. 344). 35
Studies of inelastic scattering of 185 MeV protons on carbon, H. Tyrén and Th. A. J. Maris (see also Erratum p. 344). 52
The polarization of 155 MeV protons elastically and inelastically scattered from carbon, R. Alphonce, A. Johansson and G. Tibell. 185
Polarization of high energy nucleons exciting a collective level, Th. A. J. Maris 213
Alpha-alpha scattering at 38.5 MeV, W. E. Burcham, W. M. Gibson, D. J. Prowse and J. Rotblat. 217
A new method of measurement of neutron polarization and n-He^{4} phase analysis, I. I. Levintov, A. V. Miller and V. N. Shamshev. 221
Dependence of (D+D) neutron polarization on deuteron energy, I. I. Levintov, A. V. Miller, E. Z. Tarumov and V. N. Shamshev 237
The polarization of 173 MeV protons inelastically scattered by carbon, H. Tyrén, Peter Hillman and A. Johansson 336
Scattering of fast neutrons by neon in the energy region 1.9 to 3.5 MeV, C. P. Sikkema 375
Concerning the elastic scattering of high energy particles, I. M. Khalatnikov 433
Construction of the scattering matrix of a two-nucleon system, L. Puzikov, R. Ryndin and J. Smorodinsky 436
Polarisation in the elastic scattering of neutrons by helium, R. E. White and F. J. M. Farley (see also Erratum, 689) 476
Dispersion relations for the decay of the τ-meson, E. Corinaldesi. 649

Structure of nuclei (Models and Theory). (*see also* Nuclear states)

Studies in the α-particle model of nuclei III. Calculation of the interaction between α-particles, A. Herzenberg. 1
Many-body forces and the many-body problem, J. C. Polkinghorne. 94

Sum rule for optical nuclear reactions, H. Morinaga and D. C. Peaslee 115
Niveaux de rotation de noyaux sans axe de symétrie, C. Marty 193
A note on rotational energy levels in nuclei, F. Villars 240
Nuclear surfaces and zero-energy scattering, D. C. Peaslee 255
Studies in the α-particle model of nuclei IV. The polarization forces between α-clusters in nuclei, A. Herzenberg and A. S. Roberts 314
Sur la diffusion d'électrons de haute énergie par les noyaux, J. Reignier 340
The problem of an effective mass in nuclear matter, V. F. Weisskopf 423
The dipole sum rule with an approximate Hamiltonian, J. S. Levinger, N. Austern and P. Morrison 456
Empirical determination of nuclear shape factors and moments of inertia, E. D. Klema and R. K. Osborn 571

APPEAL TO CONTRIBUTORS

Among the factors delaying the appearence of a paper, the most serious is the unsatisfactory presentation of the typescript. An appeal is made to contributors to follow the simple rules and conventions laid down in the instruction sheet which has already been widely distributed and copies of which are available on request from the publishers or the members of the Editorial Board. Attention is called in particular to the writing of formulae. Authors are especially requested *not* to typewrite formulae, but to write them in long hand, very carefully, since the compositor cannot guess the meaning of a symbol which is not legible. In future, the Editor will be forced to return unsatisfactory typescripts to the authors for the necessary material improvements.

It frequently happens that after a paper has been communicated, the author sends substantial corrections or alterations. Since the publisher and printer spare no effort to achieve prompt publication, such late alterations often arrive after the paper has already been set, and inflict on them much unnecessary trouble and cost. Contributors should realise that a too hasty writing-up of a paper thus defeats the prospect of a quick publication.

Editor and publisher trust that the authors will not shun the slight trouble which the careful preparation of the typescript entails and thank them in advance for their cooperation.

JUST OUT

QUANTUM MECHANICS

by

H. A. KRAMERS

Late-Professor of Theoretical Physics, University of Leiden

Translated by D. TER HAAR, *Clarendon Laboratory-Oxford*

This book is an English translation of the well-known pre-war monograph on Quantum Theory.

The author was closely connected with Niels Bohr's institute from **1912** until **1926**, during which period quantum theory was developed, to a large extent by the Copenhagen school, into essentially its present form. Among Kramers' own contributions to this development one may mention the so-called W-K-B method, the symbolic method for calculating intensities of spectral lines, the derivation of the wave equation for a relativistic electron (independent of and practically simultaneous with Dirac's derivation), and the idea of mass renormalisation. As a consequence, the presentation of quantum theory in the present textbook is more lively and less stereotyped than in most texts on the subject and often sheds light on details which are usually overlooked. Also, there are in this monograph a number of those mathematical gems which were so typical of Kramers.

6×9", xvi +496 pages

Guilders 45.— (90 s.)

CONTENTS:

- *I. Quantum theory of free particles.*
- *II. Non relativistic quantum theory of bound particles.*
- *III. The non-relativistic treatment of the many-body problem.*
- *IV. Transformation theory.*
- *V. Perturbation theory.*
- *VI. The spinning electron.*
- *VII. The exclusion principle.*
- *VIII. Electromagnetic radiation.*

Sole distributors for U.S.A.: Interscience Publishers, Inc. - New York

NORTH-HOLLAND PUBLISHING COMPANY-AMSTERDAM

Send your order to your bookseller or directly to the publisher